KCC2 AND NKCC1 IN THE CONTROL OF NEURONAL Cl^- AND BRAIN EXCITABILITY

By

Lei Zhu

Dissertation

Submitted to the Faculty of the

Graduate School of Vanderbilt University

in partial fulfillment of the requirements

for the degree of

DOCTOR OF PHILOSOPHY

in

Neuroscience

August, 2007

Nashville, Tennessee

Approved:

Professor Robert L. Macdonald

Professor Eric Delpire

Professor Louis J. DeFelice

Professor Danny G. Winder

Professor David M. Lovinger

ACKNOWLEDGEMENTS

I wish to express my gratitude to the following people who provided immense help to me to complete my Ph.D. degree. My mentor Dr. Eric Delpire is an enthusiastic and hardworking scientist who gave me great help for my thesis proposal, experiment design, and paper/thesis writing and from whom I am still learning the way to be a scientist. Dr. David Lovinger is also a great mentor who always came up with great ideas and advice with my research. I want to express my great gratitude to Dr. Gregory Mathews who is such a generous and wonderful person for letting me do all brain slice experiments in his laboratory. I also want to thank my other thesis committee members Dr. Robert Macdonald, Lou DeFelice, and Danny Winder. Their advice and critiques have guided me through the years of my Ph.D study. I want to thank Mike Maguire for his help with my neuronal cultures, Nathan Polley for caring and genotyping mice and everyone in the Delpire lab for the several wonderful years spent together.

I want to thank my family in China, my mother, father and brother, who has made such great sacrifices and contributions that without them, I could not have been able to come to the US to carry out my dream to become a scientist. My lovely wife Wenjuan is always by my side no matter what happens in my life and I want to let her know how grateful I am. Finally I want to show my great gratitude to my grandfather, who passed away last November. He has such great faith and passion for the education of children that the injustice and pain he suffered for most of his life didn't change his mind.

TABLE OF CONTENTS

Page

LIST OF FIGURES

CHAPTER I

INTRODUCTION

Synaptic Transmission Overview

The human brain contains more than 10^{12} neurons and these neurons are the master controllers of our perception, concentration, thoughts, and movement. Each of the 100 billion neurons communicates with other neurons via thousands of synapses on average. These synapses transmit signals from one neuron to another by converting an electrical signal from the presynaptic neuron into a chemical signal—neurotransmitter—then converting it back to an electrical signal in the postsynaptic neuron through the binding of neurotransmitter to its specific receptor, and opening of ion channels. Chemical synapses are the main method of communication between neurons, in spite of the existence of electrical synapses (Bennett et al., 2000; Kandler and Katz, 1995; Rorig and Sutor, 1996), neurotransmitter spill-over (Diamond, 2001; Kullmann et al., 1996), and retrograde signaling (Murphey and Davis, 1994; Yin and Lovinger, 2006). Although there are many neurotransmitters, the two most prominent in the brain are glutamate and γ-aminobutyric acid (GABA), with glutamate being excitatory and GABA being mostly inhibitory.

The three major modes of neurotransmission are excitatory, inhibitory and modulatory. I will focus on excitatory and inhibitory neurotransmission. Excitatory postsynaptic potentials (EPSP) depolarize the postsynaptic membrane, while inhibitory

postsynaptic potentials (IPSP) either hyperpolarize the membrane or shunt the excitatory current. One neuron can receive thousands of inputs from other neurons, with the inputs being a mixture of excitatory and inhibitory potentials. Each individual EPSP is too small to generate an action potential, although there are a few exceptions(Crepel et al., 1980; Lohof et al., 1996). The temporal and spatial summation of many EPSPs can add up to a large depolarization, and can trigger an action potential at the axon hillock if the depolarization reaches the action potential threshold (approximately -55 mV at axon hillock). At the same time, the inhibitory inputs from inhibitory interneurons generate IPSPs onto the same neuron, which tries to shunt the excitatory current and prevent the depolarization from reaching its action potential threshold. The total summation of excitatory and inhibitory inputs determines whether the neuron will fire an action potential. Inhibitory transmission not only plays a crucial part in this decision-making, but also prevents the neuron from being over-excited. In the absence of inhibitory neurotransmission, prolonged presynaptic depolarization results in large amounts of glutamate release and over-activation of glutamate receptors. Excessive Ca^{2+} moves through these receptors and activates a multitude of cellular processes involving kinases and phosphatases that leads to damage or even death to the cell. This whole process is called glutamate toxicity (Sattler and Tymianski, 2001). Large-scale over-excitation also causes synchronized neuronal firing and epileptic seizures. Overall, inhibitory neurotransmission has a crucial part in the decision-making process of the CNS and maintains the stability of the neuronal network.

The $GABA_A$ receptor in inhibition

Before I fully discuss inhibition in the CNS, it is necessary to discuss some fundamental elements of both excitatory and inhibitory neurotransmission: neurotransmitters. Excitatory neurotransmission is mostly mediated by ionotropic glutamate receptors in the CNS (by acetylcholine receptors at the neuromuscular junction). Thus, glutamate is generally considered the major excitatory neurotransmitter in the CNS. There are three types of ionotropic glutamate receptors defined by their agonists and function: the NMDA receptor, the AMPA receptor, and the kainate receptor. The ligand-gated glutamate receptors are ionophores activated by binding of agonist. After its release from the presynaptic terminal, glutamate binds to the receptors on the postsynaptic membrane and opens up ion channels, allowing cations to pass. Na^+ and K^+ move through AMPA and kainate receptors, while NMDA receptors allows another ion, Ca^{2+}, to permeate along with Na^+ and K^+. In the presence of normal physiological ionic distribution, the reversal potential for glutamate receptors lies at 0 mV because the weighted equilibrium potential for K^+ and Na^+ is approximately 0 mV. The resting membrane potential of neurons is normally more negative than -60 mV. Hence, the net driving force for cations is at least 60 mV inward. Upon opening of the ligand-gated ion channel, the current carried by cations flows into the neuron, causing a depolarization of the postsynaptic membrane.

The inhibitory neurotransmitters in the CNS are GABA and glycine. Ionotropic $GABA_A$ receptors are widely expressed in different brain regions and play the most

prominent role in inhibition of neuronal networks. Ionotropic $GABA_C$ receptors are mostly localized to the retina, and take part in modulating visual signals. Ionotropic glycine receptors are best known for their inhibitory function in the brainstem and spinal cord (Betz, 1991; Betz et al., 1994). Finally, the metabotropic $GABA_B$ receptor located on postsynaptic membranes is also inhibitory, as GABA binding results in the activation of receptor-coupled G proteins and consequently the βγ subunits of the G protein activate a K+ channel (Chebib and Johnston, 1999; Mott and Lewis, 1994). $GABA_A$, $GABA_{C,}$ and glycine receptors are ion channels permeable to Cl^- when activated, with a much weaker permeability to HCO_3 (permeability ratio $Cl:HCO_3$ is approximately 5:1). I will focus on the $GABA_A$ receptor since it is the most abundant and important receptor in the inhibitory system in the CNS. Each $GABA_A$ receptor consists of five subunits (pentameric structure) and has a conformation similar to nicotinic receptors. There are many different types of $GABA_A$ subunits in humans, including 6 α, 3 β, 3 γ, 3 ρ as well as δ, ε, π, θ (Dunn et al., 1994). All subunits have four transmembrane segments, and different combinations of subunits endow the receptor with different properties in terms of affinity, gating, deactivation, and desensitization.

There are two types of inhibition through ionotropic $GABA_A$ receptors. Firstly, due to the low intracellular Cl- concentration in most adult neurons, the reversal potential of GABA-activated current is hyperpolarized relative to the resting membrane potential. Activation of $GABA_A$ receptors hyperpolarizes the cell membrane. This hyperpolarization moves the membrane potential farther away from the threshold to

trigger an action potential, resulting in the disruption (inhibition) of incoming excitatory signals. Another form of GABA inhibition is current shunting instead of direct hyperpolarization of the membrane. An IPSP is depolarizing when the GABA reversal potential is more positive than the membrane potential. The current from EPSPs can be short-circuited by the simultaneous opening of $GABA_A$ receptors and Cl^- channels (increasing membrane conductance) and thus, the amplitude of the EPSP is reduced upon arrival at the axon hillock. Theoretically, as long as the GABA reversal potential is more negative to the action potential threshold, GABA is still inhibitory. The HCO_3^- gradient also contributes to the reversal potential of GABA. However, its effect is more prominent when the intracellular $[Cl^-]$ is low, as in most adult neurons, and is negligible when the intracellular $[Cl^-]$ is high, as in young neurons (Farrant and Kaila, 2007), also see Appendix B).

GABA excitation in developing neurons

GABA, although an inhibitory neurotransmitter in the adult brain, elicits depolarizing and excitatory effects during embryonic development and early postnatal life in rodents. In fact, GABA is the first excitatory neurotransmitter in postnatal development, as GABAergic synapses develop prior to glutamatergic synapses. GABA excitation is due to high intracellular Cl^- concentration (Avoli, 1996; Ben-Ari et al., 1994);(Ben-Ari, 2006). As I will discuss in more detail in later sections, the high $[Cl^-]_i$ is thought to be the result of high expression of the Cl^- importer Na-K-2Cl cotransporter, NKCC1, and low

expression of the Cl^- extruder K-Cl cotransporter, KCC2 (**Figure 1-1**). This "unusual" excitatory action of GABA is not adverse to the development of the CNS, but likely participates in some critical developmental processes. For instance, as glutamate receptors are "silent" and $GABA_A$ receptors are active, GABA excitation depolarizes the membrane, activates voltage-gated Ca^{2+} channels, and removes the magnesium block from NMDA receptors(Ben-Ari et al., 1997a). Giant synchronous depolarizing potentials (GDP) have been observed in the developing brain, and they are inhibited by $GABA_A$ receptor blockers, but not glutamate receptor inhibitors (Ben-Ari et al., 1989; Leinekugel et al., 1998; Sipila et al., 2005). The subsequent influx of Ca^{2+} through both types of channels triggers intracellular processes for phosphorylation and trafficking of the "silent" glutamate receptors (Ben-Ari et al., 1997a; Hennou et al., 2002) and might participate in the development and maturation of growth cones (Gao and van den Pol, 2000; Obrietan and Van den Pol, 1996). As I will also discuss later, GABA depolarization might promote the expression of KCC2 and thus the maturation of the GABA system itself (Ganguly et al., 2001).

Excitatory GABA may also have detrimental effect on the developing brain. Neonatal seizures can cause neurological dysfunction in infants in the first 28 days of life (Ronen et al., 1999), and can even possibly lead to long-term impairment of brain and behavior (Painter et al., 1986; Scher et al., 1993). Neonatal seizures are hard to treat with traditional anticonvulsant drugs such as benzodiazepines and barbiturates.

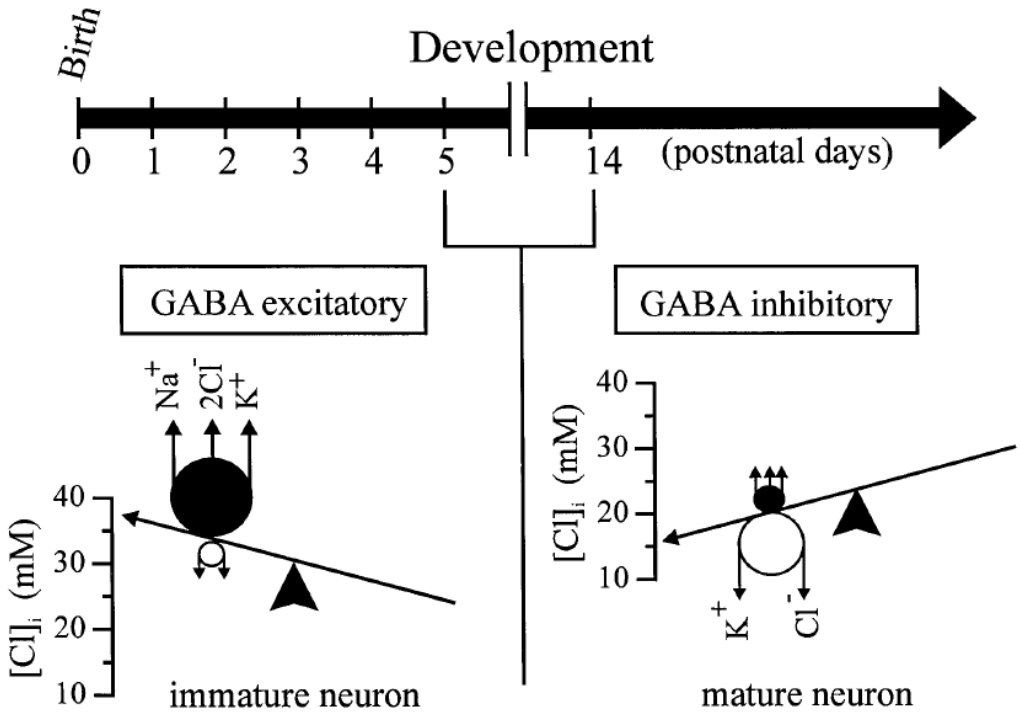

From Lu et. al. J. Neurobiol. 1999

Figure 1-1. The effect of GABA is determined by the intracellular Cl^- concentration that is regulated by two cation-chloride cotransporters: KCC2 and NKCC1.

During the first postnatal week, expression of NKCC1 is high while expression of KCC2 is low. Balance of Cl^- accumulation by NKCC1 versus Cl^- export by KCC2 favors Cl^- accumulation in the neurons, and as a result, GABA response is excitatory. As the neurons mature, the decrease of NKCC1 expression and increase of KCC2 expression results in the balance shifting in the opposite direction and GABA responses becoming inhibitory.

Since the GABAergic system matures in a caudal to rostral fashion (Stein et al., 2004), it is possible to control the motor manifestations by potentiating GABA inhibition in the spinal cord and brainstem, but seizures in the rostral structures are resistant to such treatment (Painter et al., 1986). Whether or not targeting the mechanisms that set the intracellular Cl^- concentration will have an impact on neonatal seizures needs to be addressed. In a recent paper, Dzhala et al showed that NKCC1 function facilitates seizures in the developing brain (Dzhala et al., 2005).

Excitatory GABA and Epilepsy

The intracellular chloride concentration is not unchallenged during neuronal activities. There are various situations in which intracellular Cl^- will increase, including repetitive activation of $GABA_A$ receptors, activation of large amounts of $GABA_A$ receptors during prolonged depolarization and, as we will see later, the active inward Cl^- transport by NKCC1 transporters. As the intracellular Cl^- concentration increases, GABA becomes more excitatory. In the 1980s, Thompson et al. found that repetitive activation of $GABA_A$ receptors by stimulation from bipolar electrodes causes disinhibition which is the shift of E_{GABA} in the depolarized direction possibly due to the excessive influx of Cl^- into the neuron through $GABA_A$ receptor channels (Thompson et al., 1988). In the adult CNS, especially the hippocampus where large amount of glutamatergic neurons form an interconnected network, disinhibition can lead to synchronous firing and oscillation, which usually precedes epileptic seizure. Numerous studies have examined the link

between GABA dysfunction and epileptic seizures (De Deyn et al., 1990; Macdonald et al., 2004; Prince et al., 1992). However in the research field of epilepsy, most of the work has focused on modifications and mutations of the $GABA_A$ receptor, and little attention is being paid to the driving forces that allow chloride ions to move through the receptor-activated Cl^- channel. Recently, more attention has been paid to the transmembrane chloride gradient, and this research might shed new light on the study of epileptic seizures that are resistant to the treatment with agents potentiating $GABA_A$ receptor function, such as benzodiazepines, barbiturates and ethanol (Connell et al., 1989; Dzhala and Staley, 2003; Painter et al., 1986; Scher, 2003).

Cation-Chloride Cotransporters Overview

Cation-chloride cotransporters (CCC) are a large superfamily of proteins that transport inorganic cations with chloride across the plasma membrane. There are seven functionally well-characterized members in this family, namely NCC (Na-Cl cotransporter); NKCC1, NKCC2 (Na-K-Cl cotransporters); KCC1, KCC2, KCC3, KCC4 (K-Cl cotransporters); and two additional members with unknown functions, CCC8 and CCC9(Delpire and Mount, 2002; Hebert et al., 2003; Mount et al., 1998). These cotransporters vary vastly in terms of the expression pattern, cellular localization, and their physiological functions. However, they share similarities in their protein structure, encoded genes, the electroneutral nature of the transport, and sensitivity to loop-diuretics. Most of the cation-chloride cotransporters are sensitive to cell volume changes. The

Na-K-2Cl cotransporters are activated by cell shrinkage, whereas the K-Cl cotransporters are activated by cell swelling (Delpire and Mount, 2002). The K-Cl cotransporter KCC2 is also constitutively active under isotonic conditions (Payne, 1997; Song et al., 2002; Strange et al., 2000).

Cation-chloride cotransporters do not directly utilize ATP as their source of energy. Instead, they rely on the Na^+ and/or K^+ gradients established by Na-K-ATPase to transport these ions across cell membranes. Transport is tightly coupled and therefore occurs only when all ions are present. Theoretically, the transport can occur in both directions: from the inside of the cell to the outside, or vice-versa. However, in most physiological situations, due to the activity of the Na-K-ATPase, $[K^+]_i$ is significantly higher than $[K^+]_o$, and $[Na^+]_i$ is significantly lower than $[Na^+]_o$. Thus, due to these gradients, Na-K-2Cl cotransporters move Na^+, K^+, and Cl^- into cells, while K-Cl cotransporters move K^+ and Cl^- out of cells. Since the gradients of Na^+ and K^+ are rapidly restored by Na-K-ATPase at the cost of ATP hydrolysis, only the Cl^- gradient is generally different from equilibrium (Alvarez-Leefmans et al., 2001).

There are three major functions associated with cation-chloride cotransporters. First, CCCs regulate the intracellular Cl^- concentrations in cells. As mentioned in the first section, Cl^- is the major ion permeating $GABA_A$, $GABA_C$, and glycine receptors. Abnormally high intracellular Cl^- causes the polarity of the GABA currents to switch from hyperpolarizing to depolarizing, leading to disinhibition of neuronal networks and epileptic seizures (see Chapter IV). Second, most cation-chloride cotransporters

participate in cell volume maintenance and regulation. When the osmolality of the extracellular space increases or decreases, cells shrink or swell due to the rapid movement of water across the plasma membrane. After cell shrinkage, the Na-K-2Cl cotransporter participates in the restoration of cell volume by transporting ions into the cell. This process is called regulatory volume increase or RVI (Majid et al., 2001; Russell, 2000) . In contrast, after cell swelling, K-Cl cotransporters participate in water loss by extruding K^+ and Cl^- ions. This process is called regulated volume decrease or RVD (Lauf and Adragna, 2000). Finally, CCCs participate in the secretion/reabsorption of fluid and ions in epithelia. For example, NKCC2 is expressed on the apical membrane of the thick ascending limb of Henle of the kidney where it facilitates transport of ions from the lumen (urine side) to interstitium (blood side). It is one of the main mechanisms for salt reabsorption (Gimenez and Forbush, 2003; Karolyi et al., 1998; Schnermann, 2001). On the other hand, in Cl^- secreting epithelia, NKCC1, expressed on the basolateral membrane accumulates Cl^- into the cell and provides a reservoir for Cl^- secretion at the apical membrane (Delpire et al., 1999; Haas and Forbush, 2000; Wall and Fischer, 2002).

The genes encoding the cation-chloride cotransporters share homology with eukaryotic cationic amino acid transporters as well as with prokaryotic and eukaryotic amino acid permeases (**Figure 1-2**). These cotransporters can be divided into 2 sub-families: the sodium-dependent cation-chloride cotransporters, which include NCC, NKCC1 and NKCC2, and the sodium-independent cation-chloride cotransporters, which are comprised of KCC1, KCC2, KCC3 and KCC4. Two additional genes encode not yet

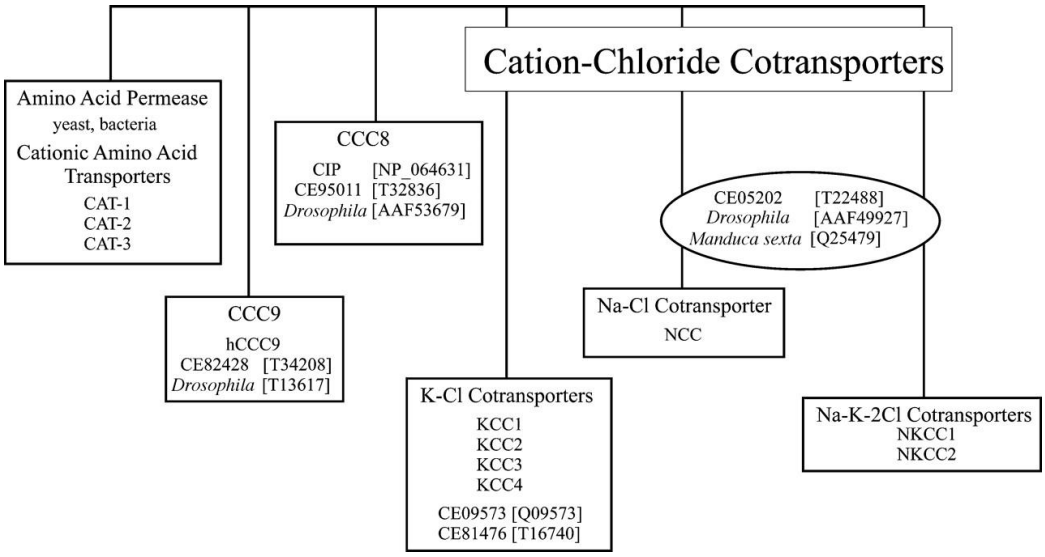

From Delpire and Mount, Annu. Rev. Physiol. 2002

Figure 1-2. The superfamily of cation-chloride cotransporters and amino acid permeases.

There are three subfamilies of electroneutral cation-chloride cotransporters, Na-Cl coupled transporters (NCC), K-Cl coupled transporters (KCC), and Na-K-Cl coupled transporters (NKCC). NKCCs consist of two isoforms NKCC1 and NKCC2, while KCCs have four different isoforms: KCC1, KCC2, KCC3 and KCC4. These cotransporters are distantly related to the amino acid permeases of yeast and bacteria, and to *Drosophila* orthologs.

functionally characterized are CCC8 and CCC9. (**Figure 1-3**). The crystal structure of these membrane proteins has not yet been resolved and their membrane topology was derived mostly based on predictions based on hydropathy analyses (e.g. Kyte-Doolittle). For the Na-K-2Cl cotransporter NKCC1, the topology was verified experimentally using an *in vitro* translation approach (Gerelsaikhan and Turner, 2000). The transmembrane domains TM3 to TM12 are homologous with a large amino acid permease domain (pfam00324), and each specific CCC is defined by TM1, TM2, and the large cytosolic N-terminal and C-terminal domains. TM2 is involved in determining the ion-binding affinity of the different cotransporters (Igarashi et al., 1995; Isenring et al., 1998). The large intracellular amino- and carboxyl-terminals of the cation-chloride cotransporters are involved in regulation of transport activity, such as through phosphorylation/dephosphorylation mechanisms (Bize and Dunham, 1994; Darman and Forbush, 2002; Jennings and Schultz, 1991; Klein et al., 1999).

Physiological roles of Cation-Chloride Cotransporters

NCC

The Na^+-Cl^- cotransporter NCC was the first cation-chloride cotransporter identified at the molecular level (Gamba et al., 1993). Although there are reports of NCC expression in bone (Nicolet-Barousse et al., 2005), the cotransporter is mostly found in kidney, located at the apical membrane of epithelial cells of the distal convoluted tubule

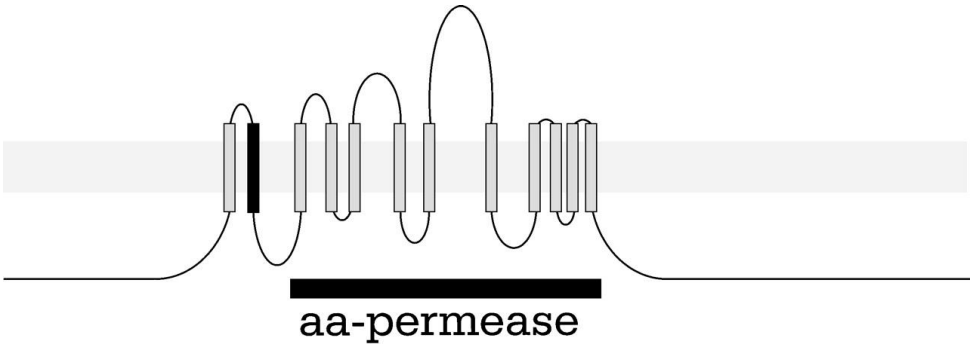

from Delpire and Mount, Annu. Rev. Physiol. 2002

Figure 1-3. Cation-chloride cotransporters share a common 12 transmembrane domain core and two large cytoplasmic termini.

Transmembrane domains TM3–TM12 share high homology among different subtypes of CCCs and are also homologous to the amino acid permease domain. The second transmembrane domain is involved in ion binding.

of the kidney (Ellison et al., 1987). In contrast to the other cation-chloride cotransporters, which are inhibited by loop diuretics, the Na-Cl cotransporter is inhibited by thiazide diuretics. Recent studies have found that NCC forms a homodimer in epithelial cells (de Jong et al., 2003). NCC is responsible for 5% of the filtered NaCl load and it also indirectly affects calcium homeostasis by increasing intracellular Cl^- and lifting the resting membrane potential of the epithelial cells (Delpire and Mount, 2002; Gesek and Friedman, 1992). NCC expression is under the regulation of hormones and the load of NaCl of the DCT itself. Both a low salt diet and mineralocorticoids can decrease the expression of NCC transcripts in the DCT (Kim et al., 1998). Inactivating mutations of NCC are involved in Gitelman syndrome, a salt wasting disorder characterized by excessive Na^+, K^+, Mg^{2+}, and Cl^- in the urine and hypocalciuria (Bettinelli et al., 1992). Disruption of the NCC gene in mice causes some, but not all, of the symptoms of Gitelman syndrome, including increased renin mRNA levels in the kidney, hypomagnesemia, hypocalciuria, and morphological changes in the distal convoluted tubule (DCT), but not hypokalemia and alkalosis which is seen in human Gitelman syndrome (Schultheis et al., 1998) (Delpire and Mount, 2002).

NKCC2

The bumetanide-sensitive Na^+-K^+-$2Cl^-$ cotransporter was cloned by screening a rat kidney cDNA library with a NCC cDNA probe (Gamba et al., 1994). NKCC2 plays an important role in the reabsorption of cations (Na^+, Ca^{2+}, Mg^{2+}), acid secretion

(Attmane-Elakeb et al., 1998), and countercurrent multiplication (Good, 1994). Human NKCC2 is 95% identical to rabbit and 93% to rat or mouse NKCC2 (Gamba, 2005a), with an approximate molecular weight of 121 kDa. Western blot analysis reveals that NKCC2 expression is restricted to the kidney (Gamba et al., 1994; Igarashi et al., 1995; Mount et al., 1999; Payne and Forbush, 1994). *In situ* hybridization and single nephron RT-PCR have localized NKCC2 transcript to the cortical and medullary thick ascending limb (Gamba et al., 1994; Igarashi et al., 1995; Yang et al., 1996). NKCC2 expression is also found in macula densa cells (Kaplan et al., 1996; Nielsen et al., 1998). Apical cotransport by NKCC2 plays a pivotal role in the transepithelial absorption of Na^+ and Cl^- by the TAL and macula densa and also the absorption of ammonium (NH_4^+) from the tubular lumen, followed by countercurrent multiplication (Good, 1994). The loop diuretics bumetanide and furosemide inhibit NKCC2, which result in large production of urine isotonic to plasma fluid. NKCC2 deficiency is involved in an autosomal-recessive form of hypokalemic hypochloremic metabolic alkalosis disorder named Bartter syndrome(Delpire and Mount, 2002; Kleta et al., 2000; Kleta and Bockenhauer, 2006).

NKCC1

Cloning of NKCC1 was obtained simultaneously from homology cloning (Delpire et al., 1994) and by screening a library using an antibody generated against the shark cotransporter (Forbush et al., 1994). NKCC1 is found in a wide variety of cells, both epithelial and non-epithelial. NKCC1 is found in the central and peripheral nervous

system, choroid plexus, lung, kidney, skeletal muscle, digestive tract, salivary gland, and testis (Haas, 1994; Haas and Forbush, 1998; Russell, 2000). Some splice variants have been found: one variant lacking a cassette exon in the C-terminus of the cotransporter (Randall et al., 1997), another containing a shorter, alternative C-terminus in muscle (Wong et al., 2001). In epithelial cells, NKCC1 is localized on the basolateral membrane, except for the choroid plexus, where the cotransporter is found on the apical membrane (Plotkin et al., 1997a). Due to its localization on the basolateral membrane of epithelial cells, and its role in ion secretion, NKCC1 is often referred to as the "secretory" Na-K-2Cl cotransporter. In non-epithelial cells the cotransporter participates in cell volume regulation. The NKCC1 protein is relatively large, with about 1,200 amino acids and 12 transmembrane domains, TM1-TM12. Transmembrane domains 1, 3, 6, 8, 10 and the intracellular loop between TM2 and TM3 are highly conserved between the two isoforms of NKCC. TM2 is responsible for cation affinity, while Cl- affinity can be affected by TM4-TM7 (Payne et al., 1995; Russell, 2000).

NKCC1 requires the presence of all 3 transported ions (Na^+, Cl^-, K^+) on the same side of the cell membrane to be active (Russell, 2000). Absence of any of these three ions will totally shut down transport by NKCC1. The ions of transport strictly follow the ratio 1Na: 1K: 2Cl in most cells and 2Na: 1K: 3Cl in giant squid axons (Russell, 1983). This stoichiometry of NKCC1 transport determines that transport activity is electrically neutral, because the net charge crossing the membrane is zero. Under physiological ionic conditions, the driving force for NKCC1 is always inward, and thus NKCC1 acts as a Cl^-

accumulator. NKCC1 is inhibited by the loop diuretics bumetanide and furosemide, with bumetanide (sensitivity varies among tissues: IC50 0.05-10 μM) being much more potent than furosemide (Russell, 2000).

KCC1

KCC1, the fourth member of the Slc12 family of transport proteins, is often referred to as a housekeeping protein, involved in the maintenance of cell volume. It is widely expressed in brain, colon, heart, kidney, liver, lung, spleen, stomach, pancreas, and muscle (Delpire and Mount, 2002; Gillen et al., 1996). The physiology of KCC1 is best studied in red blood cells (Lauf and Adragna, 2000; Lauf et al., 1992). KCC1 plays a primary role in the regulatory volume decrease (RVD) of various types of cells under hypotonic environments. KCC1 is activated by hypotonic challenge and dephosphorylation (PP1 and PP2A) and inhibited by phosphorylation (Jennings and Schultz, 1991; Kaji and Tsukitani, 1991; Krarup and Dunham, 1996). KCC1, together with a Ca^{2+}-activated K^+ channel, is involved in the dehydration of sickle erythrocytes. Thus, therapeutic methods aimed at inhibiting KCC1 might provide benefit to sickle cell patients (Brugnara, 1995). KCC1 is also inhibited by the loop diuretics furosemide and bumetanide with Ki = 40 μM and 60 μM, respectively (Gillen et al., 1996).

KCC2

KCC2, the fifth member of the Slc12 family of transport proteins (Slc12a5), was also found during an attempt to identify additional genes related to NCC and the two Na-K-2Cl cotransporters. The K-Cl cotransporter was identified by searching a database of Expressed Sequences Tags (ESTs), and the full length cDNA was then cloned from a rat cDNA library (Payne et al., 1995). Its basic transport properties were demonstrated by flux experiments after expression in HEK-293 cells (Payne, 1997).

^{86}Rb flux experiments have been used extensively for the study of K^+ channels, pumps, and transporter physiology. Due to its similar physiological properties to K^+, radioactive rubidium ions are added as a tracer for K^+ ion in these experiments. The K-Cl transport (KCC1) is well studied in red blood cells (Adragna et al., 2004; Lauf et al., 1992). Functional characterization of KCC2 has been performed in HEK293 cells by Payne and coworkers (Payne, 1997; Payne et al., 1996). When expressed in the HEK293 cell line, KCC2 showed many characteristics similar to the well-characterized KCC1 transport. K-Cl transport via KCC2 is stimulated by the alkylating reagent NEM and this NEM-stimulated K-Cl transport can be inhibited by the loop-diuretics furosemide and bumetanide, with higher sensitivity to furosemide (inhibition constant (K_i) ~25 µM) than bumetanide (K_i ~55 µM). Other known inhibitors of KCC2 and other K-Cl transport are the stilbene disulfonic acid DIDS (Delpire and Lauf, 1992) and the alkanoic acid DIOA (Vitoux et al., 1989). KCC2 transport is also sensitive to the external concentration of K^+ and Cl^-, but not Na^+, which is another trait shared by all K-Cl transporters. However,

KCC2 exhibits some unique properties which differentiate this neuronal-specific cotransporter from other K-Cl cotransporters. The K-Cl transport by KCC2 is constitutively active in isotonic solution. In HEK293 cells, KCC2 is insensitive to volume change, unlike other K-Cl cotransporters. However, Strange and coworkers found that KCC2 is sensitive to volume changes when expressed in X*enopus laevis* occytes, suggesting that HEK293 cells have lost some components of cell volume activation of transport pathways (Strange et al., 2000). KCC2 also exhibits high affinity for extracellular K^+ (K_m = 5.2mM) (Payne, 1997), in contrast to the low affinity of KCC1 to extracellular K^+ (Km > 25mM) (Gillen et al., 1996). This characteristic of the KCC2 isoform suggests the K^+ buffering capability for KCC2, as the neuronal K-Cl cotransporter works very close to equilibrium and extracellular K^+ can rise to 10 – 12 mM during sustained neuronal activity (Heinemann and Lux, 1977). The difference between KCC2 and other K-Cl transporters may be attributed to the low homology of the cation binding domain of TM2 between the K-Cl cotransporters (only 60% between KCC2 and KCC1, while the other 11 TM domains share >90% homology between cotransporters).

KCC2 is a heavily glycosylated protein with a molecular mass of ~150kDa (Lu et al., 1999; Payne et al., 1996; Williams et al., 1999). The 150 kDa protein reduces to ~125 kDa after treatment with *N*-glycosidase F (Payne, 1997). Mutagenesis experiments have shown that the second transmembrane domain of KCC2 is responsible for the high affinity for extracellular K^+ ions (Williams et al., 1999). This high external K^+ affinity,

coupled to the weak outward driving force ($[K^+]i$ x $[Cl^-]i$ > $[K^+]o$ x $[Cl^-]o$), was speculated to underlie the possibility for KCC2 to easily reverse its direction of transport upon an increase of extracellular K^+ (Payne, 1997). As already mentioned, KCC2 has the unique property of being active under isotonic conditions. In a recent paper, Mercado et al. (Mercado et al., 2006) argue that a unique region of the C-terminus confers the isotonic transport property of KCC2. Indeed, a chimera in which the unique region of KCC2 is placed in KCC4 confers isotonic transport activity to this K-Cl cotransporter. Conversely, removal of the proline/serine- and charged residue-rich region in KCC2 eliminated the isotonic activity. These mutagenesis studies identified a 15-residue domain from 1021-1035 conferring isotonic transport (Mercado et al., 2006). KCC2 heterologously expressed in HEK293 cells is inhibited by the loop diuretics furosemide and bumetanide with Ki of 25 μM and 53 μM, respectively (Payne, 1997).

KCC2 expression is limited to the brain and spinal cord; there is no expression in colon, heart, kidney, liver, lung, spleen or stomach (Lu et al., 1999; Payne et al., 1996; Williams et al., 1999). Immunohistochemistry has shown that in the brain, expression of KCC2 is strictly confined to neurons (Lu et al., 1999; Vu et al., 2000; Williams et al., 1999). The cotransporter is also expressed in retinal neurons (Vardi et al., 2000). The neuronal-specific expression pattern of KCC2 is due to a 21-bp neuronal-restrictive silencing element located downstream of exon 1 (Karadsheh and Delpire, 2001). This element is recognized by the transcription factor NRSF, or neuronal restrictive silencing factor, which is expressed in non-neuronal cells as well as neuron precursors (Kraner et

al., 1992). In tissues other than mature neurons, expressed NRSF binds to the neuronal-restrictive silencing element, turning-off transcription of the cotransporter.

KCC3

KCC3, the sixth member of the Slc12 family (Slc12a6), was cloned independently by three groups (Hiki et al., 1999; Mount et al., 1999; Race et al., 1999). Several isoforms have been reported. Two isoforms (KCC3a and KCC3b) are generated by two alternative transcription initiation sites (Pearson et al., 2001). Transcript for KCC3a is widely expressed in the brain, lung, kidney, heart and muscle, while transcript for KCC3b is mainly located in the kidney (Mercado et al., 2004). By Western blot analysis and immunofluorescence, KCC3 protein was found in most CNS structures, including hypothalamus, hippocampus, cerebral cortex, cerebellum, brain stem, spinal cord and the white matter (Hiki et al., 1999; Mount et al., 1999; Pearson et al., 2001; Pearson et al., 2000). It is also found on the basolateral membrane of choroid plexus (Pearson et al., 2001). KCC3 is expressed in both neurons and glial cells in the brain.

KCC3 mutations have been found in patients with Agenesis of Corpus Callosum with Peripheral Neuropathy (ACCPN). The disorder is found in families sporadically throughout the world, but with a very high rate of occurrence in some counties of Quebec, Canada (Deleu et al., 1997). Patients with ACCPN show mental retardation and severe motor neuropathy, with or without agenesis of the corpus callosum. KCC3-null mice have been created by two different laboratories (Boettger et al., 2003; Howard et al.,

2002). Hypomyelination, demyelination, axonal swelling and fiber degeneration were observed in the homozygous mice (Howard et al., 2002). These characteristics might account for the severe locomotor deficit observed in both the knockout mouse and human patients. Sensorimotor gating deficit (pre-pulse inhibition), as well as decreased exploratory behavior, have also been demonstrated in the KCC3 knockout mice indicating central deficits. KCC3 null mice also exhibit arterial hypertension and a slowly progressive, age-related deafness (Boettger et al., 2003). KCC3 is expressed in many supporting cells of the inner ear involved in the K^+ recycling pathway, and these cells slowly degenerate in $KCC3^{-/-}$ mice. KCC3 is also inhibited by the loop diuretics furosemide (Ki ~ 10μM) and bumetanide (Ki ~ 40μM)(Hiki et al., 1999).

KCC4

KCC4 was also identified through an EST database search (Mount et al., 1999). It is encoded by the *SLC12A7* gene. KCC4 is found in a variety of tissues, which include kidney, the peripheral nervous system and the spinal cord. In the kidney, KCC4 is found on the basolateral membrane of type-A intercalated cells of the medullary collecting duct, and in the proximal tubule (Boettger et al., 2002). KCC4 expression in the CNS is not as abundant as other KCCs. It is mostly expressed on the apical membrane of the choroid plexus, as well as in cranial nuclei and cranial nerves (Karadsheh et al., 2004). KCC4 expression in the brain is also developmentally regulated, but in the opposite direction to KCC2 (Karadsheh et al., 2004). The KCC4 transcript has been found to be abundant in

the proliferative zone around embryonic day E14.5, and is only found in choroid plexus and epithelial lining the brain and ventricles by P0 (Li et al., 2002). No human disorder has been associated with KCC4. $KCC4^{-/-}$ mice generated by targeted deletion have normal hearing abilities until P14, when hearing begins to deteriorate. The mice lose all hearing ability after P21 (Boettger et al., 2002). KCC4 is thought to absorb K^+ ions from the fluid around the outer hair cells into the supporting Deiters' cells, thus moving K^+ into the gap junction pathway. KCC4 therefore participates in the K^+ recycling pathway of the inner ear. KCC4 is also responsible for the Cl^- extrusion across the basolateral membrane of acid-secreting ∝-intercalated cells in the kidney. Disruption of this function in $KCC4^{-/-}$ mice results in (Boettger et al., 2002). Unlike other KCCs, KCC4 shows a very low affinity for the loop diuretics bumetanide and furosemide (~ 900 μM for both) (Mercado et al., 2000b).

Regulation of cation-chloride cotransporters

Cation-chloride cotransporters are regulated by a variety of stimuli, including osmotic, oxidative, hormonal, etc. All signaling pathways leading to cation-chloride cotransporter regulation seem to converge to the final phosphorylation or dephosphorylation of the transport protein. For the K-Cl cotransporters, dephosphorylation stimulates transport activity, whereas phosphorylation reduces transport activity (Adragna et al., 2004; Di Fulvio et al., 2001; Gamba, 2005b; Jennings and Schultz, 1991; Lauf, 1985; Lauf et al., 1992; Mercado et al., 2000a; Starke and Jennings, 1993). For the Na-K-2Cl cotransporter,

it is phosphorylation that activates transport, whereas dephosphorylation results into cotransporter inactivation. A variety of protein kinases have been shown to be involved in the regulation of cation-chloride cotransporters; including PKA (Kurihara et al., 2002), PKC (Kurihara et al., 2002), and PKG (Di Fulvio et al., 2001; Selvaraja et al., 2000). Whether or not these protein kinases directly phosphorylate the transporters is unknown. Recently, mutations found in WNK1 and WNK4 have been shown to induce PHA2 (pseudohypoaldosteronism type II), an autosomal-dominant syndrome of hypertension with hyperkalemia and metabolic acidosis (Wilson et al., 2001). This discovery led to the demonstration that WNK (With No Lysine) kinases regulate the trafficking of NCC to the apical membrane of the distal convoluted tubule (Cai et al., 2006). Mutations in the carboxyl-terminus of the kinases led to increased insertion of transporters in the membrane, resulting in increased salt reabsorption and hypertension. Recent studies also showed that WNK3 and WNK4 inhibit the activities of all KCCs (Garzon-Muvdi et al., 2007; Kahle et al., 2006). WNK3, when co-expressed with either NCC, NKCC1 or NKCC2, resulted in a significant activation of these cotransporters in flux experiments (Kahle et al., 2005). These effects are also seen in hypotonic condition in which NCC, NKCC1 and NKCC2 are normally dephosphorylated and inhibited. On the other hand, co-expression of WNK3 and KCCs results in complete inhibition even in hypotonicity. Interestingly, a kinase-inactive mutant of WNK3 (KI-WNK3) had the opposite effect on all cation-chloride cotransporters. When co-expressed, the catalytically inactive kinase dephosphorylates and inhibits KCCs, and activates NKCCs. The activation of KCCs by

KI-WNK3 is reversed by PP1 inhibitor calyculin A and PP2B inhibitor cyclosporine A. These results imply that instead of being a volume sensor kinase, WNK3 regulates the cotransporters through its interaction with protein phosphatases (de Los Heros et al., 2006). WNK3 likely phosphorylates the protein phosphatase and inhibits it, resulting in increased NKCC activity and reduced KCC activity. It can be concluded that WNK3 affects cell volume through reciprocal regulation of NKCCs and KCCs (**Figure 1-4**) and keeps a balance between the net transport of KCCs and NKCCs. The expression of WNK3 co-localizes with the cation-chloride cotransporters NKCC1 and KCC2 in hippocampal, cerebellar, and cortical GABAergic neurons. Interestingly, expression of WNK3 is also developmentally regulated in a pattern nearly identical to that of KCC2: low at birth and gradually up-regulated during postnatal development. Since KCC2 is responsible for the developmental down-regulation of intracellular chloride and the subsequent switch of GABA responses from excitatory to inhibitory, WNK3 could be an important modulator of the developmental GABA switch (Kahle et al., 2005).

Our laboratory also demonstrated the first direct interaction between a kinase and the cation-chloride cotransporters NKCC1, NKCC2, and KCC3. Indeed, the N-terminal tail of the cotransporters possesses one or two anchoring sites for the Ste20p-related serine/threonine kinases SPAK (Ste20-related, proline alanine-rich kinase), and OSR1 (oxidative stress kinase 1). SPAK, also known as PASK and STK39, has homologues in *Drosophila* (*Fray)*, and *C. elegans (Gck-3).*

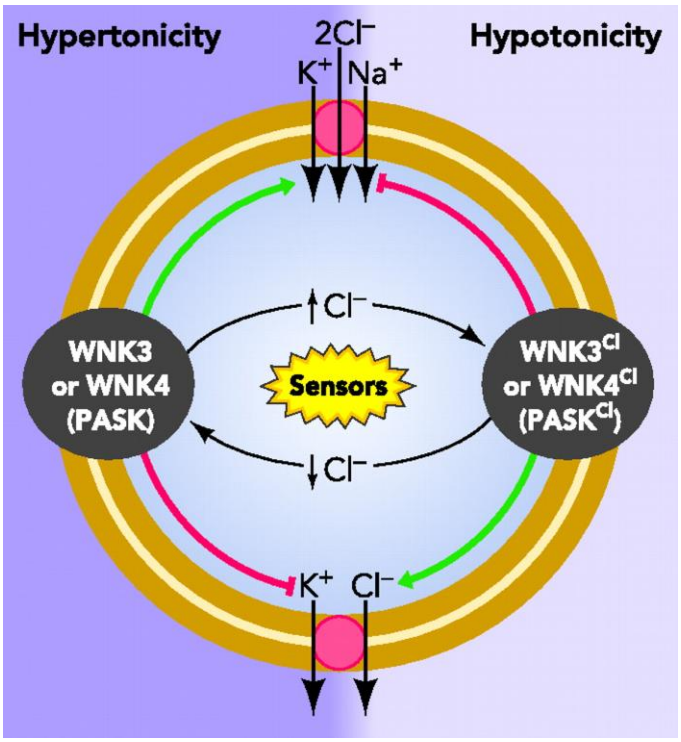

Kahle KT et. al., Physiology 2006

Figure 1-4. WNK kinases regulate cation-chloride cotransporters through inhibition of protein phosphatase in a signaling cascade.

WNK4 phosphorylates and activates SPAK under low intracellular Cl^- or cell swelling, which in turn phosphorylates the cotransporters. WNK3 is proposed to act as an intracellular Cl^-/cell volume sensor, inhibiting protein phosphates by phosphorylating them. The activation of both WNK4 and WNK3 results in a net increase of phosphorylation level of the cotransporters. Phosphorylation results in NKCC1 activation and KCC2 inhibition. High intracellular Cl^- would result in the opposite effect, the activation of KCC2 and inhibition of NKCC1.

SPAK and OSR1 were found to interact with the NKCC1 N-terminus in the yeast-two-hybrid assays (Piechotta et al., 2003). SPAK is also found to interact with several other proteins including the MAPK p38, gelsolin, heat shock protein 105, apoptosis-associated tyrosine kinase (AATYK), and WNK4 (Piechotta et al., 2003). When overexpressed, a dominant-negative form of SPAK inhibited 70% of the NKCC1 transport in HEK cells, while wild type SPAK only increased NKCC1 activity by 10% (Dowd and Forbush, 2003; Gagnon et al., 2006a; Kahle et al., 2005). SPAK is also sensitive to intracellular Cl^- concentration (Gagnon et al., 2006b). Our laboratory has also demonstrated that co-expression of WNK4 and SPAK, but neither WNK4 nor SPAK alone, is required to activate NKCC1 activity or inhibit KCC2 activity (Gagnon et al., 2006a). It was later demonstrated that WNK4 phosphorylates and activates SPAK, and phosphorylated SPAK in turn phosphorylates the N-terminus of NKCC1, turning NKCC1 into its activated state (Gagnon et al., 2006a; Moriguchi et al., 2006; Vitari et al., 2005). It is very likely that WNKs and Ste20-type kinases are components of a signaling complex, which regulate NKCCs and KCCs via phosphorylation/ dephosphorylation (**Figure 1-5**).

Role of KCC2 in neurons

During synaptic transmission and propagation of the action potential, the electrochemical driving force for Cl^- ions varies significantly in neurons as the membrane potential fluctuates. Provided that passive pathways for Cl^- movement across the plasma

membrane exist, changes in membrane potential will tend to affect the Cl^- concentration. In addition, both $GABA_A$ and glycine receptors contain intrinsic Cl^- channels, and during activation of these receptors, Cl^- ions flow across neuronal membranes. The mechanisms regulating intracellular Cl^- concentrations in neurons are not fully understood. Cl^- is rarely distributed passively across the plasma membrane, and thus maintenance of its concentration requires consumption of energy. After maturation, CNS neurons exhibit a Cl^- concentration that is lower than electrochemical potential equilibrium, due to an active Cl^- transport mechanism responsible for extruding Cl^- from the neuron.

Already in the second part of the 1980s, there were indications that a K^+-dependent and furosemide-sensitive K-Cl cotransporter was responsible for maintaining intracellular Cl- below equilibrium (Misgeld et al., 1986; Thompson et al., 1988). Thompson et al also found that repetitive stimulation of $GABA_A$ receptors reduces the driving force of the IPSP (Thompson and Gahwiler, 1989a; Thompson and Gahwiler, 1989b). In 1996, a neuronal-specific isoform of K-Cl cotransporters, KCC2, was cloned and its function was characterized (Payne et al., 1996). Expression of KCC2 in the CNS follows very precise spatial and temporal patterns. The global expression of KCC2 is low at birth and increases gradually during postnatal development (Clayton et al., 1998; Lu et al., 1999). This timeline of KCC2 expression coincides with a decrease in the intracellular Cl^- concentration and the well-known switch of GABA and glycine responses from excitatory to inhibitory during postnatal development (DeFazio et al., 2000; Owens et al., 1996; Stein et al., 2004). KCC2 expression also follows an interesting differential pattern

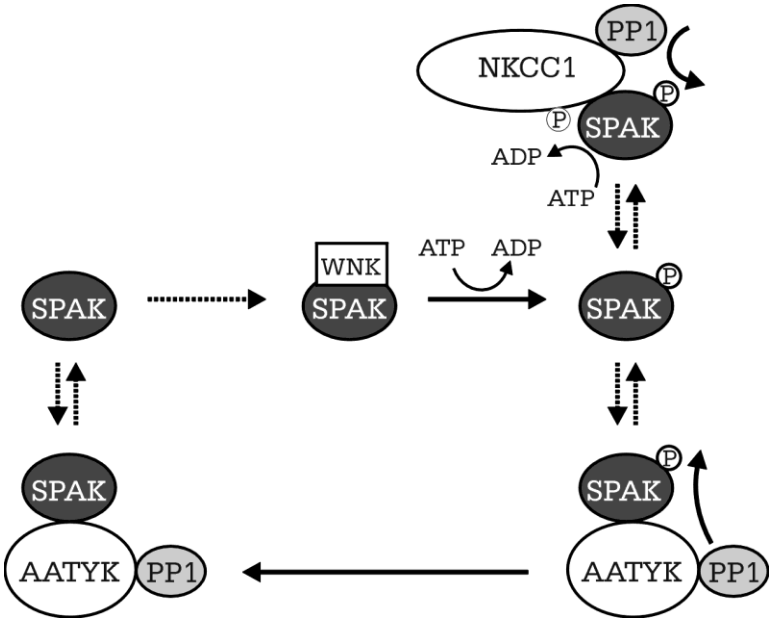

from Gagnon et al, Am. J. Physiol. 2007

Figure 1-5. Model of NKCC1 regulation by the STE20 kinase SPAK.

SPAK and OSR1 anchor to the N-terminus of the cotransporter and phosphorylate specific threonine residues located downstream of the binding site. For its catalytic activity, SPAK needs to be activated by an upstream kinase (WNK1 or WNK4). SPAK inactivation is mediated by PP1. PP1 dephosphorylation of SPAK is mediated through a scaffold protein such as AATYK.

from rostral to caudal with high expression at birth in the brainstem and extremely low expression in forebrain structures such as hippocampus and cerebral cortex (Balakrishnan et al., 2003; Kanaka et al., 2001; Li et al., 2002; Mikawa et al., 2002; Wang et al., 2002). KCC2 also shows different spatial expression patterns between different cell types in rat motorneurons (Ueno et al., 2002), rat substantia nigra (Gulacsi et al., 2003), rat visual system (Ikeda et al., 2003), thalamus (Bartho et al., 2004) and olfactory bulb (Wang et al., 2005). For example, in the rat retina KCC2 colocalizes with neurons that express $GABA_A$ receptors and temporally different expression patterns were found between the inner retina and outer plexiform layer (Vu et al., 2000). Studies have shown that KCC2 is highly expressed in the vicinity of excitatory inputs in the hippocampus, possibly to provide fast Cl^- extrusion to negate rapid Cl^- rises in small subcellular compartments (Gulyas et al., 2001).

Due to the lack of specific inhibitors, genetic modification of KCC2 provides a crucial tool to study KCC2. Knock-down of KCC2 expression by anti-sense RNA in hippocampal slice cultures revealed a positive shift in the GABA reversal potential (Rivera et al., 1999). The full knockout of KCC2 by targeted deletion of exon 5 of the KCC2 gene caused immediate death upon birth due to motor deficits and respiratory arrest, possibly due to the disrupted Cl^- homeostasis in brainstem (Hubner et al., 2001). A targeted deletion of the first exon of KCC2 gene was generated in our lab. Homozygous mice showed frequent generalized seizures and died at about two weeks after birth (Woo

et al., 2002). Interestingly, 5 percent of the total KCC2 protein still persisted in the brain of homozygous mice and thus these mice are hypomorphs instead of full knockouts.

Although KCCs are regulated by phosphorylation/dephosphorylation in heterologous expression systems, not much is known about the signaling pathways that regulate KCC2 in neurons. It has been proposed that the postnatal increase of KCC2 expression is "nurtured" by the excitatory action of GABA in the young brain (Ben-Ari, 2002; Ganguly et al., 2001; Leitch et al., 2005), while later evidence argues against it(Ludwig et al., 2003; Titz et al., 2003). Reciprocally, overexpression of KCC2 by transgenic methods in young neurons induces a earlier switch of GABA response from depolarizing to hyperpolarizing (Lee et al., 1998) and even an augmentation of the functional GABA synapses (Chudotvorova et al., 2005). In the adult brain, the expression of KCC2 is altered by various insults to the brain. Recent studies indicate that ischemia, oxidative stress, epileptic seizures, and other types of neuronal injury cause a downregulation of KCC2 mRNA and protein (Bonislawski et al., 2007; Galeffi et al., 2004; Nabekura et al., 2002; Okabe et al., 2003; Rivera et al., 2004; Toyoda et al., 2003; Wake et al., 2007). Plasmalemmal KCC2 has a high turnover rate (Rivera et al., 2004) and repetitive neuronal stimuli result in a downregulation of KCC2 mRNA, which is often preceded by increased intracellular Ca^{2+} (Fiumelli et al., 2005). Trophic factors (BDNF and IGF) and sex hormones also contribute to the regulation of KCC2. IGF is believed to activate the inactive form of KCC2 and reduce the intracellular Cl^- (Kelsch et al., 2001), while BDNF was found to either increase or decrease the expression of KCC2 (Aguado et al., 2003;

Rivera et al., 2002; Rivera et al., 2004). Epileptic seizures have a higher occurrence in males than in females (Galanopoulou, 2005). Studies have found that testosterone down-regulates the expression of KCC2 in the developing substantia nigra (Galanopoulou, 2005; Galanopoulou, 2006; Galanopoulou et al., 2003; Veliskova et al., 2004) and the developing thalamus (Perrot-Sinal et al., 2007). KCC2 is also found to be involved in pain (Coull et al., 2003; Mantyh and Hunt, 2004; Morales-Aza et al., 2004; Price et al., 2005). Peripheral nerve injury causes a trans-synaptic reduction of KCC2 expression and consequent disruption of anion homeostasis in neurons of lamina I of the superficial dorsal horn, resulting in a lowered nociceptive threshold (Coull et al., 2003).

The expression pattern of KCC2 during development (Clayton et al., 1998; Lu et al., 1999; Rivera et al., 1999) and the phenotype of the KCC2 knockout (Hubner et al., 2001) and knockdown mice (Woo et al., 2002) are all consistent with the important role the cotransporter plays in supporting GABA and glycine hyperpolarizing responses. With the exception of one study that used anti-sense KCC2 oligonucleotides to decrease KCC2 expression and affect E_{GABA} (Rivera et al., 1999), demonstration of the role of KCC2 as a major Cl^- regulator in neurons comes mainly from the use of furosemide, an inhibitor of the cotransporter. However, as the loop diuretic lacks specificity, there is a serious need for additional evidence of the role of KCC2 in Cl- regulation in mature central neurons.

Role of NKCC1 in neurons

Some neurons, mostly notably adult sensory neurons that exhibit depolarizing GABA responses, have an intracellular Cl^- concentration that is much higher than adult level. These high Cl^- levels are maintained by strong Na-K-2Cl cotransport activity (Alvarez-Leefmans et al., 1988; Rohrbough and Spitzer, 1996; Sung et al., 2000). In contrast to sensory neurons which keep a high Cl^- concentration throughout adulthood, central neurons show high Cl^- levels only during development from E15-E17 in the ventricular zone (LoTurco et al., 1995; Owens et al., 1996) to postnatal days P1-P7 (Ehrlich et al., 1999; Owens et al., 1996). These high Cl^- levels are consistent with the depolarizing GABA responses that were measured in immature neurons (Ben-Ari et al., 1989; Janigro and Schwartzkroin, 1988; Luhmann and Prince, 1991; Mueller et al., 1983; Muller, 1989). LoTurco et al. (LoTurco et al., 1995) demonstrated that GABA depolarization in embryonic ventricular zone neurons was related to a furosemide-sensitive Cl^- transport process. This process is consistent with an inward Na-K-2Cl cotransporter. Expression of NKCC1, a widely expressed Na-K-2Cl cotransporter, has been demonstrated in immature neurons (Plotkin et al., 1997a) and shown to decrease with neuronal maturation (Plotkin et al., 1997b). NKCC1 is activated by the decrease of intracellular Cl^- following $GABA_A$ receptor activation in cultured cortical neurons and serves as a positive feedback mechanism for maintaining high intracellular chloride concentration (Schomberg et al., 2003). A Ca^{2+} activated Cl^- current in olfactory receptor neurons is abolished in NKCC1 deficient mice, which also indicates

that NKCC1 plays a role in neuronal Cl^- accumulation (Reisert et al., 2005). Since increased intracellular Cl^- means less GABA inhibition, NKCC1 may play roles in epileptogenesis. The role of NKCC1 in epileptic seizure has been recently studied. Abnormally high expression of NKCC1 was found in epileptic tissues from both human and rodents (Aronica et al., 2007; Okabe et al., 2003; Palma et al., 2006; Sen et al., 2007). This anomalous expression of NKCC1 was suspected to contribute to excitatory GABA actions in the epileptic brain. Dzhala and colleagues found that inhibiting NKCC1 with bumetanide or targeted deletion of NKCC1 reduced epileptic activities induced by high $[K^+]_o$ in the developing brain (Dzhala et al., 2005). They concluded that NKCC1 facilitates epileptic seizure in the developing brain.

Hypotheses and Specific Aims

Hypothesis I

A neuron is a confined compartment consisting of the soma, the dendrites and the axons. $GABA_A$ receptors are expressed on most of the neurons and they are one of the pathways for Cl^- ions to enter or exit the neuron. Activation of $GABA_A$ receptor induces either influx (hyperpolarizing action) or efflux (depolarizing action) of Cl^- ion and causes the redistribution of Cl^- across the plasma membrane (Ehrlich et al., 1999). Without a transport system, the intracellular Cl^- would be fluctuating with the membrane potential. Although it was proposed that KCC2 maintains a low intracellular Cl^- concentration and is responsible for hyperpolarizing GABA response, most of the work is based on the effect of furosemide, an inhibitor of KCC2 with unspecific effects on other KCC isoforms (Ki = 40 μM, 25 μM, and 40 μM for KCC1, KCC2 and KCC3, respectively), and other Cl^- transport proteins (see Chapter 1). The generation of $KCC2^{-/-}$ mice in the laboratory provided an excellent opportunity to study with specificity how KCC2 regulates intracellular chloride in neurons. **Here, I hypothesize that KCC2 is responsible for driving and maintaining low intracellular chloride levels in mature neurons. I also hypothesize that KCC2 is active in maintaining/regulating intracellular chloride when its concentration is under various acute challenges.** This hypothesis will be addressed by the following specific aims:

Specific Aim I: To determine the intracellular Cl^- concentration by measuring E_{GABA} (E_{Cl}) at different time points using cultured cortical neurons isolated from wild type and $KCC2^{-/-}$ mice,

Specific Aim II: To measure the changes in E_{GABA} (or E_{Cl}) after challenging the intracellular Cl^- concentration in wild-type and $KCC2^{-/-}$ neurons. This will be achieved by lowering the extracellular K^+ concentration, prolonging the application of GABA and depolarizing the membrane potential, and measuring the recovery of internal Cl^-.

Hypothesis II

GABA inhibition is critical in maintaining the stability of the neuronal network, and reduced GABA inhibition is a critical factor in the development of epileptic seizures. Therefore, as regulators of intracellular Cl^-, the cation-chloride cotransporters are likely important players in the stability of neuronal networks and important players in preventing or promoting seizure susceptibility. As KCC2 decreases neuronal Cl^-, it protects the brain from hyperexcitability and from the development of epileptic seizures. Thus, reduction of the cotransporter expression is likely to result in increased neuronal network excitability and increased susceptibility to seizure. As homozygous mice with targeted deletion of KCC2 have severe developmental problems and die early during postnatal development, they do not constitute a useful model to study the role of KCC2 in CNS hyperexcitability. In contrast, $KCC2^{+/-}$ mice, by expressing half the amount of KCC2 protein in the brain, are viable and exhibit increased susceptibility to behavioral

seizure induced by pentylenetrazol (PTZ), as shown in a previous publication from our laboratory (Woo et al., 2002).

As discussed in Chapter 1, the role of NKCC1 in neuronal Cl^- accumulation and network stability is still a matter of controversy. In P2-P4 cortical and hippocampal neurons, bumetanide produces a hyperpolarizing shift in E_{GABA} of pyramidal neurons (Sipila et al., 2006; Yamada et al., 2004) and increased seizure activity in a high K^+ seizure model (Dzhala et al., 2005). In contrast, in auditory brainstem neurons (Balakrishnan et al., 2003) and retinal neurons (Zhang et al., 2007), intracellular [Cl^-] remains high in the absence of NKCC1. As NKCC1 is not only expressed in neurons, but also in glial cells (Aronica et al., 2007; Mikawa et al., 2002; Su et al., 2002b), the cotransporter might play additional roles pertinent to brain excitability. For instance, the cotransporter might serve as a clearance route for excess K^+ in the extracellular space during elevated neuronal firing and thus prevent hyperexcitability. Therefore, **I hypothesize that KCC2 dampens network excitability and therefore reduces seizure susceptibility in the brain. I also hypothesize that through a mechanism independent of Cl- regulation in the pyramidal neurons, NKCC1 also prevents hyperexcitability in the brain.** These hypotheses will be addressed through the following two specific aims.

Specific Aim III: To demonstrate that KCC2 prevents hyperexcitability in the brain. This will be achieved by recording the network activity and seizure susceptibility to 4-aminopyridine in the hippocampus of wild-type and $KCC2^{+/-}$ slices.

Specific Aim IV: To demonstrate that NKCC1 does not accumulate Cl- in young CA3 pyramidal neurons, but prevents hyperexcitability of the hippocampal network. This will be achieved by recording the spontaneous activity of CA3 pyramidal neurons and seizure susceptibility to 4-aminopyridine in the hippocampus of wild type and $NKCC1^{-/-}$ slices, and by measuring the direction and amplitude of muscimol-induced responses in both genotypes before and after application of 4-AP**.**

CHAPTER II

MATERIALS AND METHODS

Animals

Mice used in these experiments were housed in micro-isolators in a standard animal care facility with a 12h light/dark cycle, and free access to food and water. All procedures were approved by the Vanderbilt University Animal Care and Use Committee, in agreement with the guidelines of the National Institutes of Health Guide for the Care and Use of Laboratory Animals.

Tail clips and genotyping

Due to the early postnatal lethality of the $KCC2^{-/-}$ knockdown animals (Woo et al., 2002), wild-type, heterozygote, and homozygote mice were generated from heterozygote $KCC2^{+/-}$ matings. Genotyping was performed by clipping 1 mm of the tail of newborn (P0-P1) or P15 pups (from $KCC2^{+/-}$ parents), and from P8 pups (from $NKCC1^{+/-}$ parents). The tail clip was treated with 200 μl solution containing 25 mM NaOH, 0.2 mM EDTA, pH ~ 12 for 20 min at 95^{o}C. The sample was neutralized by the addition of 200 μl solution containing 40 mM Tris-HCl, pH ~ 5. After mixing, the digested tail sample was centrifuged for 6 min at 14,000 rpm and 200 μl of supernatant was collected for genotyping. Separate polymerase chain reactions were performed on 1-2 μl tail DNA to

amplify fragments specific to the KCC2 control and KCC2 mutant genes. For KCC2, the oligonucleotide primers for the control gene were: forward 5’ AGCGTGTGTCCGTGTG CGAGTG 3' and reverse 5' TTGTTGAGCATGGTGGC TGCGC 3' oligonucleotide primers. To amplify the mutant gene, I used the same forward primer and reverse 5'-CCAGAGGCCACTTGTGTAGCGC 3' primer. The reactions generate fragments of 207 and 204 bp, respectively. For NKCC1, the primers for the control gene were: forward 5’ TATCTCAGGTGATCTTGC 3' and reverse 5' ACACTGCAATTCCTATGTAAACC 3'; and for the mutant gene: forward 5’ TGCAACTGGTATTCTAGCTGGAGC 3’ and reverse 5’ TACAACACACACTCCAACCTCCG 3’. In this case, the sizes of the fragments are 184 bp and 497 bp, respectively.

Cortical neuronal cultures

Mouse cortical neurons were grown in dissociated cultures according to the method of Huettner and Baughman (Huettner and Baughman, 1986) with modifications. Briefly, cortices from wild-type $KCC2^{+/+}$, heterozygotes $KCC2^{+/-}$, and homozygotes $KCC2^{-/-}$ mouse brains were isolated at postnatal days 0 or 1, and the meninges were removed. Cortices were then cut into small pieces and incubated in 5 ml solution containing 100 U papain, 1 mM L-cysteine, 0.5 mM EDTA, 500 U DNase1 in Earle’s balanced buffered solution (EBSS) for 60-90 min at 37^{o}C. Following digestion, the tissue was rinsed briefly in EBSS containing 1 mg/ml trypsin inhibitor, 100 U/ml DNase1 and 1 mg/ml BSA, then triturated gently in MEM without serum. Cortical neurons were further purified by

centrifugation for 6 min at 70g, room temperature through a density gradient consisting of 10 mg/ml trypsin and 10 mg/ml BSA in 5 ml EBSS. The cell pellet was then resuspended in MEM without serum, counted, and plated at a density of 15,000-40,000 cells on glial feeder layers consisting of growth-arrested rat astrocytes grown on 0.1 mg/ml poly-D-lysine and 33 μg/ml laminin in 35-mm glass bottom dishes. After 3 hours, 1.5 ml conditioned growth medium was added to the dishes. The conditioned growth medium consists of MEM supplemented with 20 mM glucose, 0.5 mM glutamine, 5% fetal bovine serum, 50 U/ml penicillin G, and 50 μg/ml streptomycin and conditioned by cortical astrocytes as previously described (Baughman et al., 1991). The cultures were kept up to 21 days in 5% CO_2, 37^{o}C, and fed once a week with 1.5 ml conditioned growth medium.

Immunostaining

Cells were washed with PBS and fixed for 30 min in 2% paraformaldehyde. After fixation, the cell membranes were permeabilized with 0.075% saponin in PBS for 10 min at room temperature (RT), followed by blocking with 0.2% BSA/saponin/PBS for 30 min at RT. Rabbit polyclonal anti-KCC2 antibody (Lu et al., 1999) was diluted 1:200 in BSA/saponin/PBS and incubated with the cells for 1 hour at RT. Following several washes in BSA/saponin/PBS, the cells were incubated with goat anti-rabbit immunoglobulin G (Jackson Immunoresearch, West Grove, PA) at a dilution of 1:800 for 1 hour at RT, and then washed several times with BSA/saponin/BSA. For double-staining

experiments, cells were incubated successively with anti-KCC2 antibody for 1 hour, followed by cy3-conjugated secondary antibody and then with monoclonal anti-MAP2 (microtubule associated protein-2, clone AP20, Roche, Indianapolis, IN), 1 hour at RT, followed by FITC-conjugated anti-mouse immunoglobulin G. Fluorescence signal was visualized using a Zeiss Axiovert S100 microscope equipped with a Photometrics Coolsnap^{Cf} CCD camera (Roper Scientific, Tucson, AZ) connected to a G4 Apple computer.

HPLC analysis

The concentration of GABA in the culture medium was assayed by HPLC. To obtain the fluorescent derivatives, 10 μl samples were added to 70 μl of borate buffer and 20 μl 6-aminoquinol-N-hydroxysuccinimidyl carbamate solution (both from AccQ-Tag Chemistry Package kit, WAT052875, Waters, Milford MA). After heating the mixture for 10 minutes at 37°C, 10 μl of labeled samples were injected into the HPLC system consisting of a Waters 712 autosampler, two 510 HPLC pumps, a column heater (37^{o}C) and a Waters 474 scanning fluorescence detector. Separation of the amino acids was accomplished using a Waters amino acid column and supplied buffers (buffer A: 19% sodium acetate, 7% phosphoric acid, 2% triethylamine, 72% water; buffer B: 60% acetonitrile), using a specific gradient profile. HPLC control and data acquisition was managed by Millennium 32 software. Using this HPLC solvent system, the following amino acids elute in the following order: cysteine, homocystetine, aspartic acid, serine,

glutamate, glycine, taurine arginine, threonine, alanine, proline, GABA, cystine, tyrosine, valine, methionine, lysine, isoleucine, leucine, and phenlyalanine. Calibration was obtained by running daily calibration curves, consisting of known concentrations of each amino acid (10 pmole/μl – 100 pmole/μl) to which the internal standard (γ-aminobutyric acid, 250 pmol/μl) was added. Peak height of each amino acid was compared to that of the internal standard.

Brain Slice Preparation

Brain slices were prepared from P9-P13 $NKCC1^{+/+}$ and $NKCC1^{-/-}$ mice and P19-P25 $KCC2^{+/+}$ and $KCC2^{+/-}$ mice. Animals were anesthetized with isoflurane and decapitated. Following the dissection of the skull, the brain was rapidly removed and immersed in oxygenated (95%O_2 / 5%CO_2) ice-cold high sucrose/high magnesium cutting solution of the following composition (in mM): sucrose 248, KCl 2.8, $MgSO_4$ 2.0, $MgCl_2$ 6.0, $NaHCO_3$ 26, NaH_2PO_4 1.25, glucose 10 (PH 7.4) for less than 30 seconds. The brain was quickly lifted and glued onto a 4% agar block, which was attached to a pre-chilled cutting stage. The stage was then mounted onto a vibratome (Vibratome, St. Louis, MO), and the cutting chamber was filled with oxygenated ice-cold cutting solution. Hippocampal transverse slices of 350-400 μm were cut and transferred to 37^{o}C oxygenated artificial cerebral spinal fluid (aCSF) containing (in mM): NaCl 124, KCl 2.8, CaCl2 2, $MgCl_2$ 1, $NaHCO_3$ 26, NaH_2PO_4 1.25, glucose 10. After 30 minutes incubation, the slices were

gently transferred into room temperature oxygenated aCSF and kept for at least one hour before use.

Western Blot

Wild-type mice of different ages were anesthetized, decapitated, and 500 μm brain slices were prepared following the procedure described above. Slices were then placed on an ice-cold metallic block and 0.41 mm tissue punches were taken from CA1 and CA3 hippocampus using a tissue puncher (VWR Scientific, West Chester, PA). A small volume of lysis buffer containing 150 mM NaCl, 1 mM EDTA, 10 mM TrisCl, pH 7.4, and 1 complete minitablet/10 ml protease inhibitors (Roche Applied Science, Indianapolis, IN) were added to the slices and the samples were homogenized using a Kontes pellet pestle grinder (VWR Scientific). Protein concentrations were quantitated using a standard Bradford assay (Biorad, Hercules, CA). Protein samples were then denatured in SDS-PAGE loading buffer at 75°C for 20 min and separated on a 7.5% polyacrylamide gel. Proteins were then transferred from the gels onto polyvinylidine fluoride membranes (BioRad), and the membranes blocked for 2 h at room temperature (RT) in TBST (NaCl, 150 mM; Tris-Cl, 10mM, pH 8.0, Tween 20 [polyoxyethylene-sorbitan monolaurate], 0.5%) supplemented with 5% non-fat dry milk. Membranes were then incubated with anti-KCC2 (Lu et al., 1999) or anti-transferrin receptor (Invitrogen, Carlsbad, CA) primary antibodies at 1:1000 dilution in blocking solution at 4°C overnight. Following extensive TBST washes, membranes were incubated

in horseradish peroxidase-conjugated anti-rabbit (KCC2) or anti-mouse (TR) secondary antibodies in blocking solution (1:4000; Jackson Immunoresearch, West Grove, PA) for 1 h at RT, and then rinsed for 2 h in TBST. Finally, protein bands detected by antibodies were visualized by chemiluminescence using ECL Plus (Amersham Biosciences, Arlington Heights, IL).

Electrophysiology—Cultured cortical neurons

Electrophysiological responses of cultured cortical pyramidal neurons were recorded at room temperature using the gramicidin perforated-patch whole cell recording technique with an Axopatch 200 amplifier (Axon Instruments, Foster City, CA) and pCLAMP 8.2 software (Axon Instruments). A 35-mm culture dish of cultured cortical neurons was placed onto an inverted microscope and an external solution was perfused at a rate of 1 ml/min. The external solution contained 150 mM NaCl, 5 mM KCl, 0.5 mM $CaCl_2$, 1 mM $MgCl_2$, 10 mM glucose, 26 mM sucrose, and 10 mM HEPES, pH 7.4. For the low K^+ experiments, the KCl concentration of the external solution was decreased to 1 mM and the NaCl concentration was increased to 154 mM. Pyramidal neurons were identified by their typical morphology under the microscope. Patch pipette electrodes with resistances of 2-4 MΩ were made from borosilicate glass capillaries (World Precision Instruments Inc., Sarasota, FL) using a horizontal pipette puller (Sutter Instruments Co., Novato, CA). The electrodes were first dipped in gramicidin free internal solution consisting of 140 mM KCl, 5 mM EGTA, 10 mM HEPES, pH adjusted to 7.4 using Tris

base, then backfilled with internal solution containing 20-50 μM gramicidin D (Sigma, St. Louis, MO). Gramicidin stock solution (30μg/ml in DMSO) was kept on ice and gramicidin-containing internal solution was made fresh every hour to maintain the activity of the ionophore. After the formation of a tight seal, the progress of gramicidin perforation was evaluated by following the series resistance. Recordings started after the series resistance stabilized (15-40 MΩ). Whole cell capacitance (5-30 pF) was compensated before recording. Recordings were low pass filtered at 2 KHz. Drugs were dissolved in external solution and delivered using a 3-barrel SF-77B stepper motor-driven system (Warner Instruments Co., Hamden, CT) controlled by pClamp 8.2.

The chloride equilibrium potential was estimated from the reversal potential observed during activation of $GABA_A$ receptors ($E_{Cl} = E_{GABA}$). Reversal potentials were recorded using a voltage ramp protocol consisting of a step to -80 mV for 50 milliseconds, followed by a voltage ramp to -20 mV at a rate of 300 mV/sec. At this rate, the current through the membrane capacitance is negligible. The error in E_{GABA} caused by the series resistance was corrected using the following calculation: $E_{GABA} = E_{GABA0} - (E_{GABA0}-E_m) * R_s/(R_{input1}-R_{input2})$ (where R_s is the series resistance; R_{input1} and R_{input2} are the input resistance with and without GABA application, respectively; E_m is the resting membrane potential; E_{GABA0} the original reversal potential recorded by ramp). Series resistance was compensated by 70-80% in recordings other than voltage ramps.

After each perforated patch recording, additional negative pressure was applied to the pipette in order to break the membrane patch under the pipette tip and obtain the whole

cell configuration. E_{GABA} was recorded with voltage clamp at different potentials. The value was always measured around 0 mV, indicating absence of voltage drift during the recording. The intracellular chloride ion activity was calculated using the *Nernst* equation: $E_{Cl} = RT/F*\ln(aCl_i/aCl_o)$, where R is the gas constant, T is the absolute temperature and F is the Faraday constant (96485.309 C/mol). The extracellular Cl^- activity is $aCl_o = \gamma[Cl]_o$, where γ is the activity coefficient calculated using the Extended Debye-Hückel equation (Harris, 2003). To block voltage-dependent Na^+ currents, all experiments were performed in the presence of 0.3 μM tetrodotoxin (Alomone Labs, Jerusalem, Israel). Furosemide (Sigma, St. Louis, MO) was used at a concentration of 1 mM.

Electrophysiology—Brain slices

All electrophysiological experiments were performed at 29-30^oC in a submerged chamber perfused with oxygenated aCSF. All data were filtered by Bessel filter (0.1-2000Hz), amplified by multiclamp 700B and analyzed by pCLAMP 9.0 (Axon Instruments, Foster City, CA). For extracellular recordings, 4-6 MOhm pipettes pulled from thin wall Borosilicate glass capillaries (World Precision Instruments, Sarasota, Fl) were filled with normal aCSF. The tip of the recording pipette was placed in the *stratum pyramidale* of CA3. For cell-attached experiments, the whole tip (from beginning to the end of taper) of the glass pipette (2-4 MOhm) was filled with gramicidin-free pipette solution containing (in mM): KCl 140, HEPES 10, pH 7.2. Then, the pipette was backfilled with pipette solution containing less than 5 μg/ml gramicidin D (Sigma, St Louis, MO). Gramicidin

was use to reduce R_{patch} (See Appendix A) to a value much lower than the value for conventional cell-attached mode (Perkins, 2006). With low gramicidin, the series resistance drops to less than 200MOhm in a few minutes and $V_{pipette}$ reaches a value very close to the resting membrane potential (-65 to -75 mV). All recordings were done in current clamp mode with holding current set at 0, so that no artificial current is injected into the neuron from the headstage. Bumetanide (10 μl) was applied to the aCSF perfusing the slice from a stock in DMSO to reach a final concentration of 10 μM. 4-aminopyridine (Sigma, St. Louis, MO) was used at a final concentration of 50 μM in aCSF. Power spectrum analysis was done in Prism 3.0 (Graphpad Software, San Diego, CA).

CHAPTER III

CORTICAL NEURONS LACKING KCC2 EXPRESSION SHOW IMPAIRED REGULATION OF INTRACELLULAR CHLORIDE

Introduction

During synaptic transmission and propagation of the action potential, the electrochemical driving force for Cl^- ions varies significantly in neurons as the membrane potential fluctuates. Provided that passive pathways for Cl^- movement across the plasma membrane exist, changes in membrane potential will tend to affect the Cl^- concentration. In addition, both $GABA_A$ and glycine receptors contain intrinsic Cl^- channels, and during activation of these receptors, Cl^- ions flow across neuronal membranes. The mechanisms regulating intracellular Cl^- concentrations in neurons are not fully understood. Cl^- is rarely distributed passively across the plasma membrane, and thus maintenance of its concentration requires consumption of energy.

The Cl^- concentration could be maintained by secondary active transporters which are mechanisms that use the energy of ion gradients set by other enzymes such as carbonic anhydrase for the generation of a HCO_3^- gradient and the Na^+/K^+-ATPase for the generation of Na^+ and K^+ gradients. Some neurons, most notably adult sensory neurons that exhibit depolarizing GABA responses, have an internal Cl^- concentration much higher than electrochemical potential equilibrium. These high Cl^- levels are maintained by a strong Na-K-2Cl cotransport activity (Alvarez-Leefmans et al., 1988; Rohrbough

and Spitzer, 1996; Sung et al., 2000). In contrast to sensory neurons which keep a high Cl^- concentration throughout adulthood, central neurons show high Cl^- levels only during development ((from E15-E17 in the ventricular zone), (LoTurco et al., 1995; Owens et al., 1996) to postnatal days P1-P7 (Ehrlich et al., 1999; Owens et al., 1996)). These high Cl^- levels are consistent with the depolarizing GABA responses that were measured in immature neurons (Ben-Ari et al., 1989; Janigro and Schwartzkroin, 1988; Luhmann and Prince, 1991; Mueller et al., 1983; Muller, 1989). Lo Turco et al. (1995) demonstrated that GABA depolarization in embryonic ventricular zone neurons was related to a furosemide-sensitive Cl^- transport process. This process is consistent with an inward Na-K-2Cl cotransporter. Expression of NKCC1, a widely expressed Na-K-2Cl cotransporter, has been demonstrated in immature neurons (Plotkin et al., 1997a) and shown to decrease with neuronal maturation (Plotkin et al., 1997b). Further support for the role of NKCC1 in Cl^- accumulation in immature neurons has been provided in recent functional studies (Schomberg et al., 2003).

After maturation, CNS neurons exhibit a Cl^- concentration that is lower than electrochemical potential equilibrium, due to an active Cl^- transport mechanism which is responsible for extruding Cl^- from the neuron. This transporter was shown to be K^+-dependent and furosemide-sensitive, consistent with a K-Cl cotransporter (Misgeld et al., 1986; Thompson et al., 1988). In 1996, a neuronal-specific K-Cl cotransporter, KCC2, was cloned (Payne et al., 1996). The expression pattern of KCC2 during development (Clayton et al., 1998; Lu et al., 1999; Rivera et al., 1999) and the phenotype of the KCC2

knockout (Hubner et al., 2001) and knockdown mice (Woo et al., 2002) are all consistent with the important role the cotransporter plays in supporting GABA and glycine hyperpolarizing responses. With the exception of one study that used anti-sense KCC2 oligonucleotide to decrease KCC2 expression and affect E_{GABA} (Rivera et al., 1999), demonstration of the role of KCC2 as a major Cl^- regulator in neurons comes mainly from the use of furosemide, an inhibitor of the cotransporter. However, as the loop diuretic lacks specificity, there is a serious need for additional evidence of the role of KCC2 in Cl- regulation in mature central neurons.

In this study, I sought to examine the role of KCC2 in controlling and regulating intracellular Cl^- by comparing the reversal potentials of GABAA receptor-mediated Cl- currents in cortical neurons cultured from wild-type and $KCC2^{-/-}$ mice. We show that the normal developmental decrease in $[Cl^-]i$ in neurons is absent in mice lacking KCC2 and also show that active Cl^- regulation is severely impaired in $KCC2^{-/-}$ neurons, strongly supporting the idea that that KCC2 is critical for Cl^- homeostasis in mature cortical neurons.

Results

Disruption of KCC2 expression abolishes the down-regulation of $[Cl^-]_i$ in developing cortical neurons in culture

A postnatal increase in KCC2 expression has been demonstrated in mouse and rat CNS by Northern blot analysis (Lu et al., 1999; Rivera et al., 1999), RNAse protection assay (Clayton et al., 1998; Ganguly et al., 2001), *in situ* hybridization (Balakrishnan et al., 2003; Clayton et al., 1998), RT-PCR (Balakrishnan et al., 2003), Western blot analysis (Lu et al., 1999; Vu et al., 2000), and immunohistochemistry (Lu et al., 1999; Vu et al., 2000). Using the KCC2 specific antibody developed in our laboratory (Lu et al., 1999; Vu et al., 2000), I observed low KCC2 expression in young, immature cortical neurons in culture and high expression levels in older cells (**Figure 3-1A & C**). Immunostaining of cortical neurons in culture reveals punctate KCC2 expression at the cell plasma membrane of both soma (**Figure 3-1C**) and dendritic spines (inset of **Figure 3-1C**). This expression pattern is absent in $KCC2^{-/-}$ cells (**Figure 3-1E**). Neurons at all stages are easily identified by MAP2 staining (**Figure 3-1B, D & F**). The patterns of KCC2 and MAP2 staining are observed in 87% of 284 neurons examined from 2 wild type DIC14 cultures.

The developmental regulation of intracellular Cl^- concentration in cultured wild-type $KCC2^{+/+}$ and homozygous $KCC2^{-/-}$ cortical neurons was followed using gramicidin perforated patch clamp recordings. Because the neurons selected for our electrophysiological recordings were small pyramidal neurons (10-30 pF), only brief

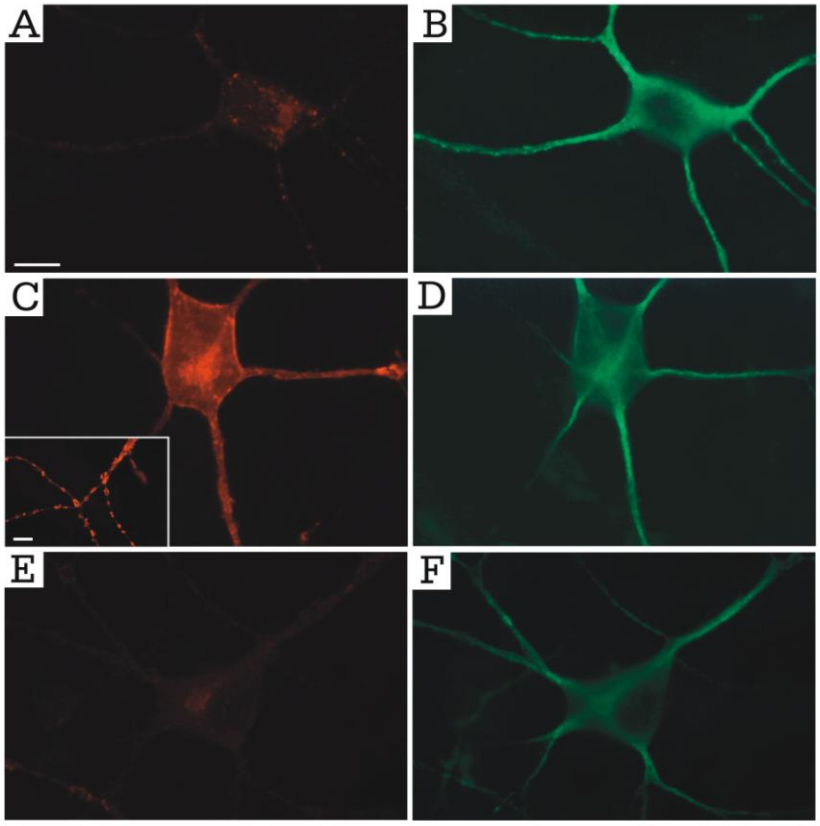

Figure 3-1. Double-immunofluorescence staining showing that the expression of KCC2 protein in cultured cortical neurons is developmentally up-regulated.

(A)Young, DIC 4, pyramidal neuron from cortical neuronal culture is stained with anti-KCC2 antibody. Expression of KCC2 is low, with a punctate pattern at cell soma and dendrites. (C) KCC2 expression is much higher in an older, DIC 10, pyramidal neuron. Intense immunostaining is observed at the soma membrane and dendrites. (Inset) KCC2 signal is concentrated on dendritic spines. (E) Absence of staining in DIC 10 $KCC2^{-/-}$ neurons. (B, D, and F) same DIC 4 and DIC 10 neurons as in (A, C, and E), but stained with anti-MAP2 antibody. The MAP2 signal is similar in the young and old neurons. The neurons are cultured on a layer of astrocytes that can be seen under differential interference contrast microscopy (data not shown). These glial cells are not immunostained by either KCC2 or MAP2 antibody, as indicated by the absence of signal under the neurons. Bars = 20 μm (A-F) and 10 μm for inset in C.

GABA (100 μM, 80 ms) pulses were applied. These short applications of GABA did not induce significant changes in the reversal potential of GABA-activated current, indicating no effect on intracellular Cl^-. I used voltage-ramp recordings to measure the GABA reversal potential (E_{GABA}) in cortical neurons cultured for 1 day (DIC1) to 20 days (DIC20). Because the external recording bath is nominally free of HCO_3^-, the recorded E_{GABA} is equivalent to the chloride ion equilibrium potential or E_{Cl}. Two major observations were made from these experiments. First, depolarized E_{Cl} (or high Cl^- concentrations) were measured in wild-type cortical neurons of very young age (**Figure 3-2A**). To ensure that these high Cl^- levels did not originate from a pipette leak, I repeated the measurements at DIC2 with low Cl^- (10 mM Cl^-, 130 mM gluconate) in the pipette. As shown by the open symbol in **Figure 3-2A**, the Cl^- activity (24.1 ± 1 mM, n = 4) measured using a low pipette Cl^- concentration was identical to the one determined using high Cl^- in the pipette. Furthermore, as shown in inset c of **Figure 3-2A**, E_{GABA} (as measured with high Cl^- in the pipette) remains stable during a relatively long period of recording time in both young and old neurons. Second, during development of the wild-type cortical neuron in culture, the E_{Cl} varied from -42.4 $\pm$ 1.7 mV to -71.3 $\pm$ 0.9 mV (n = 180, 28). This corresponds to a gradual decrease in intracellular Cl^- activity aCl_i (see Materials and Methods) from 25.0 $\pm$ 1.7 mM (mean ± SEM) at DIC2 to 7.3 $\pm$ 0.3 mM at DIC20 in (**Figure 3-2A**). The significant decrease in aCl_i and the ensuing shift in E_{Cl} underlie the switch of the GABA response from a large average inward current at rest in young CNS neurons to smaller inward current, and in many cases outward current, in

mature neurons. I also measured the resting membrane potential in young and older wild type and $KCC2^{-/-}$ neurons (**Figure 3-2B**). Although there were no significant differences between the four groups (ANOVA $P>0.05$), I measured a slightly more depolarized potential in older neurons. This small difference, irrespective of the genotype, is consistent with previous reports showing a more depolarized resting membrane potential in cortical neurons of newborn animals (Mienville and Pesold, 1999; Zhou and Hablitz, 1996). However, this more depolarized potential in young neurons could be due to shunting through the seal resistance, as these cells have a higher input resistance and no difference in resting membrane potential was measured between young and older neurons when a cell-attached method was used (Tyzio et al., 2003). At resting membrane potential, the size and direction of the GABA current was also determined (**Figure 3-2A & C**). GABA elicited inward currents in young immature wild-type neurons and on average outward currents in older neurons. However, not all older neurons expressed outward GABA currents: a fraction of them still exhibited inward current, despite the fact that ~87% of the older neurons showed immunoreactivity with the KCC2 antibody. Consistent with absence of $[Cl]_i$ downregulation in $KCC2^{-/-}$ neurons, GABA-evoked currents remain inward in more mature $KCC2^{-/-}$ neurons (**Figure 3-2C**).

In contrast to wild-type neurons, cultured cortical neurons isolated from $KCC2^{-/-}$ animals failed to exhibit the E_{Cl} shift towards more hyperpolarized potentials. Thus, the intracellular Cl^- activity was maintained around 25 mM (from 25.1 $\pm$ 1.6 mM (n = 5, 2) at DIC 2 to 23.2 $\pm$ 1.2 mM (n= 5, 2) at DIC 20. In addition, I found that in the $KCC2^{+/-}$

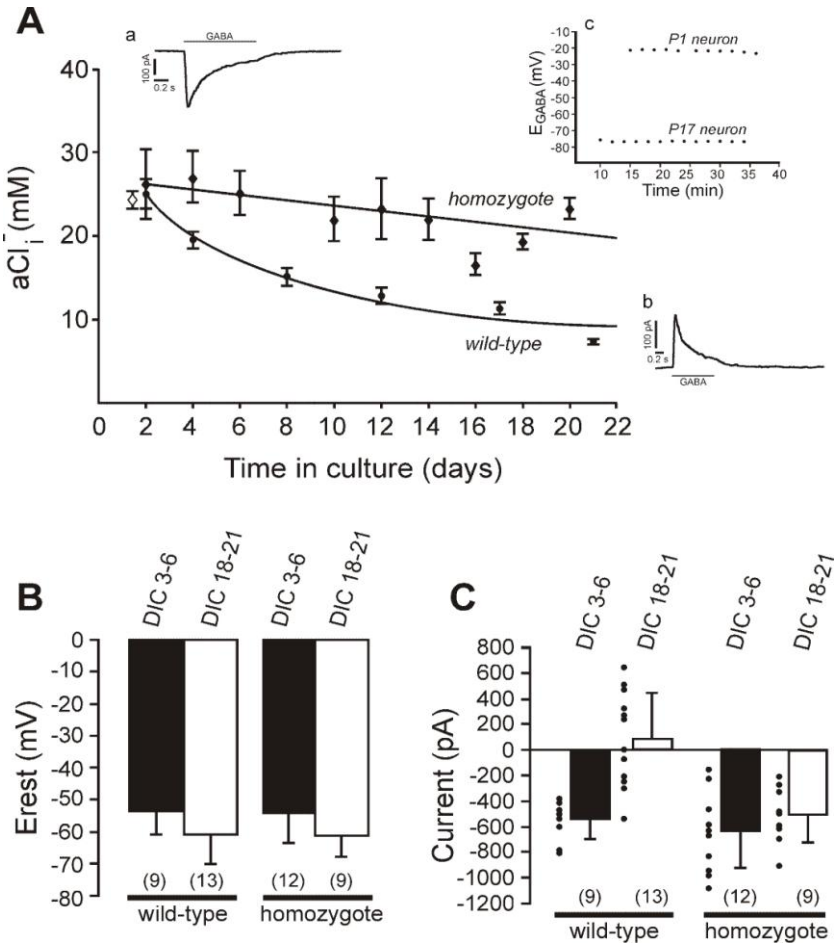

Figure 3-2. Developmental decrease of Cl^- is abolished in $KCC2^{-/-}$ neurons.

(A) Intracellular Cl^- was determined through measurements of the GABA reversal potential (E_{GABA}) using the gramicidin perforated patch-clamp method. $[Cl^-]_i$ was calculated from the Nernst equation. In cultured neurons from wild-type mice, intracellular Cl^- undergoes a significant developmental decrease. In contrast, in $KCC2^{-/-}$ neurons, the intracellular Cl^- levels did not change significantly during neuronal maturation in culture. Data represent mean ± S.E.M. For wild-type neurons (closed circles), data were obtained from a total of 180 cells (28 mice). For $KCC2^{-/-}$ cells (closed diamonds), data were obtained from a total of 67 cells (7 mice). E_{GABA} (and intracellular Cl^- activity) was also determined at DIC2 using low Cl^- (10 mM) in the pipette (open symbol). Insets a, b: sample traces showing typical GABA-induced currents during voltage-clamp at resting potential. c: stable E_{GABA} measured for ~20 min in typical neurons of ages DIC1 and DIC17. (B) Resting membrane potentials determined in young (DIC3-6) and older (DIC18-21) neurons. (C) Currents evoked by exogenously applied GABA at resting membrane potential are inward in young wild-type and young and old $KCC2^{-/-}$ neurons. In older wild type neurons, GABA evokes either outward or inward currents.

(heterozygote) neurons, the $[Cl]_i$ also undergoes a developmental decrease, but with a significant delay when compared to wild-type neurons. The Cl_i activity decreased from 20 $\pm$ 1.2 mM (n = 12, 5) to 13 $\pm$ 1.2 mM (n = 13, 5). As the neurons differentiate and increase the numbers of synaptic connections in the culture, the concentration of GABA in the culture medium could increase, resulting in increased GABA activity and enhanced Cl^- flux across the membrane. However, this is unlikely to occur in the culture system used in the present study because glial cells are a major source of ambient GABA, and the glial cells used for the feeder layer in both $KCC2^{+/+}$ and $KCC2^{-/-}$ cultures were derived from rat. This enhanced tonic GABA activity could account for the observed gradual decrease in aCl_i towards electrochemical equilibrium. To minimize the accumulation of GABA, I plated the cortical neurons at low density and replaced part of the medium every 5-7 days. To measure the GABA content in the culture, I sampled the culture medium at different time points, and subjected the samples to high pressure liquid chromatography. As shown in **Figure 3-3**, the basal level of GABA in the conditioned medium was measured at 6 μM, which increased progressively to 10 μM until replacement of part of the medium every 7 days in both $KCC2^{+/+}$ or $KCC2^{-/-}$ neuronal cultures. Since the GABA concentration measured in wild-type and $KCC2^{-/-}$ cultures was similar, the absence of aCl_i decrease in $KCC2^{-/-}$ neurons argues against a role for tonic GABA activity in the gradual decrease that I observed in cultured wild-type control cortical neurons. Taken together, our results demonstrate that the Cl^- transport mechanism, KCC2, is critical for the decrease in aCl^- during postnatal development.

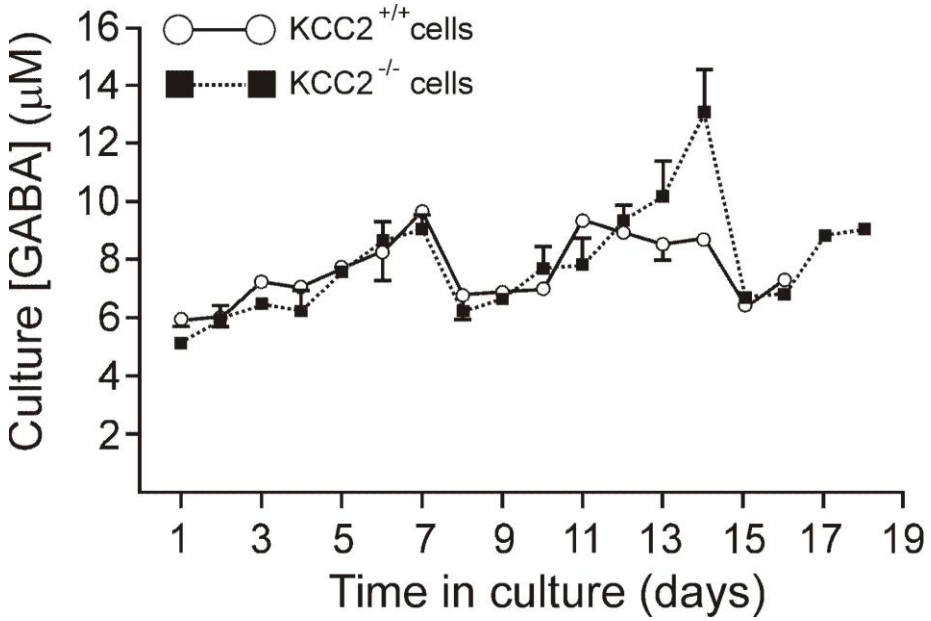

Figure 3-3. Ambient GABA is similar in wild type KCC2$^{+/+}$ and KCC2$^{-/-}$ neuronal cultures. GABA concentration was measured by HPLC.

GABA concentration was measured by HPLC. The concentration of GABA in conditioned medium was measured at 6 μM and this concentration increased progressively in the culture, due to the release of GABA from both astrocytes and neurons. The culture medium was replaced every 7 days with fresh conditioned medium, leading to a periodic decrease in GABA concentration. The GABA concentration in KCC2$^{-/-}$ neuronal cultures (filled squares) is very similar to that of wild-type KCC2$^{+/+}$ cultures (open circles). Each data point represents the mean ± SEM GABA concentration in the culture medium (n = 4, KCC2$^{+/+}$ and n = 2 KCC2$^{-/-}$).

Intracellular Cl^- in neurons is acutely regulated by KCC2

Since the Cl^- content of mature neurons is significantly below the concentration for passive distribution, energy is required to drive Cl^- away from equilibrium. **Figures 3-1 and 3-2** demonstrate that the K^+-coupled Cl^- transporter, KCC2, is expressed in more mature neurons and is responsible for setting the neuronal Cl^- concentration to low values. Whether or not the cotransporter also acutely regulates and maintains intracellular Cl^- upon challenge is addressed in the next experiments. Using 200 ms ramp protocols, E_{GABA} was measured every 2 minutes in a DIC14 wild-type neuron. As indicated in **Figure 3-4A**, the measurement procedure did not affect the intracellular Cl^- concentration. Upon addition of furosemide (1 mM), I observed a progressive shift in E_{GABA} towards more positive potentials, indicative of a rise in intracellular Cl^-. Upon removal of the cotransporter inhibitor, the intracellular Cl^- returned towards control levels. The effect of furosemide was significant in older neurons but not in young neurons, in agreement with the increased expression of KCC2 in the more mature neurons (**Figure 3-4**). The effect of furosemide on $KCC2^{-/-}$ neurons was examined in later experiments. The driving force for KCC2 results from the difference in the transmembrane ionic gradient of both potassium and chloride. Thus, changing the K^+ concentration in the recording bath solution directly affects the intracellular Cl^- concentration (Kakazu et al., 2000). In the following experiment, after a steady E_{GABA} was observed, the cell perfusion was switched from standard external bath solution containing 5 mM K^+, to a bath solution with lower K^+ (1 mM, see methods and materials). In a DIC13 wild type neuron, E_{GABA} dramatically

shifted in the negative direction when external solution was switched to 1mM K^+ and this effect was reversed by applying 1mM furosemide (**Figure 3-4C**). In young wild-type neurons, lowering K^+ had little effect on E_{GABA} (**Figure 3-4D** left, n = 4, 2). In contrast, in older wild-type neurons, exposure to low K^+ significantly depleted cell Cl^-, resulting in a negative shift of E_{GABA} (**Figure 3-4D** right, n = 14, 2). This effect of low K^+ was counteracted by the addition of 1 mM furosemide (**Figure 3-4C**). The same manipulations were performed in DIC11-13 $KCC2^{-/-}$ neuron cultures and I observed that the $[Cl^-]_i$ only slightly decreased when the cells were exposed to low K^+ (**Figure 3-4D** right, n = 8, 1). These data indicate that KCC2 plays a key role in coupling neuronal Cl^- with neuronal K^+. Other cation-chloride cotransporters, such as KCC1, KCC3, or KCC4, may also participate in the cation-anion coupling; although they may not be active at resting conditions (see discussion).

KCC2 counteracts $[Cl^-]_i$ challenges imposed by excessive Cl^- influx

I have shown that KCC2 plays a critical role in the developmental down-regulation of intracellular Cl^-. Because of low internal Cl^-, mature neurons are always under the challenge of excessive influx of Cl^- ions driven by the large Cl^- gradient across the membrane. When $GABA_A$ receptors are activated, especially when the neuron is also depolarized, the $[Cl]_i$ of small compartments such as dendritic spines can increase significantly through the anion channels associated with $GABA_A$ receptors. Different mechanisms, including cation-chloride cotransporters and passive chloride channels, may

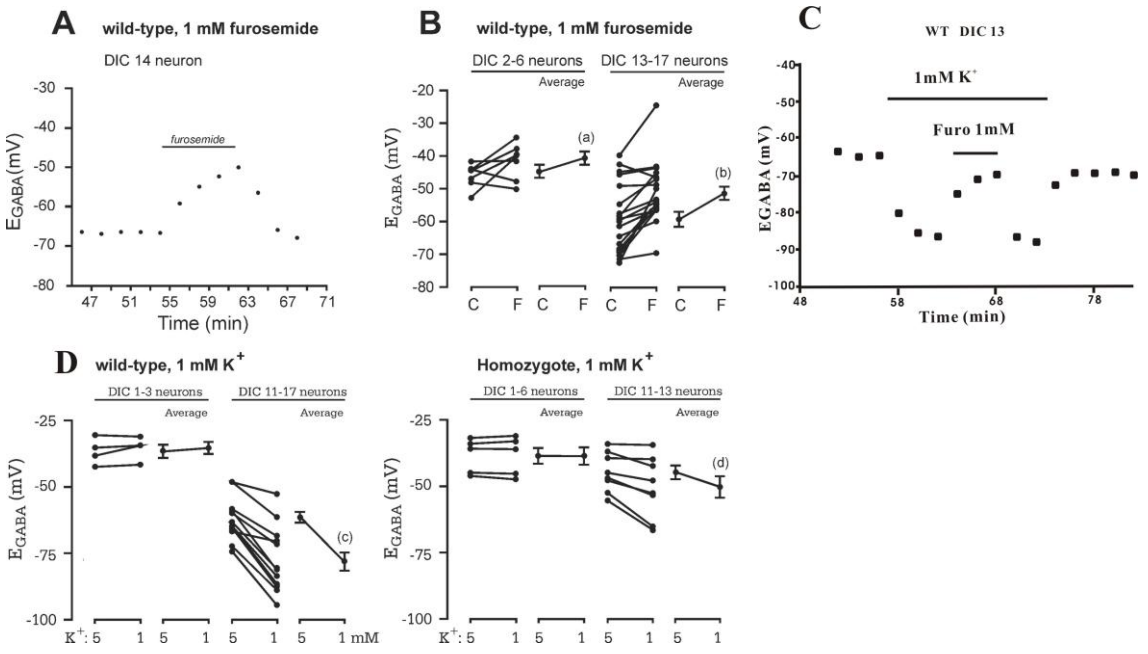

Figure 3-4. Evidence for a furosemide-sensitive K-Cl cotransporter in older cortical neurons in culture.

(A) Typical experiment in a wild-type DIC14 cortical neuron showing a stable E_{GABA}, as measured every two minutes for a period of 8-10 minutes in control conditions. Addition of furosemide induces a shift in E_{GABA} towards more positive values, indicating an increase in intracellular Cl^- concentration. (B) In contrast to older neurons where furosemide induces a significant positive shift in the GABA reversal potential (b) ($P = 0.0001$), in young neurons, furosemide has no significant effect on E_{GABA} (a) ($P = 0.087$). (C) Reducing extracellular $[K^+]$ from 5 mM to 1mM greatly decreases intracellular $[Cl^-]$, and this effect is neutralized by furosemide. (D) Decreasing the external K^+ concentration induces a significant E_{GABA} shift in older $KCC2^{+/+}$ neurons, corresponding to a 38 ± 8 % decrease in $a[Cl^-]i$ (c) ($P < 0.0001$). In old homozygous $KCC2^{-/-}$ neurons, reduction in external K^+ results in a much smaller decrease in E_{GABA}, corresponding to a 16 ± 13 % decrease in $a[Cl^-]i$ (d) ($P < 0.005$). In younger neurons from both genotypes, there was no effect of K^+ reduction on E_{GABA}.

immediately be activated to fight excessive Cl^- influx, and maintain the Cl^- equilibrium. To study the role of KCC2 in the acute regulation of $[Cl^-]_i$, I utilized a long 6 sec GABA (100 μM) application coupled to a depolarizing step (30-40 mV away from the measured resting membrane potential) to induce a large amount of Cl^- influx into the recorded neuron. E_{GABA} was monitored using repetitive (every 2 minutes) brief GABA pulses (80 ms) with voltage ramp recording. Every experiment started when stable series resistance and stable E_{GABA} were achieved.

During each 6 sec GABA application under depolarization, the intracellular Cl^- significantly increased as demonstrated by the significant positive shift in E_{GABA} (**Figure 3-5B, 3-5D**). Although the extent to which E_{GABA} changed was different in young and older neurons, the intracellular $[Cl^-]_i$ returned to its original value within 8-10 minutes in both groups. The decrease in E_{GABA} during the initial 2 min period were 8.64 ± 2.46 mV (n=5) and 1.94 ± 0.52 mV (n=8) in wild-type DIC14-18 and DIC2-6 neurons, respectively (**Figure 3-5D, 3-5F**). After recovery, a second 6 sec GABA application under depolarization was performed, followed in order by an immediate E_{GABA} measurement and the perfusion of 1mM furosemide. It was only in wild-type neurons older than P10, that furosemide greatly inhibited the initial decrease in E_{GABA} (from 8.64 ± 2.46 mV to 1.76 ± 0.74 mV (n=5), see **Figure 3-5B, 3-5D, and 3-5F**). The loop diuretic failed to affect the initial decrease in E_{GABA} in the young wild-type neurons, in agreement with absent or low KCC2 expression in immature wild-type neurons. Identical experiments were performed in cortical neuronal cultures obtained from $KCC2^{-/-}$ mice.

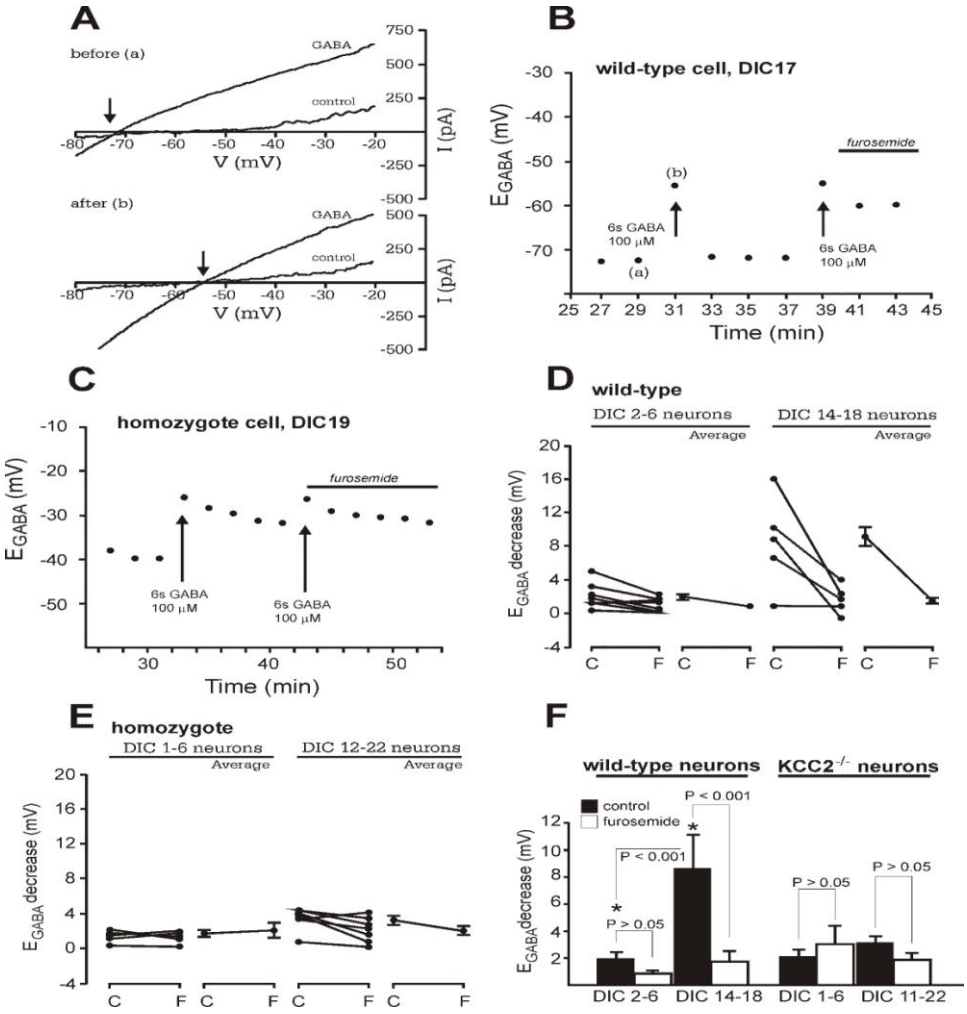

Figure 3-5. Deletion of KCC2 abolishes $[Cl^-]_i$ regulation after acute loading of Cl^-.

(A) I-V traces recorded using voltage ramps before and after loading the cell with Cl^-. E_{GABA} shifts to more depolarized values after Cl^- loading. The letters (a) and (b) correspond to 2 specific recordings depicted in panel B. (B) Typical experiment performed in a wild-type mature neuron. After steady E_{GABA} values were obtained, intracellular chloride loading was obtained using long (6 sec) GABA application combined with membrane depolarization (holding at -20mV). Voltage ramps were applied every 2 minutes to record E_{GABA}. In wild-type neurons, the E_{GABA} decrease during the first 2 min was greatly delayed by 1 mM furosemide. (C) In $KCC2^{-/-}$ neuron, the initial $[Cl^-]_i$ (E_{GABA}) decrease was unaltered by furosemide. (D) The initial E_{GABA} decrease was calculated from the first 2 time points or first 2 min interval. Each dotted-line set represents one experiment as shown in A. In wild type and $KCC2^{-/-}$ neurons, only more mature cells of wild type mice (DIC14-18), which have high KCC2 expression, showed high E_{GABA} decrease and responsiveness to 1mM furosemide. (F) Only the inhibition of recovery rate by furosemide in more mature wild-type neurons is significant ($P<0.001$).

As seen in **Figure 3-5C** and **3-5E**, $KCC2^{-/-}$ neurons also recovered their Cl^- content after Cl^- loading, but the decrease was much smaller (3.12 $\pm$ 0.52 mV in DIC11-22 neurons). In these neurons, furosemide did not affect the E_{GABA} decrease (**Figure 3-5C, 3-5E, and 3-5F**), consistent with the absence of the cotransporter in these cells. A more physiological example of Cl^- loading is the co-application of glutamate and GABA (**Figure 3-6**). I thus conclude that KCC2 in control neurons actively promotes the rapid extrusion of the anion from the neurons during acute loading of Cl^-. Other Cl^- mechanisms, probably passive Cl^- channels, also take part in the recovery process.

KCC2 maintains neuronal Cl^- during prolonged depolarization

Due to the presence of passive chloride permeation pathways, prolonged depolarization induced by persistent activation of GABAergic synapses will tend to increase intracellular Cl^- concentration and move E_{Cl} in the depolarized direction. In the next set of experiments, I demonstrate that KCC2 is able to prevent such changes in E_{Cl} due to depolarization. Again, cortical neurons obtained from wild-type and homozygote $KCC2^{-/-}$ animals were analyzed. In these experiments, the membrane potential was first clamped to obtain zero current (E_{rest}) and a steady recording of E_{GABA}. The cells were then voltage clamped 30 mV higher than E_{Cl} for the entire remainder of the experiment, with the exception of the time during ramping protocols used for E_{GABA} (E_{Cl}) measurements. As indicated in **Figure 3-7A & 3-7C-D**, in older wild-type neurons, the E_{Cl} remained steady during depolarization (only a slight increase from -62.4 $\pm$ 1.9 mV to -60.3 $\pm$ 1.9 mV).

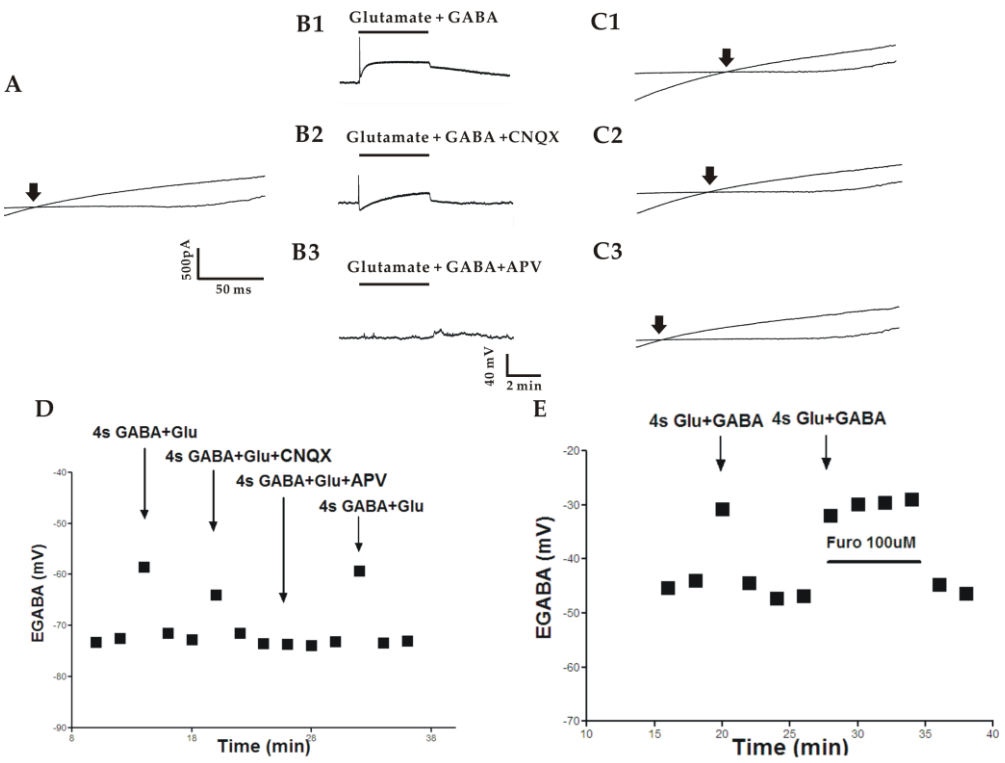

Figure 3-6 Intracellular Cl^- loading with co-application of GABA and glutamate shifts GABA in the depolarized direction.

(A) Voltage ramp recording was used to measure the GABA reversal potential E_{GABA}. After a stable baseline of E_{GABA} was established, Glutamate (100μM) and GABA (100μM) with or withour glutamate receptor antagonists were co-applied to the neuron for 4 seconds. The response of the membrane potential to the co-application of GABA and glutamate is shown in (B) (current clamp, I=0). Immediately after the evoked response, same voltage ramp was applied to measure the E_{GABA} (C). After the depolarization induced by co-aplication of GABA and glutamate (B1), EGABA shifts from -73mV of control (A) to -58mV (C1). Co-application of GABA/glutamate/CNQX induces a smaller depolarization (B2) and less shift in E_{GABA} (C2). However DL-APV totally blocks the depolarization (B3) and E_{GABA} shift (C3) when it is co-applied with GABA and glutamate. The data from the same P15 neuron is plotted in panel (D). KCC2 inhibitor furosemide blocked the recovery of E_{GABA} (E).

Upon addition of furosemide, the E_{Cl} significantly increased from -60.3 $\pm$ 1.9 mV to -48.6 $\pm$ 1.6 mV, indicating a large increase in the intracellular Cl^- concentration (**Fig 3-7**). In contrast, $KCC2^{-/-}$ neurons reacted directly to the depolarization, as indicated by the marked increase in E_{GABA} from 49.2 $\pm$ 1.5 mV to 38.8 $\pm$ 1.3 mV (**Figure 3-7B & 3-7E-F**). As anticipated, in these neurons lacking the cotransporter, furosemide did not affect E_{GABA}. These data demonstrate that in older neurons, KCC2 renders the neuron resistant to changes in the intracellular Cl^- concentration during depolarization.

Interestingly, in young wild-type neurons, neither depolarization alone nor furosemide significantly affected E_{GABA} (E_{Cl}), indicating that only relatively low levels of passive chloride channel pathways are expressed/active in early postnatal development. The absence of a furosemide effect in $KCC2^{-/-}$ neurons not only confirms the absence of the cotransporter in these cells, but also confirms (under our recording conditions) the specificity of the furosemide effect on the cotransporter in wild-type neurons.

Discussion

In contrast to KCC2 knockout mice, which die at birth from respiratory failure (Hubner et al., 2001), genetically modified $KCC2^{-/-}$ mice generated in our laboratory survive for about 2.5 weeks (Woo et al., 2002). In the brain of these mice, 2-5% KCC2 protein is still detected by Western blot analysis. This leakage is likely due to the targeting of exon 1 and may explain the survival of the mice beyond birth. In their publication, Hubner and coworkers (Hubner et al., 2001) showed that E_{GABA} in wild type E18.5 spinal cord motor

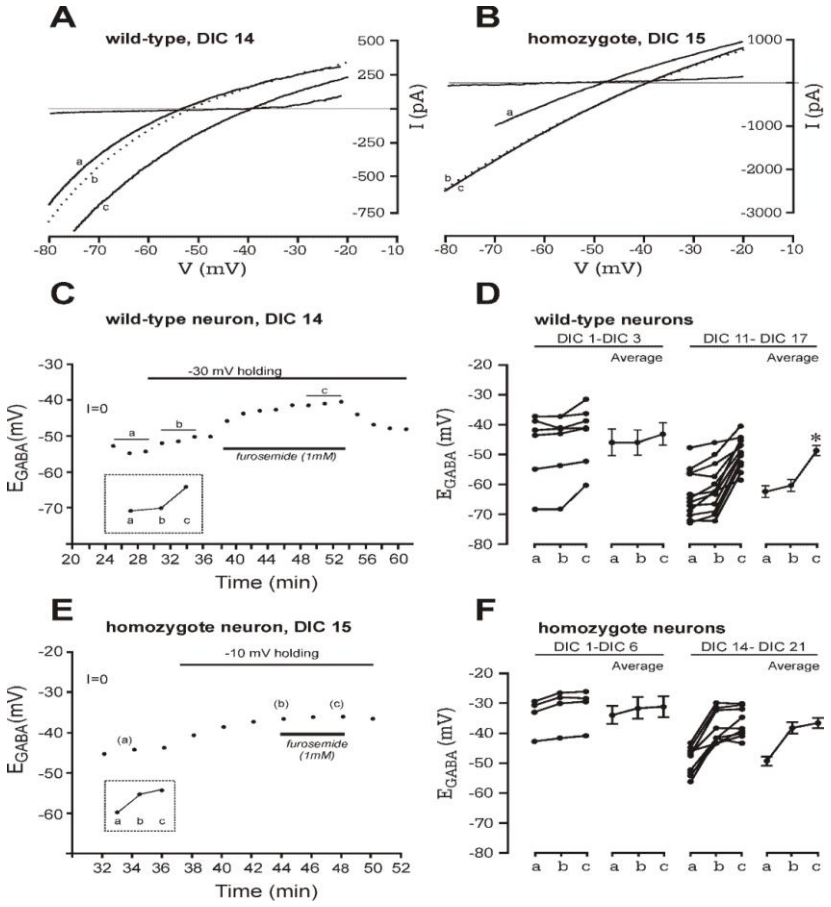

Figure 3-7. Depolarization greatly affects intracellular Cl^- in the absence of KCC2.

(A-B) I-V traces recorded in wild-type and $KCC2^{-/-}$ neurons using voltage ramps before depolarization (a), after depolarization (b), and in the presence of 1 mM furosemide (c). In A, the reversal potential shifts to more depolarized potentials only in the presence of furosemide, whereas in B, the reversal potential shifts to more depolarized potentials only during depolarization. (C) In a typical experiment, after stable E_{GABA} recordings were established at E_{rest} (a), the holding potential of the cell was stepped to a more depolarized potential (-30 mV). The absence of E_{GABA} change (b) indicates that the intracellular Cl^- concentration is not affected by depolarization in mature $KCC2^{+/+}$ neuron. As expected, furosemide induces a shift in E_{GABA} towards more positive potentials (c). (D) Recordings in several neurons at different ages. Each recording is from a single neuron and consists of three different E_{GABA} values (see inset in C: E_{GABA} before depolarization (a), during depolarization (b), and depolarization + 1mM furosemide (c)). (E) Typical experiment in mature $KCC2^{-/-}$ neuron showing a marked effect of depolarization on E_{GABA} and absence of furosemide effect. (F) Recordings in several $KCC2^{-/-}$ neurons at different ages.

neurons is already hyperpolarized (−52 mV), whereas in $KCC2^{-/-}$ neurons, it is more depolarized (-33 mV). Expression of KCC2 is already high in the spinal cord at late embryonic stage (Li et al., 2002; Stein et al., 2004). In our $KCC2^{-/-}$ mouse model, 2-5% KCC2 expression may be enough to slightly shift the E_{GABA} towards the shunting range of $GABA_A$ receptor activation, preventing the severe motor deficits that cause neonatal death in the full knockout mice. Of interest is the demonstration here that mature $KCC2^{-/-}$ cortical neurons have lost their ability to regulate $[Cl^-]_i$.

Several studies conducted in a variety of GABA-responsive neurons have shown that, from late embryonic days to the second postnatal week, E_{GABA} progressively shifts to more negative potentials (Ben-Ari et al., 1994; Fukuda et al., 1998; Kandler and Friauf, 1995l; Owens et al., 1996; Wu et al., 1992). This shift is due to a gradual decrease in the neuronal intracellular Cl^- content (Fukuda et al., 1998; Owens et al., 1996). Since this decrease of intracellular Cl^- is against the inward driving force, Cl^- transport must require energy. The identification of a neuronal-specific K-Cl cotransporter (Payne et al., 1996) and the demonstration of its up-regulation during postnatal neuronal maturation (Clayton et al., 1998; Lu et al., 1999; Rivera et al., 1999), makes the cotransporter a good candidate for this developmental decrease in neuronal Cl^-. Indeed, the tight coupling of Cl^- and K^+ movements through K-Cl cotransport, allows for an uphill Cl^- transport using the large K^+ gradient generated by the Na^+/K^+ pump. Two additional K-Cl cotransporters could potentially be expressed in cortical neurons. In total, there are four genes encoding K-Cl cotransporters. KCC1 is widely expressed throughout the brain (Payne et al., 1996)

where it fulfills housekeeping roles in volume maintenance and regulation. KCC3 expression has been found in large cortical pyramidal cells (Pearson et al., 2001), whereas KCC4 is only expressed in cranial nerves (Karadsheh et al., 2003). Out of the four cotransporters, only KCC2 exhibits substantial basal transport activity (Payne, 1997; Song et al., 2002; Strange et al., 2000), the other transporters require swelling activation (Mercado et al., 2000b; Mount et al., 1999). In our experimental conditions there is no indication that an additional K-Cl cotransporter participates in Cl^- regulation in older neurons since this regulation is abolished in neurons lacking KCC2.

In agreement with Ganguly et al. (Ganguly et al., 2001), I have shown that isolated neurons reproduce in culture the developmental up-regulation of KCC2 and the concomitant decrease in internal Cl^-. An issue that remains unresolved concerns the nature of the mechanism underlying the high Cl^- concentration in young immature neurons. Although our data were consistent with many reports showing GABA depolarization in young neurons, I sought to exclude the possibility that the measured high Cl^- concentration in the young cultured cortical neurons resulted from a leak from the high Cl^--containing pipette. First, I measured identical GABA reversal potentials in DIC2 neurons when either low Cl^- (10 mM) or high Cl^- (140 mM) was present in the patch pipette (**Figure 3-2A**). In addition, once the gramicidin perforation was large enough to allow current measurements, I showed that E_{GABA} was very stable despite the high Cl^- in the pipette. A progressive leakage of Cl^- would have resulted in a progressive shift of E_{GABA} towards more positive potentials. A Cl^- activity of 25 mM or more in

young neurons suggests the participation of an active inward Cl^- transport mechanism. Based on expression studies in CNS neurons, the laboratory proposed in the past that the Na-K-2Cl cotransporter might participate in Cl^- accumulation in immature neurons (Plotkin et al., 1997a; Plotkin et al., 1997b). However, out of four DIC1-DIC4 neurons recorded, only one responded to 10 μM bumetanide (0.1 ± 0.6 mV after 6 minutes in bumetanide, n = 4) .The lack of bumetanide effect is consistent with the absence of effect of decreasing the external K^+ concentration (**Figure 3-4C** and (DeFazio et al., 2000)). These data suggest either that the NKCC1 cotransporter is not expressed or is not active in the young cultured cortical cells or that the Cl^- leak in these immature neurons is too small to expose the effect of NKCC1 inhibition. Because bumetanide can directly inhibit GABA receptors (Sung et al., 2000), I did not incubate the neurons in the inhibitor for extended periods of time. The potential participation of NKCC1 in Cl^- accumulation can be more directly examined in future studies using an NKCC1 knockout mouse model (Delpire et al., 1999).

In this study, I provided evidence for a direct relationship between KCC2 and the developmental decrease in intracellular Cl, as neurons deficient in cotransporter expression fail to undergo this developmental decrease (**Figure 3-2**). The mechanisms underlying the postnatal up-regulation of KCC2 expression are still unknown. The laboratory recently demonstrated the presence of a neuronal-restrictive silencing element in proximity of exon 1 (Karadsheh and Delpire, 2001). Activation of KCC2 transcription concurs with the decreased expression of neuronal-specific silencing factor after birth

(Schoenherr and Anderson, 1995). Based on their findings that chronic blockade of $GABA_A$ receptors in hippocampal neuronal cultures abolished the KCC2 increase and shift of E_{GABA}, Ganguly et al. also suggested that the GABA activity promotes the shift of the GABA response (Ganguly et al., 2001). However, results from two other groups argue against this effect of chronic $GABA_A$ inhibition on KCC2 expression levels (Ludwig et al., 2003; Titz et al., 2003).

In older wild-type neurons (**Figure 3-2**), the internal Cl^- concentration is consistent with gradients set by a K-Cl cotransport mechanism: $[K^+]_i \times [Cl^-]_i = [K^+]_o \times [Cl^-]_o$. For known external concentrations of $[K^+]_o$ at 5 mM, and $[Cl^-]_o$ at 158 mM, and estimated $[K^+]_i$ at 140 mM, the calculated $[Cl^-]_i$ is 5.6 mM. The $[Cl^-]_i$ estimated by measurements using gramicidin perforated patch clamp in DIC21 neurons is 7.3 $\pm$ 0.2 mM (n=4). Thus, the agreement between calculated and recorded $[Cl^-]_i$ indicate that KCC2 is the major mechanism setting $[Cl^-]_i$ in older neurons. From these data and in agreement with Payne (Payne, 1997), I can also conclude that under physiological conditions, KCC2 is working close to its equilibrium. Also consistent with an obligatory coupled K^+ and Cl^- transport, alteration of extracellular K^+ has a significant impact on intracellular Cl^- levels. In experiments depicted in **Figure 3-4 (C-D)**, I showed substantial reduction in Cl^- content in older neurons expressing KCC2 upon lowering external K^+. In young immature neurons, a decrease in $[K^+]_o$ showed no effect on $[Cl^-]_i$. In older homozygous $KCC2^{-/-}$ neurons, the decrease in $[K^+]_o$ induced a smaller but still significant reduction in $[Cl^-]_i$. Whether or not the $[Cl^-]_i$ reduction is due to redistribution associated with a change in

membrane potential or to a K^+ coupled mechanism remains to be determined. KCC2 was shown to be highly expressed in the vicinity of excitatory synapses (Gulyas et al., 2001). Thus, strong synaptic excitation or pathological conditions leading to increased extracellular K^+ will likely result in a significant increase in $[Cl^-]_i$. Increased $[K^+]_o$ and $[Cl^-]_i$ should both lead to hyperexcitability.

During neuronal inhibition, $GABA_A$ receptors are activated and Cl^- is driven into the cell down its electrochemical gradient. During frequent network synaptic activity, intracellular Cl^- accumulates due to prolonged $GABA_A$ receptor activation, and as a result, E_{GABA} shifts to more positive potentials. During membrane depolarization, Cl^- ions can also accumulate through passive chloride conductances (**Figure 3-5** and (Staley et al., 1995). If repeated membrane depolarization is large enough, intracellular Cl^- could rise to values where GABA becomes depolarizing. In our experiment of **Figure 3-5**, long GABA application combined with depolarization tends to mimic this process. Co-application of GABA and glutamate can also induce similar result, indicating the possibility of such a Cl^- loading process in physiological conditions. NMDA receptor activation may provide the depolarization for such a Cl^- loading through $GABA_A$ receptors. $GABA_A$ receptor activation will no longer efficiently inhibit and might even lead to excitation if the accumulated Cl^- is not readily removed from the cell. Although other chloride regulating mechanisms such as ClC2 (Staley, 1994; Staley et al., 1996) (Whether the expression of ClC2 is altered in KCC2 knockout mice hasn't been investigated) and passive chloride conductance will eventually lower the intracellular Cl^-,

KCC2 is the major determinant mechanism for the rapid extrusion of excessive Cl^- (**Figure 3-4**).

In wild-type neurons expressing high amounts of KCC2, depolarization alone does not affect E_{GABA}, whereas in $KCC2^{-/-}$ neurons, a significant shift of E_{GABA} is observed. These data demonstrate that KCC2 is able to regulate intracellular Cl^- during membrane depolarization and thus suggest a critical role for KCC2 in efficiently "clamping" intracellular Cl^- during neuronal network activities. The activity of KCC2 greatly shortens the recovery time of the neuronal Cl^- from excited state to resting state.

In summary, our study provides a comprehensive look at the role of KCC2 in Cl^- regulation in isolated CNS neurons. By comparing neurons isolated from genetically modified mice deficient in KCC2 with wild-type neurons, I demonstrate that the cotransporter is critical in lowering intracellular Cl^- during postnatal development of cortical principal neurons, a process that occurs progressively during the first 10 days of postnatal life in the forebrain of rodents. I also show that KCC2 neurons lacking the cotransporter are unable to regulate and maintain their intracellular Cl^- during conditions in which the internal Cl^- is challenged. In contrast, control neurons use the cotransport of Cl^- and K^+ to fight Cl^- changes completely independently of membrane potential effects (electroneutrality of cotransporter), during GABA inhibition and membrane depolarization. Importantly, I show the absence of a difference in Cl^- levels and in acute regulation of Cl^- between young neurons from wild-type and $KCC2^{-/-}$ mice, but an increasing difference between the two genotypes during maturation of these neurons. The

inability of KCC2$^{-/-}$ cortical primary neurons to regulate Cl^- may result in disinhibition and hyperexcitability in the cortical region, but because of the wide distribution of KCC2 within the brain, disregulation of this cotransporter would likely result in defects involving most brain regions. For instance, disinhibition and hyperexcitability is likely to lead to the generation of seizures (Rivera et al., 2002; Woo et al., 2002). A role for KCC2 in disinhibition and hyperexcitability has also been shown in the spinal cord in a model of chronic pain (Coull et al., 2003).

CHAPTER IV

ROLES OF THE CATION-CHLORIDE COTRANSPORTERS KCC2 AND NKCC1 IN PROMOTING/PREVENTING HYPEREXCITABILITY IN THE HIPPOCAMPUS

Introduction

The hippocampus is an important CNS structure involved in temporal lobe epilepsy (Aronica and Gorter, 2007; Blumcke et al., 1999; French et al., 1993; Liu et al., 2007; Mathern et al., 1996). Inhibition provided by ionotropic $GABA_A$ receptors is essential in maintaining normal brain function and protecting against seizures. Indeed, the GABAergic tone, by hyperpolarizing postsynaptic membranes and increasing membrane conductance (shunting), dampens excessive glutamatergic excitation and prevents synchronization of neuronal networks into epileptiform activity. $GABA_A$ receptors mediate their effects through the opening of a Cl^- channel, allowing Cl^- to move into the cell driven by high external Cl^- and low internal Cl^-, leading to plasma membrane hyperpolarization. The low neuronal Cl^- is maintained by a secondary active transport mechanism, the neuronal-specific K-Cl cotransporter, KCC2. This overall process matures concomitant with the development of glutamatergic excitation (Ben-Ari et al., 1997b; Ben-Ari et al., 1994; Cherubini et al., 1991; Stein et al., 2004), which in rodents translates to the first two weeks of postnatal life. At birth, however, neuronal Cl^- is elevated, far above the extracellular concentration of the anion (LoTurco et al., 1995;

Luhmann and Prince, 1991; Owens et al., 1996). This implies that the absence of KCC2 expression at birth, alone, cannot account for the high neuronal Cl^-.

Accumulation of the anion in immature neurons is thought to be mediated by the inward Na-K-2Cl cotransporter NKCC1 (Fukuda et al., 1998; Plotkin et al., 1997b; Sipila et al., 2006; Yamada et al., 2004). Furthermore, expression of NKCC1 was found to be high in immature CNS neurons and down-regulated during postnatal development, opposite to that of KCC2 (Dzhala et al., 2005; Plotkin et al., 1997b; Wang et al., 2002). However, NKCC1 is not always involved in the accumulation of intracellular Cl^-. Indeed, in the developing brainstem (Balakrishnan et al., 2003) and immature retinal neurons (Zhang et al., 2007), intracellular Cl^- is high in the absence of NKCC1 expression. In these neurons, the mechanism of Cl^- accumulation is unknown. Furthermore, there is evidence that NKCC1 may not be ubiquitously down-regulated in the developing hippocampus, but instead undergoes a change of localization from the soma of interneurons and pyramidal neurons to dendritic compartments (Marty et al., 2002), or from neuronal layers to glial formations (Hubner et al., 2001). These observations are significant since NKCC1-mediated elevation of Cl^- in GABAergic interneurons may reduce their inhibition by GABA, resulting in increased inhibitory output to pyramidal neurons and higher network activity. Furthermore, glial cells also play an important role in epileptic activity by regulating the K^+ ion concentration in the extracellular space (D'Ambrosio, 2004; Lux et al., 1986) and glial NKCC1 may be important for clearance of extracellular K^+ (Chen and Sun, 2005).

The formation of neuronal connections during brain development depends on a precise balance between inhibition and excitation, which is maintained throughout brain development and adulthood (Ben-Ari, 2002). As the rodent brain switches from GABA excitation to GABA inhibition during the first two week of postnatal life, this period constitutes a critical moment as excessive GABAergic excitation might lead to increased seizure susceptibility (Dzhala and Staley, 2003; Khazipov et al., 2004) while excessive GABAergic inhibition might prevent growth or synapse formation (Ben-Ari, 2002). A recent report showed that NKCC1 may facilitate seizures in the developing brain (Dzhala et al., 2005). However, as the seizure model used in that study utilized 8.5 mM external $[K^+]$, it is a concern for studying K^+-dependent transport pathways (see discussion). In addition, in their experiments inhibition of NKCC1 by bumetanide shifted the E_{GABA} of postnatal day 4 CA3 pyramidal neurons by -3 mV from -37 $\pm$2.7 mV to -40.4 $\pm$2.7 mV (Dzhala et al., 2005), a rather small change in the reversal potential.

To further understand how inhibition or disruption of NKCC1 affects neuronal excitability and seizure susceptibility, in this study I make use of NKCC1 knockout mouse (Delpire et al., 1999; Woo et al., 2002) and a 4-aminopyridine (4-AP) seizure model in this study. To understand how 4-AP induced seizure-like activity affects the intracellular chloride concentration, I also combine two existing single cell patch clamp techniques, gramicidin perforated patch and cell-attached patch, into a new technique to continuously monitor the E_{GABA} in CA3 pyramidal neurons. The experiments are done in P9-P13 neurons, when NKCC1 expression is still much higher than adult level (Dzhala et

al., 2005). As a continuation from previous study of KCC2 in cultured cortical neurons, I also compare the susceptibility of wild type and KCC2+/- hippocampus slices to 4-AP induced epileptic seizures.

Results

Hippocampal expression of KCC2 Protein increase during development

Many studies have examined the spatial and temporal distribution of KCC2 mRNA transcript and protein during postnatal development (Clayton et al., 1998; Lu et al., 1999; Mikawa et al., 2002; Rivera et al., 1999; Shimizu-Okabe et al., 2002; Wang et al., 2002). There is a consensus that KCC2 expression in rodents is low at birth in the forebrain, and increases steadily during the first 2-3 weeks of postnatal life. To examine the level of KCC2 expression in the regions of hippocampus where our electrophysiological measurements are made, I acquired tissue samples from either CA1 or CA3 by making 0.41 mm punches. **Figure 4-1A** shows that KCC2 protein in the CA1 region increased steadily. It was undetectable at postnatal day P1 and reached adult levels after P15 (**Figure 4-1B**). In the CA3 sub-region, KCC2 expression was much lower than in the CA1 during the first 2 postnatal weeks and then increased thereafter. Western blots were re-probed using anti-transferrin receptor to verify that punches were made in the neuronal layers. Unfortunately, due to the low abundance of NKCC1 and the small amount of tissue, the punches did not allow us to test for NKCC1 expression.

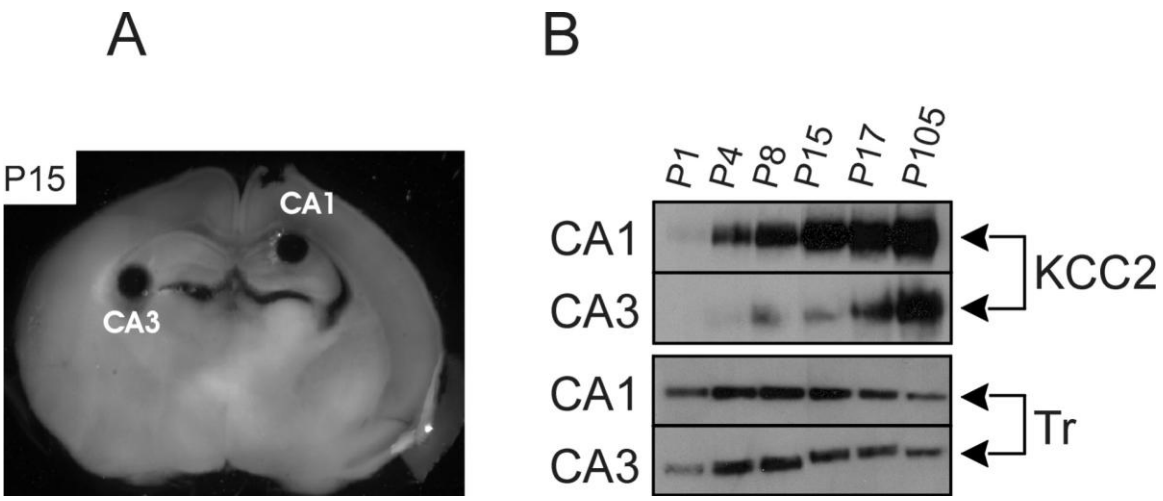

Figure 4-1. **Postnatal expression pattern of KCC2 protein in the CA1 and CA3 regions**.

(A) Example of 0.41 mm sample punches taken from CA1 and CA3 hippocampal regions in a 500 μm whole brain slice from a P15 wild-type mouse. (B) Expression of KCC2 in CA1 hippocampus increases gradually from P1 to P17, but remains low in the CA3 until P17. P105 shows the level of KCC2 in the adult mouse. Anti-transferrin receptor antibody was used as control.

Hyperactivity and seizure susceptibility in KCC2$^{+/-}$ slices

To assess the role of KCC2 in the excitability of the hippocampus, I performed extracellular field recordings in brain slices isolated from wild-type and KCC2$^{+/-}$ mice under control and 4-aminopyridine conditions. Extracellular recordings were obtained from the hippocampal CA1 subregion. In control aCSF, fewer spontaneous events were identified in wild type slices (**Figure 4-2A**) than in KCC2$^{+/-}$ slices (**Figure 4-2B**) which express one half of the KCC2 protein content of wild-type animals (Woo et al., 2002). At age P19-P24, when KCC2 is maximally expressed in wild-type brain, expression of only one copy of KCC2 results in network hyperactivity (**Figure 4-2C**). Blocking voltage-gated potassium channels with 4-aminopyridine (4-AP) is a well-established model to increase the release of excitatory neurotransmitter and trigger epileptiform discharges and seizure-like events in hippocampal slices. As seen in **Figure 4-3A2**, 4-AP induced seizure-like events in the CA1 subregion of hippocampus in brain slices isolated from P24 KCC2$^{+/-}$ mice. Each event was typically longer than 20 seconds and consisted of an interictal, tonic, and clonic phase (**Figure 4-3A4**). In contrast, 4-AP treatment induced interictal-like events in slices isolated from wild-type mice (**Figure 4-3A1, A3**), and in some slices induced ictal events lasting less than 5 seconds in duration. **Figure 4-3B** shows the power spectra for twenty minute consecutive recordings of CA1 hippocampus from wild-type and KCC2$^{+/-}$ slices (traces taken from **Figures 4-4A1 and 4-4A2**). Power spectrum analysis showed that the power density in KCC2$^{+/-}$ was greater than in wild-type, in the EEG frequency band (1-100HZ), as well as in the fast ripple frequency band

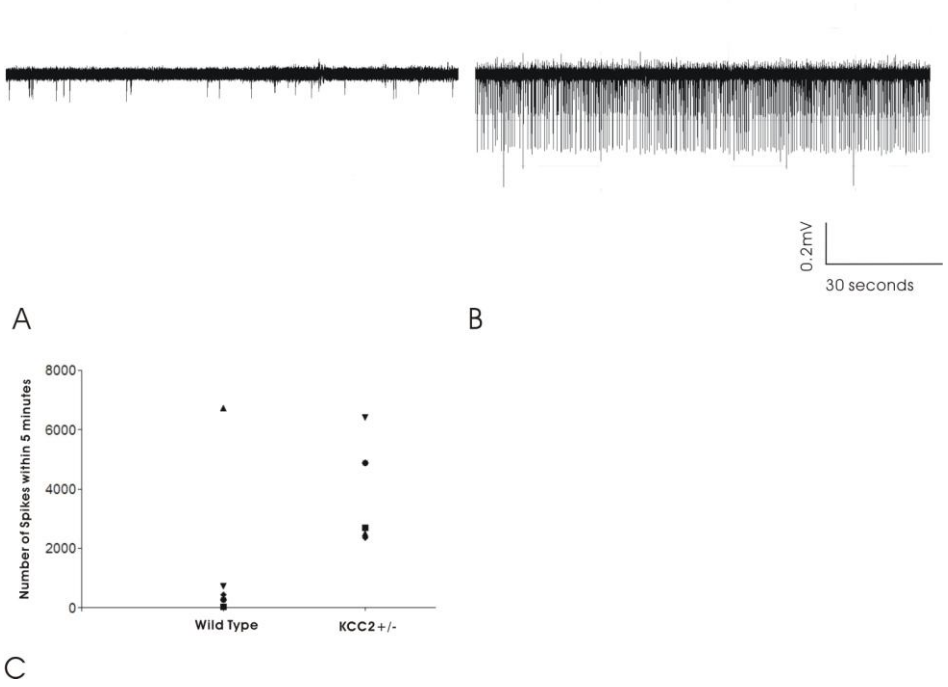

Figure 4-2. Recording of spontaneous spikes from wild type and KCC2$^{+/-}$ slices in normal aCSF.

Both the amplitude and frequency of extracellularly recorded spontaneous events are increased in slice from a KCC2$^{+/-}$ mouse (A) (P18) compared to wild type mouse (B) (P19). No drugs are added to the perfusion during the recording. (C) Pooled data from both wild type and KCC2+/- slices. Number of spikes within 5 min are counted and analyzed by Clampfit 9.2. KCC2$^{+/-}$ slices have a higher occurrence of spontaneous events (n = 5, 2 mice) than wild type slice (n = 5, 2 mice).

(200-400HZ). To quantify seizure susceptibility of $KCC2^{+/-}$ brain slices and wild-type brain slices, the area under the power spectrum for frequencies ranging from 1-100HZ was measured for each recording, and averaged from seven 1-min windows for each trace, 10 min after the application of 4-AP (**Figure 4-3C**). The power obtained from $KCC2^{+/-}$ CA1 hippocampal recordings (4.6 ± 1.4) x 10^{-3} mV^2, n = 6 from 5 mice, P19-P25) was significantly greater than the power obtained from wild-type CA1 hippocampal recordings: (6.9 ± 2.4) x 10^{-4} mV^2, n = 5 from 4 mice, P18-P24, P = 0.038). These results indicate that a reduction in KCC2 expression increases the susceptibility of the hippocampus to seizure-inducing agents such as 4-AP.

Increased spontaneous activity in CA3 pyramidal neurons of $NKCC1^{-/-}$ slices

In contrast to the expression of KCC2 which is highest in mature CNS neurons (Lu et al., 1999; Mikawa et al., 2002; Rivera et al., 1999; Wang et al., 2002), the expression of NKCC1 is highest in immature CNS neurons (Kanaka et al., 2001; Li et al., 2002; Mikawa et al., 2002; Plotkin et al., 1997b; Wang et al., 2002). Whereas KCC2 functions to decrease intracellular Cl^- and thus promote GABAergic inhibition, NKCC1 might function to accumulate intracellular Cl^- and promote excitatory effects of GABA. To assess the role of NKCC1 in regulating intracellular Cl^-, I first attempted to use the gramicidin-perforated patch method in brain slices to determine the GABA reversal potential without disrupting the chloride gradient. Because of the positive pressure applied to the pipette while advancing into the slice and the relatively high concentration of

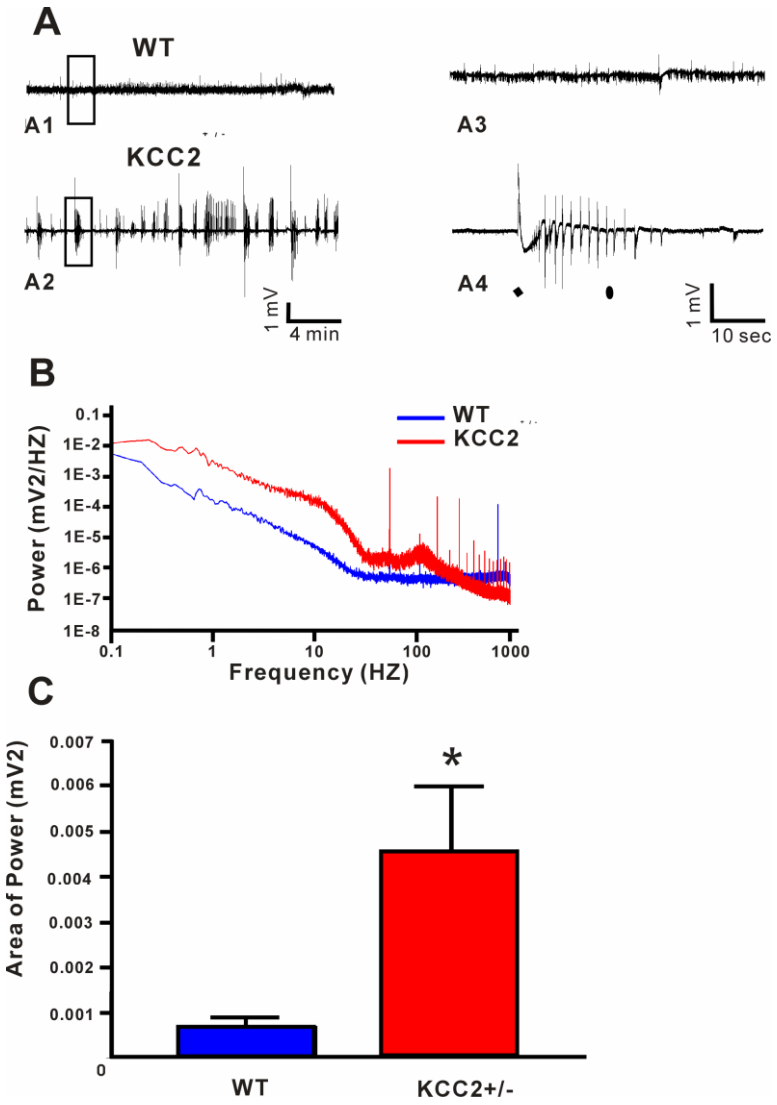

Figure 4-3. Extracellular field recording shows 4-AP induces more seizure-like activities in CA1 region of hippocampal slices from KCC2$^{+/-}$ mice.

(A) 4-AP induces seizure-like events in KCC2+/- brain slice (P24, A2), but much less activities in its wild type counterpart (P24, A1). The boxed region is expanded in A3 and A4 for wild type and KCC2$^{+/-}$, respectively. Each seizure-like event in the KCC2$^{+/-}$ slices consists of a tonic phase (filled diamond) and clonic phase (filled oval). (B) Power spectra from the two traces of (A) in consecutive 20 minutes time windows (window starts at 10 minutes after 4-AP application). EEG (1-100 HZ) and fast ripple (200-400 HZ) frequency range are shown. (C) Average power of extracellular field activity (1-100 HZ band) in 1 minute windows of seizure-like events region 10 minutes after 4-AP application Wild-type: 5 slices from 4 mice P18-24; KCC2$^{+/-}$: 6 slices from 5 mice P19-25.

gramicidin contained in the pipette, gramicidin often disrupted the GΩ seal. Furthermore, by leaking into the slice, the ionophore also produced depolarization of surrounding neurons. Thus, instead of using the gramicidin-perforated patch method, I modified the conventional cell-attached patch recording method (Mason et al., 2005; Perkins, 2006) by adding a low concentration of gramicidin in the pipette. In the cell-attached patch mode, the recorded voltage (V) and the membrane potential (Em) have the relationship shown in **Figure A-5A** (See Appendix A). As R_{seal} is usually greater than 2 GΩ, and R_m (with the exception of young neurons) is by and large uniform and low, the value of R_{patch} typically determines the accuracy of the membrane potential measurement. When R_{patch} is large, V approaches 0, whereas when R_{patch} is small, V approximates Em. Thus, by adding very low concentrations of gramicidin in the pipette solution (less than 5 μg/ml), R_{patch} can be minimized and V becomes a good measure of Em at reasonable seal resistances. As mentioned above, due to the high resistance (Rm) of young pyramidal neuron membranes (Tyzio et al., 2003), this technique has its limitations. However, when the GABA agonist muscimol (20 μM) is applied to the cell and the low membrane conductance (high Rm) is shunted by the high GABA conductance; the peak of the muscimol response V becomes again a good measurement of E_{GABA} (**Figure A-5A,** equation 3). The E_{GABA} measurement becomes more accurate with increased $GABA_A$ conductance. Using this technique, I studied the spontaneous membrane activity of CA3 principal neurons. As seen in **Figure A-5B**, the membrane potential can be followed accurately as the action potential threshold was measured at – 56.6 ± 1.6 mV (n = 40 spikes from 4 CA3 pyramidal neurons).

Because NKCC1$^{-/-}$ mice are viable and do not show any behavioral signs of seizure activity, I examined the spontaneous activity in brain slices prepared from wild-type, NKCC1$^{+/-}$ and NKCC1$^{-/-}$ mice. Under control perfusion conditions, I found that CA3 pyramidal neurons from P10 NKCC1$^{-/-}$ mice exhibited much higher action potential firing rates than the same neurons from P10 wild-type mice (**Figure 4-4A**). I then quantified the number of action potentials (AP) over a 5 min period. As shown in **Figure 4-4B**, there were 706 ± 210 APs per five minutes in CA3 pyramidal neurons from NKCC1$^{-/-}$ mice (n = 7 from four P10-P13 mice), in comparison to 20 ± 9 AP spikes in neurons from wild-type mice (n = 8 from five P9-P13 mice, P = 0.0022). In addition, I tested whether bumetanide (10 μM), a potent inhibitor of NKCC1, would alter excitability in wild type slices similar to NKCC1$^{-/-}$ slices. Five-minute time windows were taken from the recorded trace before or after perfusion of bumetanide (at least 15 minutes after the start of bumetanide). As seen in **Figure 4-4C**, the number of APs recorded from CA3 pyramidal neurons after bumetanide treatment (237 $\pm$ 87, n = 9 from 8 mice) was significantly larger than the number of AP spikes measured using control aCSF (54 ± 25, n = 9 from 8 mice, P = 0.027). Together, these results indicate that NKCC1 likely facilitates a tonic inhibition for the CA3 pyramidal neurons, and in the absence of NKCC1, their spontaneous firing rate increases.

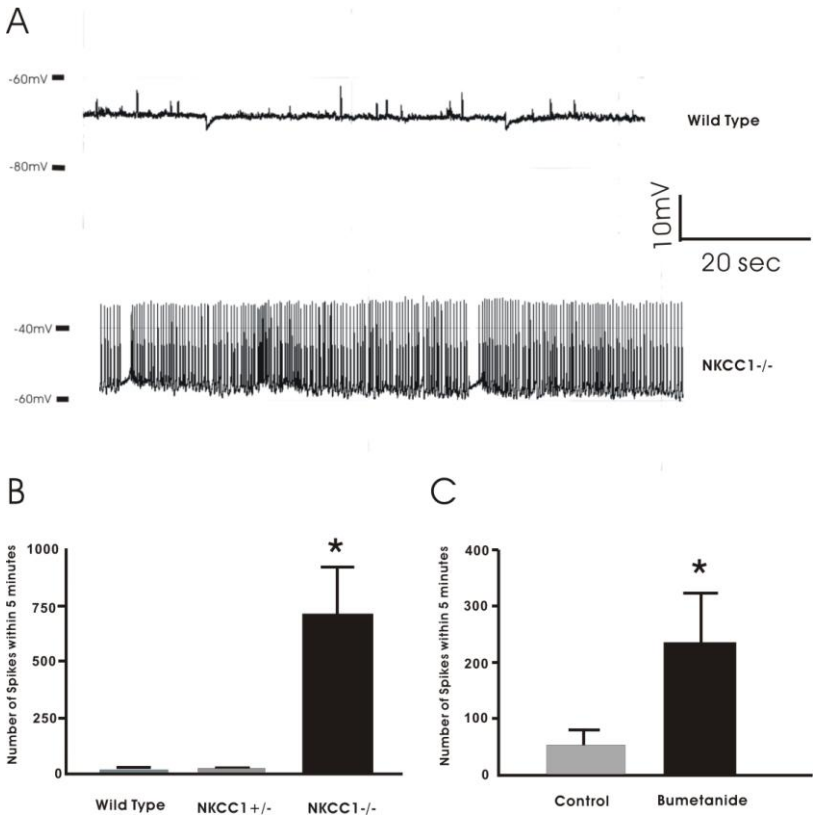

Figure 4-4. **Recordings of spontaneous action potential spikes from CA3 pyramidal neurons of wild-type and NKCC1$^{-/-}$ slices in normal aCSF.**

The number of action potential spikes is much higher than in NKCC1$^{-/-}$ slices (A) than wild type slices. (B) The number of action potential spikes within 5 minutes of recording from NKCC1$^{-/-}$ slices (n = 7, 4 mice) is significantly larger than NKCC1+/- (n = 3, 2 mice) and wild type (n = 8, 5 mice). (C) In the presence of the loop diuretic bumetanide (10 μM), the number of action potential spikes within a 5 minute recording was significantly increased in wild type slices (n = 9, 8 mice).

Positive shift of the Cl^- driving force in CA3 pyramidal neurons of both NKCC1$^{-/-}$ and wild-type slices

As the driving force of chloride determines the polarity of an evoked GABA response, the response of neurons to muscimol, a potent and selective agonist of ionotropic $GABA_A$ receptors but not metabotropic $GABA_B$ receptors, provides an estimation of the neuronal Cl^- concentration. While the majority of excitatory glutamatergic synapses are located on the dendrites of the pyramidal neurons of the hippocampus, a great portion of inhibitory GABAergic synapses are formed on the proximal dendrites or the cell soma. In the following experiments, I applied short puffs (6-8 ms) of muscimol (20 μM) onto the cell soma to mimic synaptic release of GABA. When P10-old wild-type CA3 pyramidal neurons were current-clamped at 0 current, muscimol puffs evoked a slight hyperpolarization of the membrane potential from -54.5 mV to -59.5 mV (**Figure 4-5A1**), indicating that the driving force for chloride was inward. Differences between neurons in the muscimol peak response were due to variations in resting membrane potentials (**Figure 4-5B**), and all driving force values (V_{delta}) measured with muscimol application were under 10 mV (**Figure 4-5C**). Interestingly, there was little difference in the chloride driving force between NKCC1$^{-/-}$ neurons (-1.8 ± 2.6 mV, n = 3) and wild-type neurons (0.1 ± 2.8 mV, n = 3). Upon addition of 4-AP to the perfusing solution, the same application of muscimol induced a depolarization of the V_{peak} (-63.8 mV to -51.0 mV) along with increased activity and interictal-like events in the slice (**Figure 4-5A2**). Hyperpolarization of the resting membrane potential is known to be an effect of 4-AP and was similar between NKCC1$^{-/-}$ and WT (NKCC1$^{-/-}$, -65.83 $\pm$ 4.7 mV, -77.72 $\pm$ 3.5 mV,

-75.76 ± 3.4 mV, -80.61 ± 4.7 mV at 0, 5, 10, 15 minutes after 4-AP application respectively; WT, -68.36 ± 1.6 mV, -74.95 ± 4.5 mV, -75.69 ± 4.3 mV, -75.99 ± 2.2 mV at 0, 5, 10, 15 minutes after 4-AP application respectively, P = 0.700, 1.000, 1.000, 0.700, respectively). This spontaneous hyperpolarization of the membrane is due to increased $GABA_B$ receptor-mediated activation of membrane conductance to K^+ (Avoli et al., 1994; Jarolimek et al., 1994). Under 4-AP application, the driving force of chloride rapidly reversed its direction and GABA became excitatory. Again, there was no measurable difference in the chloride driving force between P10-P13 $NKCC1^{-/-}$ neurons (16.2 ± 8.1 mV, 22.7 ± 7.5 mV, and 26.4 ± 5 mV at 5, 10, 15 min respectively, n = 3), and P11-P13 wild-type neurons (14.6 ± 7.6 mV, 16.8 ± 6.8 mV, and 20.0 ± 4.6 mV at 5, 10, 15 min respectively, n = 3) after 4-AP treatment (**Figure 4-5C**). Both the change in E_{Cl} and the hyperpolarization of the resting membrane potential contribute to the change of the driving force after 4-AP application (**Figure 4-5B**). Of interest is the fact that the 4-AP induced change in E_{Cl} was rapidly eliminated upon addition of 20 μM DNQX, a potent antagonist of non-NMDA glutamatergic receptors (**Figure 4-5A3**). These results indicate that although NKCC1 accumulates chloride in neurons, the cotransporter had little effect on the chloride driving force in CA3 pyramidal neurons from P10-P13 mice in the presence of increased network activity.

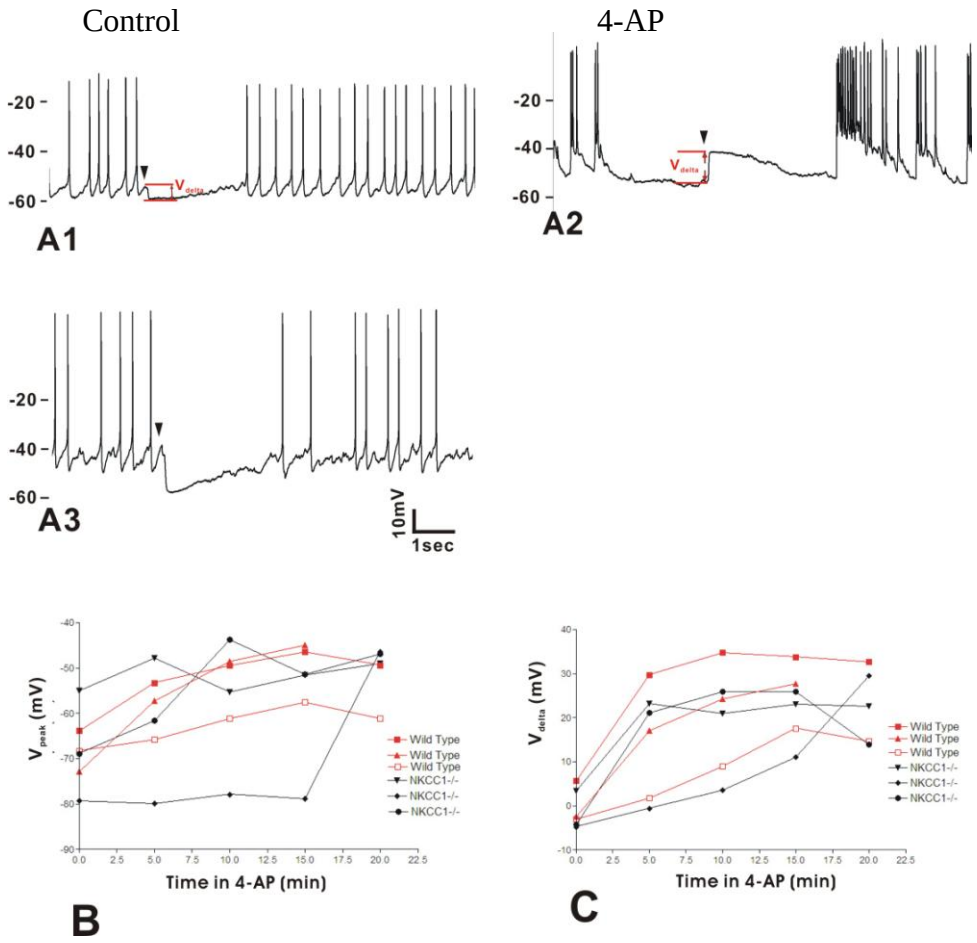

Figure 4-5. GABA response becomes more depolarized in brain slices treated with 4-AP, and this shift in GABA response is inhibited by suppressing the seizure-like events with DNQX.

(A), In a CA3 pyramidal neuron from P10 mouse, brief (8ms) GABA application depolarizes the membrane from -63.8mV to -51.0 mV 10 minutes in aCSF with 50μM 4-AP (A2), in comparison to the slight hyperpolarization from -54.5mV to -59.5mV induced by same GABA application in normal aCSF (A1). This shift of GABA response is abolished 4 minutes after perfusing the slice with aCSF contains 50μM 4-AP and 20 μM DNQX (A3). Arrow indicates the time of the GABA application. (B) The absolute peak of GABA responses (V_{peak}) every 5 minutes are plotted against time from the perfusion of aCSF containing 4-AP. The peak of GABA responses shifts to more depolarized potentials in the presence of 4-AP in both NKCC1-/- (red symbols and lines, n = 3 from 3 mice) and wild type slices (dark symbols and lines, n = 3 from 3 mice). (C) The amount of depolarization (or hyperpolarization) (V_{delta}) induced by GABA also increase in the presence of 4-AP for both NKCC1-/- and wild type slices.

NKCC1$^{-/-}$ slices showed more susceptibility to 4-AP induced epileptiform activity

Since CA3 neurons of brain slices from NKCC1$^{-/-}$ mice demonstrate hyperexcitability when compared to wild-type CA3 neurons, I tested the effect of 50 μM 4-AP in the two genotypes (**Figure 4-6**). Cell-attached recordings (upper traces of Panels **4-6A** and **4-6B**) and extracellular field recordings (lower traces of **Figure 4-6A** and **4-6B**) were carried out simultaneously in the CA3 region of the hippocampus. Shortly after the application of 4-AP, ictal-like epileptiform activities arose in NKCC1$^{-/-}$ slices (**Figure 4-6B**), whereas only interictal-like activities appeared in wild-type slices (**Figure 4-6A**). The ictal-like and interictal-like events were synchronized between cell-attached recordings and field recordings (**Figure 4-6 A and B**). Therefore what was recorded in the cell-attached mode is not only the activation of a single CA3 neuron, but a reflection of the synchronized network activity. The ictal-like epileptic events seen in NKCC1$^{-/-}$ slices consist of a tonic and a clonic phase. I quantified the number of seizure-like events during the first 15 min after addition of 4-AP to the perfusing solution (**Figure 4-6C**). In P10-P13 NKCC1$^{-/-}$ slices, we recorded 7.2 ± 1.8 seizure-like epileptic events (n = 6, from 3 mice). This number is significantly greater than the number of ictal events recorded in wild-type slices (0.4 ± 0.2, n = 8 from 4 mice). Of interest, the number of seizure-like events in P11-P12 NKCC1$^{+/-}$ mice was closer to wild-type slices: 1.5 ± 0.9 (n = 4 from 2 mice). As a summary of these results, targeted deletion of NKCC1 lowers the seizure threshold and facilitates the development of seizure activity at age P9-P13.

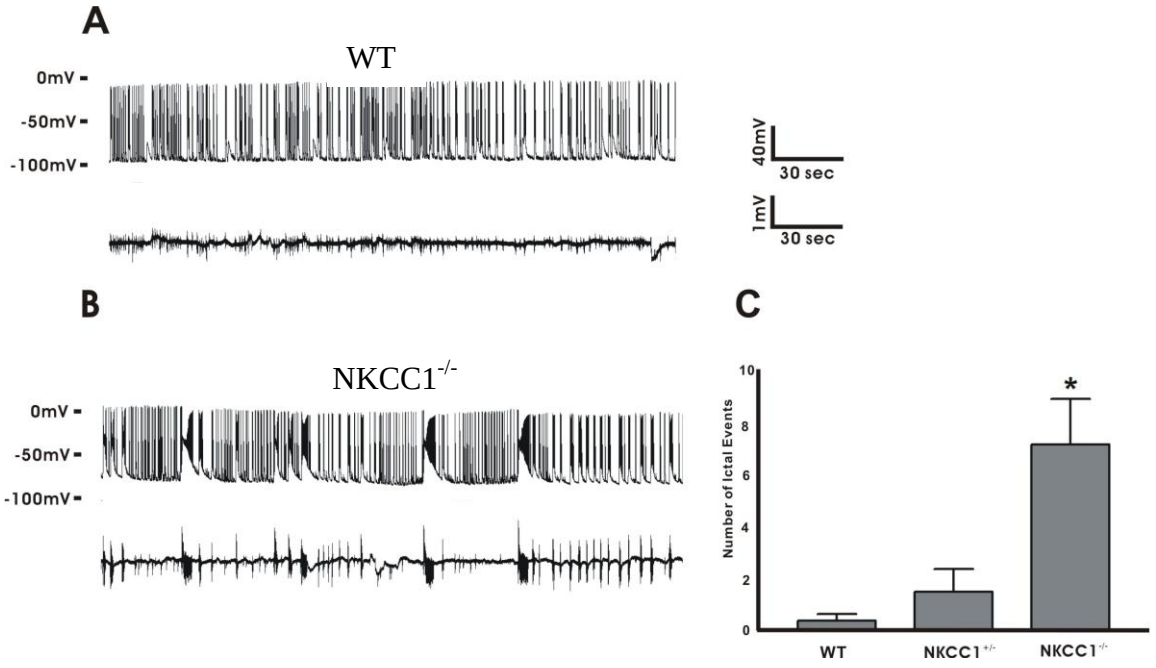

Figure 4-6. 4-AP induces more ictal events in NKCC$^{-/-}$ slices than in wild type slices.

(A) 4-AP application increases the level of spontaneous activities in both wild type and NKCC1$^{-/-}$ slices (B), but ictal events (20-40 seconds duration) are more often seen in NKCC1$^{-/-}$ slices. Cell-attached recording from CA3 pyramidal neurons (upper traces) and field recordings from CA1 *stratum pyramidale* (lower traces) show that the ictal events are synchronized (B). (C) The number of ictal events (duration > 20 seconds) of NKCC$^{-/-}$ slices (7.2 $\pm$ 1.8, n = 6 from 3 mice, P10-P13) are significantly greater than that of wild type slices (0.4 $\pm$ 0.2, n =8 from 4 mice, P10-P13). The number of ictal events seen in NKCC1$^{+/-}$ slices is 1.5 $\pm$ 0.9 (n = 4 from 2 mice, P11-P12).

Discussion

Recent studies have uncovered multiple roles for the Na-K-2Cl cotransporter, NKCC1, in volume and ion homeostasis in the brain, and in diverse pathologies of the CNS. For instance, the endothelial NKCC1 is involved in the increased salt and fluid movement into the brain that is associated with ischemic brain injury (Chen and Sun, 2005; Pedersen et al., 2006). Furthermore, the cotransporter is also involved in glial cell swelling and glutamate release, leading to neuronal excitotoxicity (Chen and Sun, 2005; Su et al., 2002a; Su et al., 2002b). The role of NKCC1 in central neurons is still controversial. Based on an overall decrease in NKCC1 expression during postnatal development, measured by Western blot analysis and immunofluorescence, our lab proposed in 1997 that NKCC1 might accumulate intracellular Cl^- above the concentration predicted by its electrochemical equilibrium potential (Plotkin et al., 1997b). Indeed, NKCC1 is a well-established mechanism of Cl^- accumulation in sensory DRG neurons (Alvarez-Leefmans et al., 1988; Sung et al., 2000). Accumulation of Cl^- through the cotransporter is possible due to the large Na^+ gradient generated by the Na^+/K^+ pump. The combination of down-regulation of NKCC1 expression and up-regulation of KCC2 expression would account for the Cl^- decrease from values above electrochemical potential equilibrium to values below. In fact, in P2-P4 cortical and hippocampal neurons, NKCC1 accumulates Cl^-, as bumetanide application results in >10 mV hyperpolarizing shift in the GABA reversal potential (Sipila et al., 2006; Yamada et al., 2004). However, recent studies in auditory brainstem neurons (Balakrishnan et al., 2003) and retinal

neurons (Zhang et al., 2007) have demonstrated that NKCC1 is not involved in the Cl^- accumulation, as high Cl^- concentrations were still measured in the absence of NKCC1. Whether or not the cotransporter accumulates Cl^- in some central neurons but not in others is still a matter of debate.

At P9-P13, when NKCC1 expression is still relatively high (Dzhala et al., 2005), and KCC2 expression has not yet increased (**Figure 4-1B**), I showed that the pyramidal CA3 neuron E_{Cl} is close to Em (**Figure 4-5C**), indicating that at this age NKCC1 is not active in Cl^- accumulation.

Despite the fact that NKCC1 is not active in accumulating Cl^- at P9-P13, I showed that absence of NKCC1 resulted in significant hyperexcitability, as the number of action potentials measured per unit of time increased significantly (**Figure 4-4B**). Because I was examining the brain of a knockout animal which might have developmental abnormalities, I treated wild-type slices with bumetanide, an inhibitor of the cotransporter with a K_i ranging from 0.5-2 μM. Complete inhibition of cotransporter function by 10 μM bumetanide also induced a significant increase in the number of action potentials measured per unit of time (**Figure 4-4C**), indicating that the increased hyperexcitability observed in the knockout resulted directly from the absence of the cotransporter rather than from developmental abnormalities.

The increased spontaneous electrical activity of pyramidal CA3 neurons in $NKCC1^{-/-}$ slices therefore suggests a different role for the Na-K-2Cl cotransporter. One possible role is the regulation of external K^+ concentration by glial NKCC1 during neuronal activity.

As cells are tightly packed *in vivo* and in brain slices, the K^+ concentration in the extracellular space can increase rapidly during neuronal activity (Avoli et al., 1993; Louvel et al., 1994; Nicholson and Hounsgaard, 1983; Roberts and Feng, 1996). Several studies performed in isolated astrocytes have demonstrated involvement of NKCC1 in the clearance of K^+ (Hertz, 1978; Su et al., 2002a; Su et al., 2002b; Tas et al., 1987; Walz and Hertz, 1984). Thus, the absence of the cotransporter in glial cells would reduce the rate of clearance of K^+ during synaptic activity, resulting in the accumulation of the cation in the extracellular space and hyperexcitability. Alternatively, differential expression of NKCC1 in inhibitory neurons could regulate their excitability, and, if so, its reduction in the knockout mouse or with bumetanide would result in hyperexcitability by decreasing inhibitory tone.

In this study, I also made use of 4-aminopyridine as a seizure-inducing agent. I showed that addition of 50 μM 4-AP induced hyperexcitability in both wild-type and $NKCC1^{-/-}$ slices (**Figure 4-5A2** and **Figure 4-6**). Consistent with the hyperexcitability demonstrated in CA3 pyramidal cells from $NKCC1^{-/-}$ mice or from wild-type mice in the presence of bumetanide, 4-AP induced seizure-like activity in CA3 pyramidal neurons. These seizure activities, synchronous between CA3 and CA1, were rarely seen in wild-type slices under 4-AP treatment. These data confirm that NKCC1 in P9-P13 wild-type brains actively participate in preventing hyperexcitability and the development of uncontrolled, synchronous seizure-like activity. Thus, our data are contrary to those of Dzhala and coworkers who suggested that NKCC1 expression instead facilitates the

development of seizures in the juvenile brain (Dzhala et al., 2005). However, they used high extracellular K^+ (8.5 mM) to induce seizure activity. This high external K^+ concentration alters the function of NKCC1 by increasing the inward driving force for chloride ions. High K^+ also alters the function of KCC2, even though its expression level is relatively low in the developing brain (DeFazio et al., 2000; Rivera et al., 1999). High external K^+ also leads to the accumulation of ions and water in glial cells, and to the release of excitotoxic glutamate (Chen and Sun, 2005). Prevention of this effect in the NKCC1 knockout mouse or by applying the NKCC1 inhibitor, bumetanide, might have contributed to the conclusion that NKCC1 promotes hyperexcitability in the juvenile brain (Dzhala et al., 2005).

At the age when KCC2 expression in the forebrain is much lower than its expression level in the adult CNS, the intracellular chloride level of principal neurons was dramatically affected by the level of neuronal activity in the hippocampus. Indeed, in both $NKCC1^{-/-}$ and wild-type neurons, when hyperactivity and frequent membrane depolarization were induced by 4-aminopyridine, the muscimol response shifted from slightly inward to strongly outward, indicating a rise in the intracellular chloride concentration. This increase in intracellular chloride is likely caused by the chloride influx through the extra-synaptic tonic GABA receptor channels or synaptic GABA receptor channels, or both, during the frequent depolarization of membrane potential. These data indicate the lack of a mechanism for rapid Cl^- regulation. These data are also consistent with previous findings in isolated cortical neurons (See Chapter III) or auditory

brain stem neurons (Ehrlich et al., 1999), that showed that young neurons are unable to handle large shifts in the intracellular Cl^- concentration. The change in the driving force measured under 4-AP (more than 20 mV) is large enough to produce depolarizing GABA responses. Furthermore, the hyperpolarization of resting membrane potential (a side effect of 4-AP) also contributes to increased Cl^- driving force (Avoli and Perreault, 1987; Avoli et al., 1993). The increase in intracellular chloride was fully activity dependent as it could be reversed by blocking non-NMDA glutamate receptors with the antagonist DNQX (**Figure 4-5A3**).

In this study, I have also seen increased frequency of seizure-like activities in CA1 $KCC2^{+/-}$ slices in comparison to wild-type slices in the presence of 4-AP, thus confirming the increased susceptibility to seizure in $KCC2^{+/-}$ mice that was previously reported by us (Woo et al., 2002). Given the importance of the hippocampus in epileptic seizures, and together with the lack of specific inhibitors of KCC2 and the lethality of the KCC2 knockout mouse, the $KCC2^{+/-}$ mouse also provides an excellent model for further studies of seizure development. In summary, I have shown that both NKCC1 and KCC2 participate in important neuronal function as mechanisms preventing the development of hippocampal epileptiform activity.

CHAPTER IV

FINAL CONCLUSIONS AND FUTURE DIRECTIONS

Final Conclusions

The goal of my project was to understand how the cation-chloride cotransporters KCC2 and NKCC1 regulate neuronal $[Cl^-]_i$ and excitability of the hippocampus network. I have addressed the role of KCC2 in active neuronal $[Cl^-]_i$ regulation using cultured cortical neurons and its role in reducing neuronal excitability and seizure susceptibility, using brain slices. I have also revealed that, contrary to previous belief, pharmacological inhibition or genetic deletion of NKCC1 increases neuronal activity and susceptibility to seizures in the developing (P9-P13) hippocampus. The exact mechanism by which NKCC1 is involved in reducing hyperexcitability in the hippocampus remains to be further investigated.

This work provided the first direct and thorough evidence that the developmental increase in the expression of KCC2 causes the developmental decrease of intracellular Cl^-. Indeed, while several studies indicated that KCC2 lowers intracellular $[Cl^-]$, these studies used an nonspecific inhibitor (furosemide), recorded GABA responses using the whole-cell patch configuration, which disrupts the intracellular $[Cl^-]$ (DeFazio et al., 2000), or were not performed in a developmental context (Hubner et al., 2001; Rivera et al., 1999). Here, I showed that the developmental down-regulation of chloride was a

direct consequence of KCC2 activity, as it was abolished in $KCC2^{-/-}$ neurons. In these experiments, I used the gramicidin-perforated patch configuration which is non-invasive to measure the intracellular chloride concentration.

Second, I showed that KCC2 actively counteracts challenges to the intracellular Cl^- concentration and decreases seizure susceptibility. These data provide evidence that acute challenges to intracellular chloride can be rapidly neutralized by the activity of KCC2. Indeed, influx of excessive amounts of chloride due to prolonged (or repetitive) $GABA_A$ receptor activation, or due to depolarization (possibly through passive Cl^- channels (Kakazu et al., 1999)), or due to co-activation of GABA and NMDA receptors renders GABA excitatory, which is detrimental to the normal function of CNS. In support of the role of KCC2 in regulating intracellular Cl^- and GABA function, I also showed that brain slices from $KCC2^{+/-}$ mice, which express half the normal level of KCC2 protein, exhibited increased seizure susceptibility.

Taken together, my work not only confirms previous findings that KCC2 is responsible for the long-term developmental decrease of intracellular $[Cl^-]$ and the developmental switch in the GABA response from depolarizing to hyperpolarizing, but also revealed that KCC2 is active in acutely regulating neuronal Cl^- during challenges and is active in maintaining the stability of neuronal networks.

Finally, I discovered that NKCC1 prevents epileptic seizures in the developing brain, in contrast to a previous report indicating that NKCC1 might facilitate neonatal seizures (Dzhala et al., 2005). I showed that at the age of P9-P13, E_{GABA} is already very

close to the resting membrane potential and NKCC1 inhibition or deletion results in increased seizure susceptibility. My experiments also demonstrated that NKCC1 does not significantly raise the intracellular Cl^- concentration in pyramidal CA3 neurons, thus providing an alternative model for the role of NKCC1 in the central nervous system. This demonstration provides new avenues of investigation. Unlike KCC2, the expression of NKCC1 is not confined to the pyramidal neurons, but this cotransporter is also expressed in epithelial cells, glial cells and interneurons (see Chapter I). Future research on NKCC1 should not be limited to the pyramidal neurons but should investigate other cell types expressing NKCC1.

Future Directions

The regulation of KCC2 in the CNS

As it is now well-established that KCC2 is responsible for the developmental decrease of intracellular chloride concentration and extrusion of excessive Cl^- during challenges, future studies should focus on the regulation of the cotransporter in the CNS. The expression of KCC2 protein in the brain is downregulated by ischemia, oxidative stress, epileptic seizures, growth factors (BDNF) and testosterone (See chapter I). It has been suggested that downregulation of KCC2 might be a general response to different neuronal insults (Rivera et al., 2004). In the case of epilepsy, downregulation of KCC2 would possible worsen seizures and cause greater damage to the brain. Future studies should

focus on the mechanisms of KCC2 downregulation, including the signaling pathways involved in triggering KCC2 removal from the plasma membrane. These studies might provide clues to the discovery and development of novel antiepileptic drugs.

The role of NKCC1 in the CNS

I have found in P9-P13 mice, that NKCC1 deletion results in increased seizure susceptibility. However, the specific mechanism of the function of NKCC1 in the CNS is not clear. Future experiments can be designed to answer the following questions.

Upon network activity, is the extracellular [K^+] accumulating in NKCC1$^{-/-}$ slices or in wild-type slices exposed to bumetanide, to a greater extent than wild-type slices incubated under control conditions? As NKCC1 is expressed in glial cells (see Chapter I), it might serve as a K^+ clearance mechanism. Its inhibition or targeted deletion would then result in K^+ accumulation in the extracellular space. This increase, in turn would depolarize the neurons and increase neuronal network activity. Two types of experiments can be done to address this question. First, the membrane potential of glial cells could be recorded in the presence of absence of NKCC1. As the membrane potential is a direct reflection of the extracellular K^+ concentration, if the extracellular K^+ increases, the glial cells will be more depolarized. Second, a direct measurement of the extracellular K^+ concentration could be made by using potassium-selective micro-electrodes. Recoding could be done under control conditions, or conditions of high network activity (with or without the presence of seizure-inducing agents).

Does the chloride concentration in interneurons play a role in pyramidal neuron excitability? The GABA response in CA3 hippocampal interneurons has been reported to be shunting throughout life due to the counter balance between KCC2 and NKCC1 (Banke and McBain, 2006). To address this question, we could measure the spontaneous IPSP frequency in the pyramidal neuron while changing the intracellular $[Cl^-]_i$ in the interneuron. First, the E_{Cl} and frequency of action potential firing of hippocampal interneurons could be measured using either gramicidin perforated patch-clamp or cell-attached recordings, at different ages in wild-type and NKCC1 knockout slices. Second, we could obtain simultaneous recordings in a CA3 pyramidal neuron and its innervating interneuron with whole-cell patch clamp. The $[Cl^-]$ of the pipette solution of interneuron recording would be varied from 10 mM to 30 mM, which mimics physiological range of intracellular $[Cl^-]$ during development. Third**,** simultaneous recordings in a CA3 pyramidal neuron with whole-cell patch clamp and its innervating interneuron could be perfomed using gramicidin cell-attached patch-clamp. Focal diffusion of bumetanide around the interneuron would also increase $[Cl^-]_i$ and disinhibit the innervated pyramidal neuron. Spontaneous IPSPs would be analyzed and compared within each experiment. The IPSP frequency should decreases in the pyramidal neuron, if the intracellular chloride concentration is reduced in the interneuron. Lucifer yellow would be included in the patch pipette to confirm the identity of the neurons by morphology at the end of each experiment (i.e. after whole-cell break-in in the perforated recording).

Would the seizure susceptibility be affected by deletion of NKCC1 in interneurons or in glia? Once the experiments outlined above are completed, interneuron-specific NKCC1 knockout animals could be generated by driving recombination using interneuron-specific protmoters such as GAD, parvalbumin, calretinin, or calbindin. Similarily, glial-specific NKCC1 knockout could be generated by driving CRE-mediated recombination under the glial acidic fibrillary protein (GFAP) promoter. The seizure susceptibility of these animals would then be evaluated using different seizure inducing agents *in vivo* (behavioral or EEG) and *in vitro* (brain slices recordings).

Summary

In this project, I have provided evidence for a direct link between KCC2 expression/activity and GABA inhibition. I confirmed the important role of KCC2 in stabilizing hippocampal neuronal networks. I also found that, *in vitro*, NKCC1 inhibits seizure activity in young animals, although the exact mechanism by which NKCC1 prevents hyperexcitability remains to be further investigated.

APPENDIX B

GRAMICIDIN PERFORATED PATCH TECHNIQUE IN CULTURED NEURONS AND BRAIN SLICES

Introduction

The patch clamp technique has revolutionized the world of neuroscience. It has been almost 30 years since the patch clamp technique was developed by Neher and Sakmann (Neher and Sakmann, 1992). During the past three decades, many improvements have been made to the basic method and today patch clamping cells plays the central role in electrophysiological studies and membrane biology. There are four major variants of the conventional patch clamp technique: whole cell mode, inside-out patch, outside-out patch, and cell attached mode. Whole cell recording is widely used because it is fairly easy to use and the macroscopic currents that are recorded are easy to analyze. But the whole cell recording technique has its problems. The dialysis of the recorded cell by the pipette solution washes out various active cytoplasmic components and thus compromises important functions such as phosphorylation-dephosphorytion, second messenger signaling, etc. Very importantly, it also artificially changes the intracellular ionic environment. A new method was introduced by the invention of the nystatin perforated patch technique (Horn and Marty, 1988) that solves most of the problems caused by the whole cell patch configuration. Today, there are several perforated patch methods that

evolved from the original nystatin perforated patch. There are three major perforated patch techniques which use nystatin, amphotericin B, and gramicidin as ionophores.

Despite the different names of the drugs, they are all ionophores that create pores in the plasma membrane allowing movement of small ions such as Na^+, H^+, K^+, and Cl^- (except gramicidin). These ions can flow through the pores in the membrane and thus provide electrical access from the recording pipette to the inside of cell. Multivalent ions such as Mg^{2+}, Ca^{2+}, and large molecules cannot pass through these pores. Consequently, whole cell currents can be recorded using these perforated patch techniques, with a minimal disturbance to the intracellular content. This technique has been widely used in studying voltage gated ion channels (Akbarali and Giles, 1993; Watsky et al., 1992), membrane transport such as Na-K pump (Oike et al., 1993; Urbach et al., 1996), cation-chloride cotransport (Ehrlich et al., 1999; Nabekura et al., 2002), and ligand gated channels (Meredith et al., 2003; Yoshimura and Tsumoto, 1994). Among the three ionophores, gramicidin has gained a lot of interest in recent years because of its unique features.

Gramicidin was first found from the soil bacterium *Bacillus brevis* and used as an antibiotic (Okuda et al., 1963; Winnick et al., 1961). Gramicidin A, B and C are small pore forming tryptophan-rich linear peptides, which share the common structure: Formyl-L-XXX-Gly-L-Ala-D-Leu-L-Ala-D-VaI-Val-L-Trp-D-Leu-L-YYY-D-Leu-L-Trp -D-Leu-L-Trp-Ethanolamine, where XXX denotes Val or Ile, and YYY denotes Trp, Phe and Tyr in gramicidin A, B, C, respectively (Andersen, 1984). Each gramicidin channel is

formed by the dimerization of two non-conducting subunits, which are bound to the lipid bilayer membrane through hydrogen bonds (Andersen et al., 2005; Wallace, 1990). Gramicidin channels are among the most extensively studied and well defined ion channels. They have restricted selectivity towards different ion species. While water and small monovalent cations such as H^+ and Na^+ can permeate with ease, anions (Cl^-, etc.) and divalent cations (Ca^{++}, etc.) cannot move easily (Sandblom et al., 1977). Due to this fact, gramicidin not only provides a great tool for the study of membrane bound ion channels, but also can serve as a solution for particular electrophysiological paradigms when it is important to preserve intracellular chloride intact.

Cl^- is one of the major ions in cells and tissues. Cl^- is important for neuronal excitability, salt secretion and reabsoprtion, cell volume regulation, and pH regulation. In the central nervous system, γ-aminobutyric acid (GABA) and glycine receptors are both Cl^- channels. The polarity of GABA or glycine response is dependent on the driving force for chloride. If the chloride equilibrium potential (E_{Cl}) is more positive than the membrane potential, Cl^- flows out of the neuron during $GABA_A$ or glycine receptor activation and the membrane is depolarized. If E_{Cl} is more negative than the membrane potential, Cl^- will flow into the neuron and the membrane will hyperpolarized. In contrast, if ECl is more positive than the membrane potential, Cl^- will flow out of the neuron and the membrane will depolarized. As we have seen in this document, intracellular Cl^- is regulated by cation-chloride cotransporters and neither conventional whole cell patch nor nystatin perforated patch can be used to record GABA or glycine receptor activity

without disturbing the intracellular Cl^-. Sharp electrode intracellular recording also somewhat influences intracellular Cl^-, although to a lesser degree. Cl^- electrodes, which have been used successfully in large cells to measure intracellular Cl^-, are too large to be practical to record activity of small CNS neurons. Gramicidin instead, when dissolved in the pipette solution, can provide electrophysiological recordings in CNS neurons without disrupting intracellular chloride concentration. The gramicidin perforated patch technique has now been developed for a decade and it truly has made a significant contribution to the study of the inhibitory transmitter system in both the central and peripheral nervous system. (Akaike, 1996; Kyrozis and Reichling, 1995) (Rhee et al., 1994; Tajima et al., 1996)

Even though the gramicidin perforated patch technique has many advantages, it does have limitations. One of the major disadvantages is that perforation takes quite a long time, from 10 minutes to almost an hour. The other disadvantage is its high series resistance, usually ranging from 40 to 70 MΩ. Many factors contribute to the perforation time and the series resistance, such as the pipette size and shape, the temperature and cell membrane properties. These problems are more acute in brain slice recordings.

The Gramicidin Perforated Patch Method

Patch pipette and solution filling

Gramicidin D (a mixture of gramicidin A, B and C, from Sigma) is commonly used in gramicidin perforated patch experiments. Gramicidin is very sensitive to humidity so any unused gramicidin needs to be refrigerated and desiccated. A stock solution of 10 mg/ml is usually made by dissolving gramicidin in methanol (Akaike, 1996) or DMSO (Kyrozis and Reichling, 1995). During my experiments, for some reason using DMSO as a vehicle for gramicidin I achieved more consistency in perforation time and series resistance than using methanol. The stock solution is then added to the pipette solution (140-150 mM KCl or CsCl, 10 mM HEPES, pH 7.4) to reach a final concentration of 5-100 μg/ml (the final DMSO concentration in the pipette should not exceed 0.2%). The large variation of final concentration required from gramicidin is probably due to different experimental conditions such as temperature, pipette solution composition, brain slices vs. isolated/cultured neurons, pipette size and ways to obtain a seal (Ebihara et al., 1995; Euler and Wassle, 1998; Singer et al., 1998; Yamada et al., 2004). Usually for recording in cultured neurons, high concentration of gramicidin (20-100μg/ml) is used, whereas relatively low concentration of gramicidin (5-20μg/ml) is used for brain slices experiments. Because gramicidin is sensitive to humidity and loses its activity in water based solutions, the final pipette solution containing gramicidin needs to be freshly made

for each experiment (i.e. every hour) and the stock solution should be discarded everday after use.

The pipette for gramicidin perforated patch is made from thin walled borosilicate glass capillaries (WPI) on vertical (Narishige) or horizontal multistage pipette pullers (Sutter). During my experiments I have used capillaries of three different dielectric constants and softening points: patch clamp capillary glass type #0010 with dielectric constant 6.7 and softening point 625 degrees (Fahrenheit), patch clamp capillary glass type #8250 with dielectric constant 4.9 and softening point 720 degrees and the thin wall single barrel glass TW150. Even though the two patch clamp capillaries form very tight seals (~GΩ) and are excellent for whole-cell and single channel patch experiments, they increase the spontaneous break-ins during perforated patch experiments and turn perforated patch conformation into whole-cell. Glass type TW150 forms less tight seal (5-10GΩ) but the spontaneous break-ins are rarely seen. Pipettes with 3-5 MΩ resistance are used for recordings in most neurons. The presence of gramicidin in the tip is well-known to disrupt GΩ seal formation and gramicidin containing pipette solution that leaks onto neurons can also cause depolarization of the neuron. To prevent this, the pipette tip is usually front-filled with gramicidin-free pipette solution, and then back-filled with gramicidin containing pipette solution. Extra care must be taken while performing gramicidin perforated patch in brain slices, since positive pressure is usually applied to the pipette tip to achieve a successful GΩ seal. Tapping of the pipette is necessary to get rid of any air bubbles in the pipette in patch clamp experiments.

However, it also accelerates the mixing of back-filled gramicidin solution with the gramicidin-free solution in the tip. Thus any tapping must be done before the back-filling of gramicidin-containing solution and careful back-filling using a fine needle can avoid any air bubble built-up in the pipette. Glass capillaries with filaments may be a better choice if it is hard to get rid of air bubbles.

Getting the seal and the perforation

For cultured cell experiments, getting the seal is quite easy since none or little positive pressure is needed at the pipette tip to reach the surface of the cell. However, for brain slice experiments, positive tip pressure is required for the pipette tip to move through a layer of dead cells and connective tissue, before touching the surface of the intended cell. If too little pressure is applied, the debris will get in the way of the pipette tip and prevent a perfect GΩ seal. If too much pressure is applied, the gramicidin inside the pipette will reach the tip prematurely and also ruin the GΩ seal. Therefore delicate control of the positive pressure is necessary. When the tip of the pipette touches the cell membrane, it can be detected visually (from the monitor) or electrically (from the sudden increase of pipette resistance). The positive pressure is released and negative pressure by suction or syringe is immediately applied to form a seal. After a GΩ seal is formed, no further negative pressure should be applied. Gramicidin molecules start to insert into the patch membrane and form ionophores as soon as the seal is formed. In voltage clamp experiments, the holding potential should be as close to resting membrane potential as

possible (-60~-70 mV), because larger holding current will depolarize the cell and induce changes to $[Cl^-]_i$ through tonic GABA receptor activity or other chloride conductances.

By applying 10mV hyperpolarizing short pulses, the series resistance is monitored and calculated from the size and decay time (τ) of the capacitive transient in membrane test of pClamp 9.0 (**Figure A-1**). In 10-30 minutes, the series resistance will usually stabilize < 100MΩ. The exact stabilized series resistance depends on the final concentration of gramicidin in the pipette and also on the temperature of the bath (Akaike, 1996). Higher concentrations of gramicidin may cause spontaneous break-ins and result in the alteration of the $[Cl^-]_i$ by the pipette solution. Fluorescent dyes (Lucifer yellow) are sometimes added to the pipette solution as an indicator of spontaneous break-ins. No series resistance compensation should be used since oscillations will probably occur because the series resistance is usually high (40-70MΩ) in perforated patch experiments.

Calculate E_{Cl} from Voltage Clamp data

Two alternative methods are typically used when E_{Cl} is to be measured by voltage clamp experiments: the vary-holding method (**Figure A-2A**), and the voltage ramp method (**FigureA-2B**). The data analysis methods that will be discussed next will pertain mostly to voltage ramp experiments, but can also be applied to vary-holding experiments. It is common knowledge that the equivalent circuits of excitable membranes comprise capacitors, resistors, and batteries (**Figure A-3**). In single-electrode voltage clamp mode, the voltage at the tip of the recording pipette is controlled by a circuit of amplifiers.

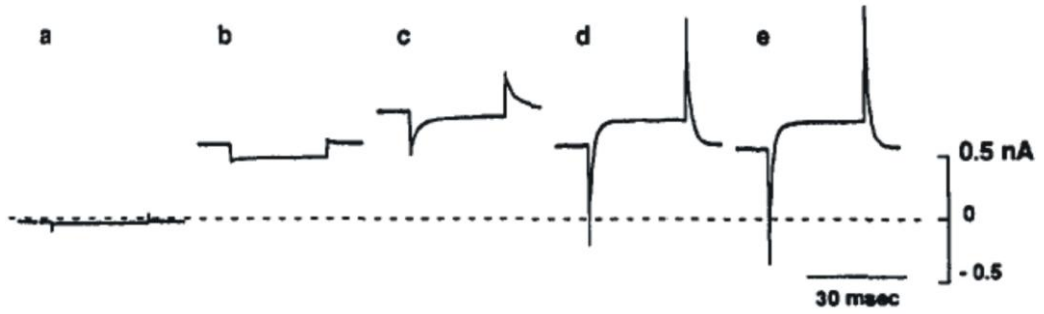

From Tajima et al. 1996.

Figure A-1. **Example pulses showing current at 0, 2, 4, 6, 10, 13 and 16 minutes after GΩ seal.**

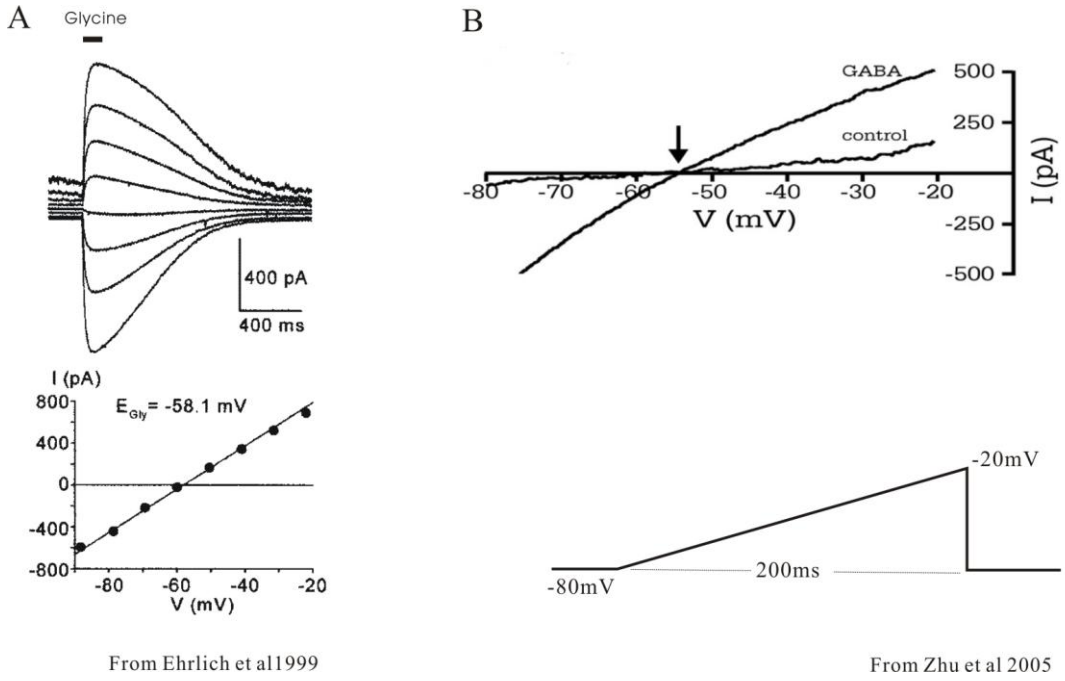

From Ehrlich et al1999

From Zhu et al 2005

Figure A-2 Vary-holding and Voltage ramp recordings.

(A) Here, GABA/Glycine receptor Cl^- current is recorded by applying glycine briefly onto a cell, which is being clamped at different voltages. The V value at the I intercept of the I-V trace is the reversal potential of GABA/Glycine (EGABA/EGly) (B) A brief ramp from -80 to -20mV is applied to the cell membrane and a current response is recorded. The V value where the control trace meets the test trace is EGABA.

Before GABA is applied, the current flow through the pipette (I_0) can be expressed using the following equation:

$$I_0 = \frac{E}{R_{seal}} + \frac{E - E_m}{R_s + R_m} + C_m \frac{\Delta V}{\Delta T}$$

C_m*$\Delta V/\Delta T$ is the capacitive current introduced by the voltage ramp. Since the whole-cell capacitance of neurons is about 10~50 pF, and $\Delta V/\Delta T$ = 300 mV/s (this is the rate for **Figure A-2B**), the capacitive current equals C*$\Delta V/\Delta T \leqslant$ 50pF * 300 mV/s = 15 pA. This current is much smaller than the current value at V=0, so it is negligible.

Then, the equation transforms into:

$$I_0 \sim \frac{E}{R_{seal}} + \frac{E - E_m}{R_s + R_m} \qquad (1)$$

However, if the ramp is too fast (for example, -80 to -20 mV in 20 ms, resulting in a rate of 3000 mV/s), the capacitive current may be too large to ignore (150 pA). Thus fast ramps need to be avoided.

After GABA is applied (**Figure A-3**, right figure), the current flowing through the pipette (I) can be expressed using the following equation:

$$I = \frac{E}{R_{seal}} + I_2$$

The above equation can be further transformed by considering the whole circuit:

$$I = \frac{E}{R_{seal}} + \frac{E - E_{Cl} + \frac{R_{GABA}}{R_m}(E - E_m)}{R_{GABA} + \frac{R_{GABA} R_s}{R_m} + R_s} \qquad (2)$$

As shown in equation (1) and (2), both currents consist of a leak component (E/R_{seal}) and a membrane component. The leak component is quite small, due to a large R_{seal} (> 2GΩ),

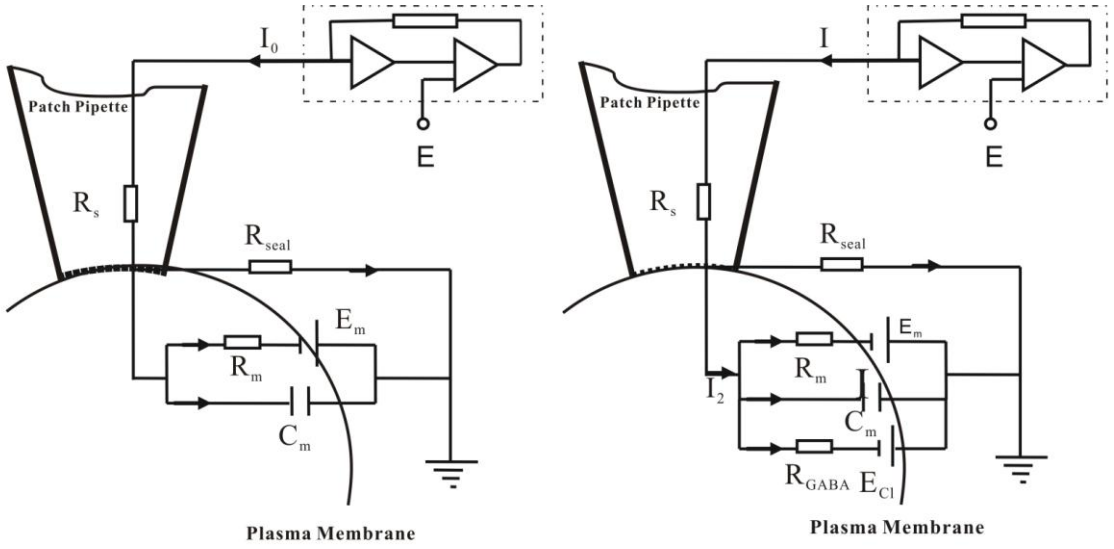

R_s: Series Resistance **R_{seal}: Seal Resistance** **E: Commanding potential**
R_m: Membrane Resistance **E: Command Potential**
E_m: Membrane Potential **C_m: Whole Cell Capacitance**

Figure A-3 Equivalent circuit of gramicidin perforated patch clamp before (left) and after (right) $GABA_A$ receptors are activated.

and can be subtracted using the leak subtraction function of Pclamp 9.0. Thus, the two equations (1) and (2) can be transformed into (3) and (4), respectively.

$$I_0 = \frac{E - E_m}{R_s + R_m} \quad (3)$$

$$I = \frac{E - E_{Cl} + \frac{R_{GABA}}{R_m}(E - E_m)}{R_{GABA} + \frac{R_{GABA}R_s}{R_m} + R_s} \quad (4)$$

From the control trace we can easily obtain:

$$E_m = V_1$$

$$R_m = \frac{1}{S_1} - R_s$$

(Rs can be measured by membrane test or fitting transient in Clampex 9.0)

And from the GABA trace and equation (4), we can obtain:

$$S_2 = \frac{1 + \frac{R_{GABA}}{R_m}}{R_{GABA} + \frac{R_{GABA}R_s}{R_m} + R_s}$$

Thus, R_{GABA} can be calculated from the results above as:

$$R_{GABA} = \frac{R_m(R_sS_2 - 1)}{1 - \frac{S_2}{S_1}} \quad (5)$$

At V_0, equation (3) equals equation (4).

$$I = \frac{V_0 - E_{Cl} + \frac{R_{GABA}}{R_m}(V_0 - E_m)}{R_{GABA} + \frac{R_{GABA}R_s}{R_m} + R_s} = \frac{V_0 - E_m}{R_s + R_m}$$

Further rearrangements of the equation yields equation (6):

$$E_{Cl} = V_0 - \frac{R_{GABA}R_s}{R_m^2}(V_0 - V_1) - \frac{R_s}{R_m}(V_0 - V_1) \quad (6)$$

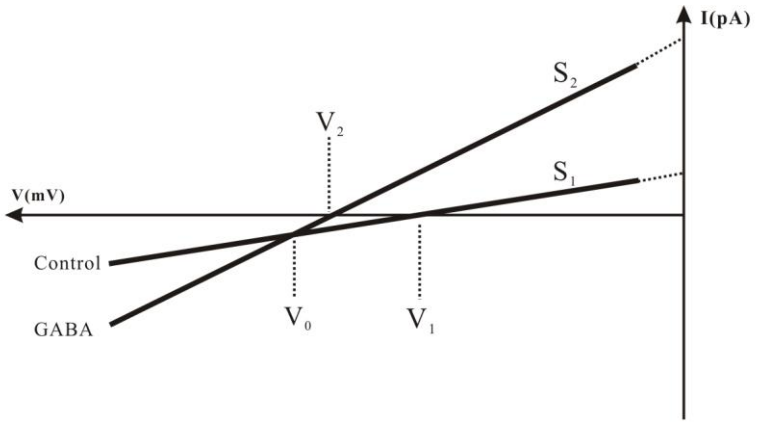

S_1: Slope of control trace S_2: Slope of GABA trace
V_1: V Intercept of control trace V_2: V intercept of GABA trace
V_0: The V value when control trace and GABA trace cross each other

Figure A-4. I-V traces after leak subtraction.

and after we substitute R_m with $(1/S_1\text{-}R_s)$ and R_{GABA} with the value from equation (5), we get the final solution to E_{Cl}:

$$E_{Cl} = V_0 + (V_0 - E_m)\frac{R_s S_2 S_1}{(S_1 - S_2)} = V_0 - (V_0 - E_m)\frac{R_s}{(\frac{1}{S_2} - \frac{1}{S_1})} \qquad (7)$$

If we name $\mathbf{R_1} = \mathbf{1/S_1}$ and $\mathbf{R_2} = \mathbf{1/S_2}$, then Equation (7) turns into Equation (8):

$$E_{Cl} = V_0 - (V_0 - E_m)\frac{R_s}{(R_1 - R_2)} \qquad (8)$$

Equation (8) is the final equation for series resistance correction for E_{Cl} measurements. From equation (8), it is obvious that E_{Cl} does not necessarily equal V_0, which is the V value when the two traces cross. However, its value is also affected by the resting membrane potential E_m, the series resistance and the input resistances of resting membrane before ($\mathbf{R_1}$) and after GABA application ($\mathbf{R_2}$). The input resistance of resting membrane is usually uniform for the same types of neuron, while the input resistance after GABA application $\mathbf{R_2}$ greatly varies with the concentration and amount of GABA applied. In whole-cell patch clamp experiments, given the fact that R_s (<10MΩ) is usually much smaller than R1 and R_s can be easily compensated, E_{Cl} is approximately equal to V_0. However, in perforated patch experiments, R_s is much higher (40 to 70 MΩ) and series resistance compensation is not practical. Thus, E_{Cl} value needs to be corrected from V_0 according to equation (8).

From the above reasoning, we can also see that in voltage clamp experiments the the membrane potential is not actually clamped. Instead, the clamped voltage is the voltage at the pipette tip. The actual potential at the membrane is the clamp voltage E minus the

voltage drop at the series resistance $I_0 * R_s$. From equation (3), we get the actual potential at the membrane $E_{actual} = E - I_0 * R_s = \frac{R_s E_m + R_m E}{R_m + R_s}$. Thus the actual potential equals control potential E only when Rs << Rm. In experiments when series resistance cannot be ignored, series resistance correction is necessary during the experiment or the recorded data must be corrected.

Gramicidin in cell-attached recordings

One critical issue related to the measurement of internal Cl^- in brain tissue is the accuracy of GABA reversal potential measurements, especially in young neurons that have high membrane resistance. The gramicidin perforated patch clamp is certainly the most used electrophysiological method to assess the intracellular Cl^- concentration in neurons. In isolated cells, the method is relatively straightforward as application of positive pressure is not necessary during the advancing of the pipette towards the cell body. However, in brain slice experiments, as the pipette has to find its way through cellular material in tissue, positive pressure is typically applied. To avoid leak of gramicidin due to the positive pressure, gramicidin-free pipette solution is typically placed into the tip of the pipette whereas the gramicidin-containing pipette solution is backfilled. This maneuver eventually lowers the effective gramicidin concentration in contact with the membrane patch. In conventional gramicidin perforated patch recordings, consistency in the series resistance is critical in measuring with accuracy the GABA reversal potential. As the overall series resistance varies due to the variability in the amount of gramicidin free

solution, the temperature, and the positive pressure applied, it is difficult to obtain accurate GABA reversal potentials. Furthermore, as it takes a long time for the series resistance to stabilize. In perforated patch experiments, a high concentration of ionophore is often added to the pipette solution to achieve low series resistance. However higher concentration of the ionophores increases the chance of spontaneous break-ins, which lead to dialysis of the cellular milieu by the pipette solution. Therefore the conventional gramicidin perforated patch method is delicate in slice preparations. To resolve these problems, I switched to and modified the convention cell-attached patch clamp by adding very little amount of gramicidin in the pipette solution (<5 μg/ml in the backfilling solution).

Cell-attached recording was first used by Fenwick et al. (Fenwick et al., 1982), and later used by other laboratories (Michelson and Wong, 1991; Perkins and Wong, 1996; Tyzio et al., 2003). Cell-attached recordings are accomplished by forming a seal with a patch electrode, without further rupture of the membrane. The internal solution can be either high KCl or high NaCl. Compared to the whole-cell or perforated patch method, the cell-attached recording method is the least invasive.

The cell-attached method has been thoroughly reviewed by Perkins (Perkins, 2006). Depending upon the quality of the seal, cell-attached recordings can either be used to record action currents (loose seal), inject current, or record membrane potential (tight seal). To record membrane potential, two conditions must be met concomitantly: a tight

seal, and the current clamped at I=0 (Mason et al., 2005; Perkins, 2006). The recorded voltage (V) and the actual membrane potential (E_m) have then the following relation:

$$V = \frac{R_{Seal}}{R_{Seal} + R_{Patch} + R_m} E_m$$

R_{Seal} is the seal resistance which is normally >2GΩ, while R_m and R_{Patch} are the whole cell membrane resistance and patch resistance, respectively. When $R_{Seal} << R_{Patch} + R_m$, V~0 (loose patch). When $R_{Seal} >> R_{Patch} + R_m$, $V = E_m$ (ideal tight patch). In reality, since R_{Patch} is smaller but somewhat comparable to R_{Seal}, the recorded membrane potential is between 0 and E_m. If R_{Seal} is 20 times more than $R_{Patch} + R_m$, V will be equal to ~95% E_m. For pyramidal neurons, $R_{Patch} + R_m$ ranges from 1GΩ to 10GΩ (Perkins, 2006). Thus, to record membrane potential with >95% fidelity, a very tight seal (20~200GΩ) is necessary but hard to achieve. However, if an effort is made to reduce $R_{Patch} + R_m$, one can achieve nearly the actual membrane potential recording with less restrictions on the seal requirement. Because the value of R_m is usually consistent for adult neurons, R_{Patch} becomes the determining factor of V. With a very low concentration of gramicidin (same for other ionophores) in the pipette solution, $R_{Patch} + R_m$ can be reduced to 200-300 MΩ (measured by membrane test in Clampex 9.0, not published). In that case, a 4-6 GΩ seal is sufficient to maintain 95% fidelity during membrane potential recordings. The final pipette concentration of gramicidin used in my experiments is less than 5 μg/ml, with a fair part of the pipette tip filled with gramicidin-free pipette solution. Compared to the traditional gramicidin perforated patch technique, this cell-attached method using a low

concentration of gramicidin provides a less invasive and faithful recording of membrane potential, with less concern of series resistance. It greatly reduces the number of spontaneous break-ins. I have only experienced one spontaneous break-in during my experiments. However, the recording mode must be current clamp at zero current since any current injection will cause large aberration in the recorded voltage due to the large R_{Patch}. By including low concentrations of gramicidin, the patch resistance is diminished significantly compared to the GΩ seal, and the recorded membrane potential becomes very close to actual membrane potential. Furthermore, with this method, the peak potential of the evoked-muscimol response is also very close to the actual E_{GABA}, as most of the current is shunted through the GABA conductance, away from the membrane resistance (**Figure A-5A**, equation (1) and (3)).

In conclusion, the gramicidin perforated patch method and the cell-attached recording (with a low concentration of gramicidin) provide us useful tools to study the regulation of intracellular chloride. These methods are much less invasive than the conventional whole-cell patch clamp technique. Thus, the data obtained with these methods are better representations of actual biological processes.

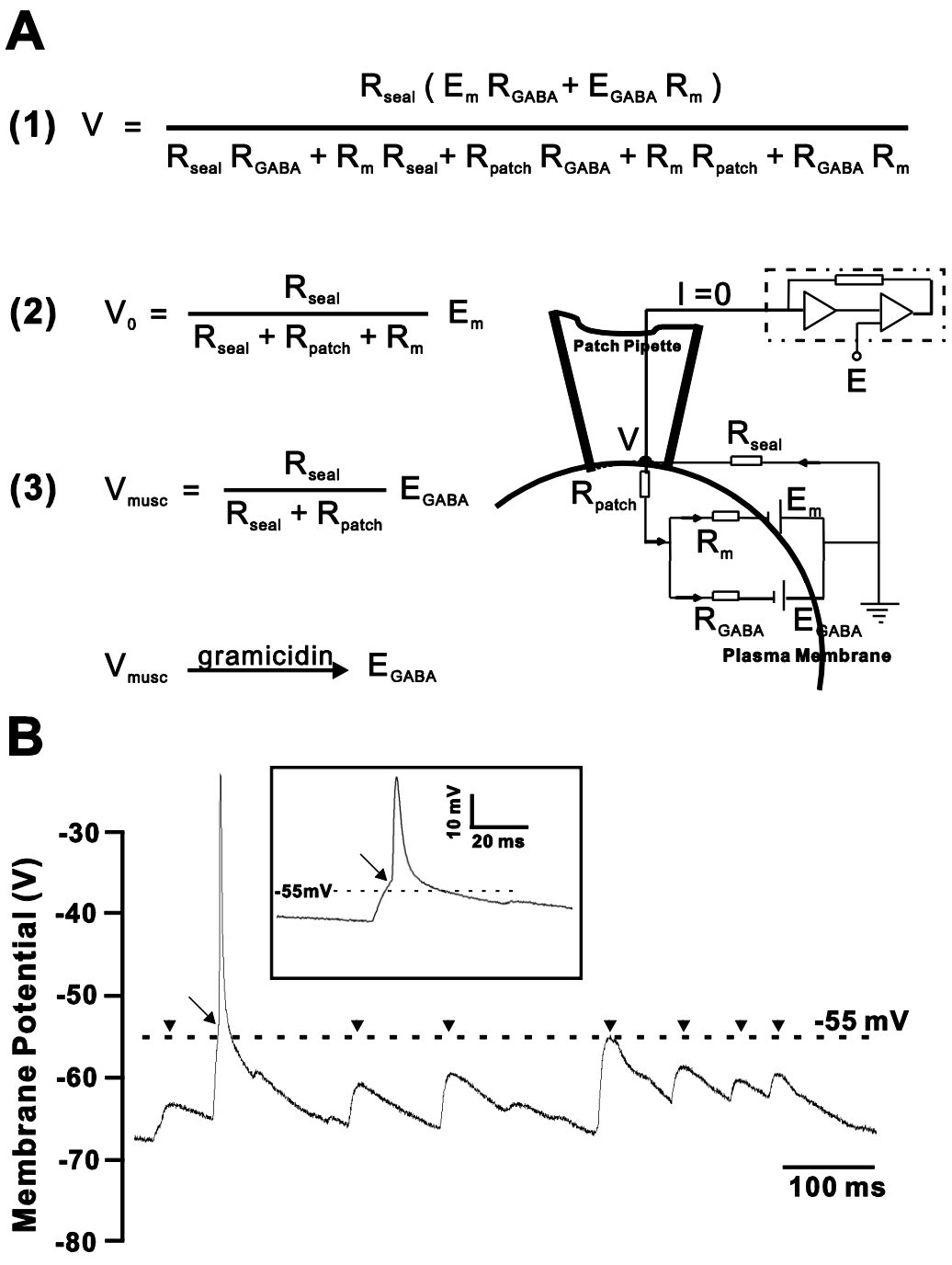

Figure A-5. The application of low-gramicidin cell-attached patch recording.

(A) Relationship between the measured potential and the membrane potential. The recorded membrane potential, V, is represented by resistances and potentials in (1). When $GABA_A$ receptor is not activated, R_{GABA} is infinite and the representation of V is reduced to (2). When $GABA_A$ receptor is activated and the cell membrane resistance is very large in young age CA3 pyramidal neurons, R_{GABA} is insignificant compared to R_{Seal} and the representation of V is reduced to (3). In our experiments, R_{Patch} is significantly reduced by gramicidin perforation, thus R_{Patch} can also be ignored and V is a very close representation of the actual E_{GABA}. R_{Seal} is the seal resistance, Rm is the whole cell membrane resistance, and R_{Patch} is the patch resistance. The equivalent circuit of cell-attached patch clamp is also drawn. When the cell is clamped at current zero, the two batteries and the seal shunting resistance forms a closed circuit resistance, E_{GABA} is GABA reversal potential, R_{GABA} is GABA resistance at peak muscimol response, and Em is the resting membrane potential. (B) Continuous measurement of membrane potential (V) by low-gramicidin cell-attached patch recording of a P13 CA3 pyramidal neuron. An action potential (arrow) is triggered at ~ -55 mV (Kandel et al., 2000) and the recorded resting membrane potential ranges from -65 to -75mV. Note that the action potential did not overshoot 0 mV, due to the artificial cut-off explained in (Perkins, 2006), and the recording in the cell body rather than axon. Membrane depolarization that did not reach threshold (arrowheads) failed to result in action potential firing. Inset shows the action potential with expanded time scale.

APPENDIX B

HCO_3^- AND THE REVERSAL POTENTIAL OF GABA (E_{GABA})

Under physiological conditions, only Cl^- and HCO_3^- can pass through the ion channel of GABAA receptors. The reversal potential of $GABA_A$ receptors (E_{GABA}) can be determined from the Goldman-Hodgkin-Katz equation,

$$\mathbf{E_{GABA} = RT/F * Ln ((P_{Cl}[Cl^-]_i+P_{HCO3}[HCO_3^-]_i)/(P_{Cl}[Cl]_o+P_{HCO3}[HCO_3^-]_o))}$$

with R being Gas Constant, T being the absolute temperature and F being Faraday's constant.

The estimated value of the ratio P_{HCO3}/P_{Cl} ranges from 0.18 to 0.6 in different culture neurons according to other ion permeability studies (Bormann et al., 1987; Fatima-Shad and Barry, 1993; Kaila and Voipio, 1987) and the variations may be methodological instead of biological (Farrant and Kaila, 2007). In the following statements, I assumed P_{HCO3}/P_{Cl} to be 0.2. Thus the E_{GABA} becomes

$$\mathbf{E_{GABA}= 59\ mV * log((5[Cl^-]_i+ [HCO_3^-]_i)/(5[Cl]_o+ [HCO_3^-]_o)).}$$

Since the HCO_3^- concentration in the cerebral spinal fluid (CSF) is 26mM and we assume $[Cl^-]_o$ is 150 mM, $[HCO_3^-]_o$ is much smaller and can be ignored in comparison to $5x[Cl^-]_o$(150 mM x 5 = 750 mM). Therefore the equation can be further converted to

$$\mathbf{E_{GABA} = 59\ mV * log(([Cl^-]_i+0.2[HCO_3]_i^-)/[Cl^-]_o).}$$

After rearrangement, we get

E_{GABA} = -59 mV * log($[Cl^-]_o$ / ($[Cl^-]_i$+0.2$[HCO_3^-]_i$)).

Typically, neurons have an intracellular pH around 7.2 and extracellular PH 7.4, so the $[HCO_3^-]_i$ is calculated to be 16 mM from **$[HCO_3^-]_i$ x $[H^+]_i$ = $[HCO_3^-]_o$ x $[H^+]_o$** (ALVAREZ-LEEFMANs, 1990). Thus the EGABA now is

E_{GABA} = -59 mV * log($[Cl^-]_o$ / ($[Cl^-]_i$+3.2)).

Thus EGABA is not exactly determined by the ratio between extracellular and intracellular chloride concentration. A modifier of 3.2mM is added on top of $[Cl^-]_i$ by HCO_3^-. In young neurons when intracellular chloride is high (20-30mM), the effect of HCO_3^- is negligible. However, in mature neurons where intracellular chloride is decreased by KCC2, HCO_3^- renders EGABA more depolarized. (Assuming that $[Cl^-]_o$ is 150mM and $[Cl^-]_i$ is 8mM, theoretically EGABA will be -75.0mM in HEPES buffer and -66.4mV in aCSF with the presence of HCO_3^-). Therefore when comparing data recorded in normal aCSF and HCO3-free aCSF, this difference in E_{GABA} needs to be taken into consideration, especially in mature neurons.

Other than directly participating in the ion flux through $GABA_A$ receptors, HCO_3^- can also cause accumulation of intracellular Cl- through the anion exchanger AE3 and further affect the reversal potential of GABA and Glycine receptor ion channels (Hentschke et al., 2006; Irie et al., 1998). The role of AE3 in the developmental regulation of intracellular chloride concentration in neurons remains to be further studied. The role of HCO_3^- in EGABA has been reviewed very recently by Farrant and Kaila (Farrant and Kaila, 2007).

In summary, HCO3- ion affects the reversal potential of GABA, especially when intracellular $[Cl^-]_i$ is downregulated in mature neurons. HCO_3^- may also increase the intracellular chloride concentration through the anion-exchanger AE3 and shift E_{GABA} to more depolarized value.

REFERENCES

Adragna, N. C., Fulvio, M. D., and Lauf, P. K. (2004). Regulation of K-Cl cotransport: from function to genes. J Membr Biol *201*, 109-137.

Aguado, F., Carmona, M. A., Pozas, E., Aguilo, A., Martinez-Guijarro, F. J., Alcantara, S., Borrell, V., Yuste, R., Ibanez, C. F., and Soriano, E. (2003). BDNF regulates spontaneous correlated activity at early developmental stages by increasing synaptogenesis and expression of the K(+)/Cl(-) co-transporter KCC2. Development *130*, 1267-1280.

Akaike, N. (1996). Gramicidin perforated patch recording and intracellular chloride activity in excitable cells. Prog Biophys molec Biol *65*, 251-264.

Akbarali, H. I., and Giles, W. R. (1993). Ca2+ and Ca(2+)-activated Cl- currents in rabbit oesophageal smooth muscle. J Physiol *460*, 117-133.

ALVAREZ-LEEFMANs, F. J. (1990). Intracellular Cl- regulation and synaptic inhibition in vertebrate and invertebrate neurones. In Chloride Channels and Carriers in Nerve, Muscle and Glial Cells. (Plenum Press, New York.).

Alvarez-Leefmans, F. J., Gamiño, S. M., Giraldez, F., and Nogueron, I. (1988). Intracellular chloride regulation in amphibian dorsal root ganglion neurons studied with ion-selective microelectrodes. J Physiol (Lond) *406*, 225-246.

Alvarez-Leefmans, F. J., Leon-Olea, M., Mendoza-Sotelo, J., Alvarez, F. J., Anton, B., and Garduno, R. (2001). Immunolocalization of the Na(+)-K(+)-2Cl(-) cotransporter in peripheral nervous tissue of vertebrates. Neuroscience *104*, 569-582.

Andersen, O. S. (1984). Gramicidin channels. Annu Rev Physiol *46*, 531-548.

Andersen, O. S., Koeppe, R. E., 2nd, and Roux, B. (2005). Gramicidin channels. IEEE Trans Nanobioscience *4*, 10-20.

Aronica, E., Boer, K., Redeker, S., Spliet, W. G., van Rijen, P. C., Troost, D., and Gorter, J. A. (2007). Differential expression patterns of chloride transporters, Na+-K+-2Cl--cotransporter and K+-Cl--cotransporter, in epilepsy-associated malformations of cortical development. Neuroscience *145*, 185-196.

Aronica, E., and Gorter, J. A. (2007). Gene expression profile in temporal lobe epilepsy. Neuroscientist *13*, 100-108.

Attmane-Elakeb, A., Mount, D. B., Sibella, V., Vernimmen, C., Hebert, S. C., and Bichara, M. (1998). Stimulation by in vivo and in vitro metabolic acidosis of expression of rBSC1, the Na-K(NH4)-2Cl cotransporter of the rat medullary thick ascending limb. J Biol Chem *273*, 33681-33691.

Avoli, M. (1996). GABA-mediated synchronous potentials and seizure generation. Epilepsia *37*, 1035-1042.

Avoli, M., Mattia, D., Siniscalchi, A., Perreault, P., and Tomaiuolo, F. (1994). Pharmacology and electrophysiology of a synchronous GABA-mediated potential in the human neocortex. Neuroscience *62*, 655-666.

Avoli, M., and Perreault, P. (1987). A GABAergic depolarizing potential in the hippocampus disclosed by the convulsant 4-aminopyridine. Brain Res *400*, 191-195.

Avoli, M., Psarropoulou, C., Tancredi, V., and Fueta, Y. (1993). On the synchronous activity induced by 4-aminopyridine in the CA3 subfield of juvenile rat hippocampus. J Neurophysiol *70*, 1018-1029.

Balakrishnan, V., Becker, M., Lohrke, S., Nothwang, H. G., Guresir, E., and Friauf, E. (2003). Expression and function of chloride transporters during development of inhibitory neurotransmission in the auditory brainstem. J Neurosci *23*, 4134-4145.

Banke, T. G., and McBain, C. J. (2006). GABAergic input onto CA3 hippocampal interneurons remains shunting throughout development. J Neurosci *26*, 11720-11725.

Bartho, P., Payne, J. A., Freund, T. F., and Acsady, L. (2004). Differential distribution of the KCl cotransporter KCC2 in thalamic relay and reticular nuclei. Eur J Neurosci *20*, 965-975.

Baughman, R. W., Huettner, J. E., Jones, K. A., and Khan, A. A. (1991). Cell culture of neocortex and basal forebrain from postnatal rats. In Culturing Nerve Cells, G. Banker, and K. Goslin, eds. (Cambridge, MA, MIT Press), pp. 227-249.

Ben-Ari, Y. (2002). Excitatory actions of gaba during development: the nature of the nurture. Nat Rev Neurosci *3*, 728-739.

Ben-Ari, Y. (2006). Basic developmental rules and their implications for epilepsy in the immature brain. Epileptic Disord *8*, 91-102.

Ben-Ari, Y., Cherubini, E., Corradetti, R., and Gaiarsa, J. L. (1989). Giant synaptic potentials in immature rat CA3 hippocampal neurones. J Physiol (London) *416*, 303-325.

Ben-Ari, Y., Khazipov, R., Leinekugel, X., Caillard, O., and Gaiarsa, J. L. (1997a). GABAA, NMDA and AMPA receptors: a developmentally regulated 'menage a trois'. Trends Neurosci *20*, 523-529.

Ben-Ari, Y., Khazipov, R., Leinekugel, X., Caillard, O., and Gaiarsa, J. L. (1997b). GABAA, NMDA and AMPA receptors: a developmentally regulated 'ménage à trois'. Trends Neurosci *20*, 523-529.

Ben-Ari, Y., Tseeb, V., Raggozzino, D., Khazipov, R., and Gaiarsa, J. L. (1994). γ-Aminobutyric acid (GABA): a fast excitatory transmitter which may regulate the development of hippocampal neurones in early postnatal life. In Prog. Brain Res., J. van Pelt, M. A. Corner, H. B. M. Uylings, and F. H. Lopes da Silva, eds. (Elsevier Science BV), pp. 261-273.

Bennett, B. D., Callaway, J. C., and Wilson, C. J. (2000). Intrinsic membrane properties underlying spontaneous tonic firing in neostriatal cholinergic interneurons. J Neurosci *20*, 8493-8503.

Bettinelli, A., Bianchetti, M. G., Girardin, E., Caringella, A., Cecconi, M., Appiani, A. C., Pavanello, L., Gastaldi, R., Isimbaldi, C., Lama, G., *et al.* (1992). Use of calcium excretion values to distinguish two forms of primary renal tubular hypokalemic alkalosis: Bartter and Gitelman syndromes [see comments]. J Pediatr *120*, 38-43.

Betz, H. (1991). Glycine receptors: heterogeneous and widespread in the mammalian brain. Trends Neurosci *14*, 458-461.

Betz, H., Kuhse, J., Fischer, M., Schmieden, V., Laube, B., Kuryatov, A., Langosch, D., Meyer, G., Bormann, J., Rundstrom, N., and et al. (1994). Structure, diversity and synaptic localization of inhibitory glycine receptors. J Physiol Paris *88*, 243-248.

Bize, I., and Dunham, P. B. (1994). Staurosporine, a protein kinase inhibitor, activates K-Cl cotransport in LK sheep erythrocytes. Am J Physiol (Cell Physiol) *266*, C759-C770.

Blumcke, I., Beck, H., Lie, A. A., and Wiestler, O. D. (1999). Molecular neuropathology of human mesial temporal lobe epilepsy. Epilepsy Res *36*, 205-223.

Boettger, T., Hubner, C. A., Maier, H., Rust, M. B., Beck, F. X., and Jentsch, T. J. (2002). Deafness and renal tubular acidosis in mice lacking the K-Cl co-transporter Kcc4. Nature *416*, 874-878.

Boettger, T., Rust, M. B., Maier, H., Seidenbecher, T., Schweizer, M., Keating, D. J., Faulhaber, J., Ehmke, H., Pfeffer, C., Scheel, O., *et al.* (2003). Loss of K-Cl co-transporter KCC3 causes deafness, neurodegeneration and reduced seizure threshold. Embo J *22*, 5422-5434.

Bonislawski, D. P., Schwarzbach, E. P., and Cohen, A. S. (2007). Brain injury impairs dentate gyrus inhibitory efficacy. Neurobiol Dis *25*, 163-169.

Bormann, J., Hamill, O. P., and Sakmann, B. (1987). Mechanism of anion permeation through channels gated by glycine and gamma-aminobutyric acid in mouse cultured spinal neurones. J Physiol *385*, 243-286.

Brugnara, C. (1995). Erythrocyte dehydration in pathophysiology and treatment of sickle cell disease. Curr Opin Hematol *2*, 132-138.

Cai, H., Cebotaru, V., Wang, Y. H., Zhang, X. M., Cebotaru, L., Guggino, S. E., and Guggino, W. B. (2006). WNK4 kinase regulates surface expression of the human sodium chloride cotransporter in mammalian cells. Kidney Int *69*, 2162-2170.

Chebib, M., and Johnston, G. A. (1999). The 'ABC' of GABA receptors: a brief review. Clin Exp Pharmacol Physiol *26*, 937-940.

Chen, H., and Sun, D. (2005). The role of Na-K-Cl co-transporter in cerebral ischemia. Neurol Res *27*, 280-286.

Cherubini, E., Gaiarsa, J. L., and Ben-Ari, Y. (1991). GABA: an excitatory transmitter in early postnatal life. Trends Neurosci *14*, 515-519.

Chudotvorova, I., Ivanov, A., Rama, S., Hubner, C. A., Pellegrino, C., Ben-Ari, Y., and Medina, I. (2005). Early expression of KCC2 in rat hippocampal cultures augments expression of functional GABA synapses. J Physiol *566*, 671-679.

Clayton, G. H., Owens, G. C., Wolf, J. S., and Smith, R. L. (1998). Ontogeny of cation-Cl^- cotransporter expression in rat neocortex. Brain Research Developmental Brain Research *109*, 281-292.

Connell, J., Oozeer, R., de Vries, L., Dubowitz, L. M., and Dubowitz, V. (1989). Clinical and EEG response to anticonvulsants in neonatal seizures. Arch Dis Child *64*, 459-464.

Coull, J. A., Boudreau, D., Bachand, K., Prescott, S. A., Nault, F., Sik, A., De Koninck, P., and De Koninck, Y. (2003). Trans-synaptic shift in anion gradient in spinal lamina I neurons as a mechanism of neuropathic pain. Nature *424*, 938-942.

Crepel, F., Delhaye-Bouchaud, N., Guastavino, J. M., and Sampaio, I. (1980). Multiple innervation of cerebellar Purkinje cells by climbing fibres in staggerer mutant mouse. Nature *283*, 483-484.

D'Ambrosio, R. (2004). The role of glial membrane ion channels in seizures and epileptogenesis. Pharmacol Ther *103*, 95-108.

Darman, R. B., and Forbush, B. (2002). A regulatory locus of phosphorylation in the N terminus of the Na-K-Cl cotransporter, NKCC1. J Biol Chem *277*, 37542-37550.

De Deyn, P. P., Marescau, B., and MacDonald, R. L. (1990). Epilepsy and the GABA-hypothesis a brief review and some examples. Acta Neurol Belg *90*, 65-81.

de Jong, J. C., Willems, P. H., Mooren, F. J., van den Heuvel, L. P., Knoers, N. V., and Bindels, R. J. (2003). The structural unit of the thiazide-sensitive NaCl cotransporter is a homodimer. J Biol Chem *278*, 24302-24307.

de Los Heros, P., Kahle, K. T., Rinehart, J., Bobadilla, N. A., Vazquez, N., San Cristobal, P., Mount, D. B., Lifton, R. P., Hebert, S. C., and Gamba, G. (2006). WNK3 bypasses the tonicity requirement for K-Cl cotransporter activation via a phosphatase-dependent pathway. Proc Natl Acad Sci USA *103*, 1976-1981.

DeFazio, R. A., Keros, S., Quick, M. W., and Hablitz, J. J. (2000). Potassium-coupled chloride cotransport controls intracellular chloride in rat neocortical pyramidal neurons. J Neurosci *20*, 8069-8076.

Deleu, D., Bamanikar, S. A., Muirhead, D., and Louon, A. (1997). Familial progressive sensorimotor neuropathy with agenesis of the corpus callosum (Andermann syndrome): a clinical, neuroradiological and histopathological study. Eur Neurol *37*, 104-109.

Delpire, E., and Lauf, P. K. (1992). Kinetics of DIDS inhibition of swelling-activated K-Cl cotransport in low K sheep erythrocytes. J Membrane Biol *126*, 89-96.

Delpire, E., Lu, J., England, R., Dull, C., and Thorne, T. (1999). Deafness and imbalance associated with inactivation of the secretory Na-K-2Cl co-transporter. Nat Genet *22*, 192-195.

Delpire, E., and Mount, D. B. (2002). Human and mouse phenotypes associated with defects in cation-chloride cotransporters. Ann Rev Physiol *64*, 803-843.

Delpire, E., Rauchman, M. I., Beier, D. R., Hebert, S. C., and Gullans, S. R. (1994). Molecular cloning and chromosome localization of a putative basolateral Na-K-2Cl

cotransporter from mouse inner medullary collecting duct (mIMCD-3) cells. J Biol Chem *269*, 25677-25683.

Di Fulvio, M., Lincoln, T. M., Lauf, P. K., and Adragna, N. C. (2001). Protein kinase G regulates potassium chloride cotransporter-3 expression in primary cultures of rat vascular smooth muscle cells. J Biol Chem *276*, 21046-21052.

Diamond, J. S. (2001). Neuronal glutamate transporters limit activation of NMDA receptors by neurotransmitter spillover on CA1 pyramidal cells. J Neurosci *21*, 8328-8338.

Dowd, B. F., and Forbush, B. (2003). PASK (Proline-Alanine-rich STE20-related Kinase), a Regulatory Kinase of the Na-K-Cl Cotransporter (NKCC1). J Biol Chem *278*, 27347-27353.

Dunn, S. M., Bateson, A. N., and Martin, I. L. (1994). Molecular neurobiology of the GABAA receptor. Int Rev Neurobiol *36*, 51-96.

Dzhala, V. I., and Staley, K. J. (2003). Excitatory actions of endogenously released GABA contribute to initiation of ictal epileptiform activity in the developing hippocampus. J Neurosci *23*, 1840-1846.

Dzhala, V. I., Talos, D. M., Sdrulla, D. A., Brumback, A. C., Mathews, G. C., Benke, T. A., Delpire, E., Jensen, F. E., and Staley, K. J. (2005). NKCC1 transporter facilitates seizures in the developing brain. Nat Med *11*, 1205-1213.

Ebihara, S., Shirato, K., Harata, N., and Akaike, N. (1995). Gramicidin-perforated patch recording: GABA response in mammalian neurones with intact intracellular chloride. J Physiol *484 (Pt 1)*, 77-86.

Ehrlich, I., Lohrke, S., and Friauf, E. (1999). Shift from depolarizing to hyperpolarizing glycine action in rat auditory neurones is due to age-dependent Cl^- regulation. J Physiol (London) *520*, 121-137.

Ellison, D. H., Velaskez, H., and Wright, F. S. (1987). Am J Physiol *253*, F546-F554.

Euler, T., and Wassle, H. (1998). Different contributions of GABAA and GABAC receptors to rod and cone bipolar cells in a rat retinal slice preparation. J Neurophysiol *79*, 1384-1395.

Farrant, M., and Kaila, K. (2007). The cellular, molecular and ionic basis of GABA(A) receptor signalling. Prog Brain Res *160*, 59-87.

Fatima-Shad, K., and Barry, P. H. (1993). Anion permeation in GABA- and glycine-gated channels of mammalian cultured hippocampal neurons. Proc Biol Sci *253*, 69-75.

Fenwick, E. M., Marty, A., and Neher, E. (1982). Sodium and calcium channels in bovine chromaffin cells. J Physiol *331*, 599-635.

Fiumelli, H., Cancedda, L., and Poo, M. M. (2005). Modulation of GABAergic transmission by activity via postsynaptic Ca2+-dependent regulation of KCC2 function. Neuron *48*, 773-786.

Forbush, B., 3rd, Lytle, C., Xu, J. C., Payne, J. A., and Biemesderfer, D. (1994). The Na, K, C cotransporter of shark rectal gland. Ren Physiol Biochem *17*, 201-204.

French, J. A., Williamson, P. D., Thadani, V. M., Darcey, T. M., Mattson, R. H., Spencer, S. S., and Spencer, D. D. (1993). Characteristics of medial temporal lobe epilepsy: I. Results of history and physical examination. Ann Neurol *34*, 774-780.

Fukuda, A., Muramatsu, K., Okabe, A., Shimano, Y., Hida, H., Fujimoto, I., and Nishino, H. (1998). Changes in intracellular Ca2+ induced by $GABA_A$ receptor activation and reduction in Cl- gradient in neonatal rat neocortex. J Neurophysiol *79*, 439-446.

Gagnon, K. B., England, R., and Delpire, E. (2006a). Characterization of SPAK and OSR1, regulatory kinases of the Na-K-2Cl cotransporter. Mol Cell Biol *26*, 689-698.

Gagnon, K. B., England, R., and Delpire, E. (2006b). Volume sensitivity of cation-chloride cotransporters is modulated by the interaction of two kinases: SPAK and WNK4. Am J Physiol Cell Physiol *290*, C134-C142.

Galanopoulou, A. S. (2005). GABA receptors as broadcasters of sexually differentiating signals in the brain. Epilepsia *46 Suppl 5*, 107-112.

Galanopoulou, A. S. (2006). Sex- and cell-type-specific patterns of GABAA receptor and estradiol-mediated signaling in the immature rat substantia nigra. Eur J Neurosci *23*, 2423-2430.

Galanopoulou, A. S., Kyrozis, A., Claudio, O. I., Stanton, P. K., and Moshe, S. L. (2003). Sex-specific KCC2 expression and GABA(A) receptor function in rat substantia nigra. Exp Neurol *183*, 628-637.

Galeffi, F., Sah, R., Pond, B. B., George, A., and Schwartz-Bloom, R. D. (2004). Changes in intracellular chloride after oxygen-glucose deprivation of the adult hippocampal slice: effect of diazepam. J Neurosci *24*, 4478-4488.

Gamba, G. (2005a). Molecular Physiology and Pathophysiology of Electroneutral Cation-Chloride Cotransporters. Physiol Rev *85*, 423-493.

Gamba, G. (2005b). WNK lies upstream of kinases involved in regulation of ion transporters. Biochem J *391*, e1-e3.

Gamba, G., Miyanoshita, A., Lombardi, M., Lytton, J., Lee, W.-S., Hediger, M., and Hebert, S. C. (1994). Molecular cloning, primary structure, and characterization of two members of the mammalian electroneutral sodium-(potassium)-chloride cotransporter family expressed in kidney. J Biol Chem *269*, 17713-17722.

Gamba, G., Saltzberg, S. N., Lombardi, M., Miyanoshita, A., Lytton, J., Hediger, M. A., Brenner, B. M., and Hebert, S. C. (1993). Primary structure and functional expression of a cDNA encoding the thiazide-sensitive, electroneutral sodium-chloride cotransporter. Proc Natl Acad Sci USA *90*, 2749-2753.

Ganguly, K., Schinder, A. F., Wong, S. T., and Poo, M. (2001). GABA itself promotes the developmental switch of neuronal GABAergic responses from excitation to inhibition. Cell *105*, 521-532.

Gao, X. B., and van den Pol, A. N. (2000). GABA release from mouse axonal growth cones. J Physiol *523 Pt 3*, 629-637.

Garzon-Muvdi, T., Pacheco-Alvarez, D., Gagnon, K. B., Vazquez, N., Ponce-Coria, J., Moreno, E., Delpire, E., and Gamba, G. (2007). WNK4 kinase is a negative regulator of K+-Cl- cotransporters. Am J Physiol Renal Physiol *292*, F1197-1207.

Gerelsaikhan, T., and Turner, R. J. (2000). Transmembrane topology of the secretory Na+-K+-2Cl- cotransporter NKCC1 studied by in vitro translation. J Biol Chem *275*, 40471-40477.

Gesek, F. A., and Friedman, P. A. (1992). Mechanism of calcium transport stimulated by chlorothiazide in mouse distal convoluted tubule cells. J Clin Invest *90*, 429-438.

Gillen, C. M., Brill, S., Payne, J. A., and Forbush, B. I. (1996). Molecular cloning and functional expression of the K-Cl cotransporter from rabbit, rat, and human. A new member of the cation-chloride cotransporter family. J Biol Chem *271*, 16237-16244.

Gimenez, I., and Forbush, B. (2003). Short-term stimulation of the renal Na-K-Cl cotransporter (NKCC2) by vasopressin involves phosphorylation and membrane translocation of the protein. J Biol Chem *278*, 26946-26951.

Good, D. W. (1994). Ammonium transport by the thick ascending limb of Henle's loop. Ann Rev Physiol *56*, 623-647.

Gulacsi, A., Lee, C. R., Sik, A., Viitanen, T., Kaila, K., Tepper, J. M., and Freund, T. F. (2003). Cell type-specific differences in chloride-regulatory mechanisms and GABA(A) receptor-mediated inhibition in rat substantia nigra. J Neurosci *23*, 8237-8246.

Gulyas, A. I., Sik, A., Payne, J. A., Kaila, K., and Freund, T. F. (2001). The KCl cotransporter, KCC2, is highly expressed in the vicinity of excitatory synapses in the rat hippocampus. Eur J Neurosci *13*, 2205-2217.

Haas, M. (1994). The Na-K-Cl cotransporters. . Am J Physiol (Cell Physiol) *267*, C869-C885.

Haas, M., and Forbush, B. I. (1998). The Na-K-Cl cotransporters. J Bioenerg Biomembr *30*, 161-172.

Haas, M., and Forbush, B. I. (2000). The Na-K-Cl cotransporter of secretory epithelia. Annu Rev Physiol *62*, 515-534.

Harris, D. C. (2003). Quantitative Chemical Analysis, 6th edn, W. H. Freeman & Company).

Hebert, S. C., Mount, D. B., and Gamba, G. (2003). Molecular physiology of cation-coupled Cl(-) cotransport: the SLC12 family. Pflugers Arch.

Heinemann, U., and Lux, H. D. (1977). Ceiling of stimulus induced rises in extracellular potassium concentration in the cerebral cortex of cat. Brain Res *120*, 231-249.

Hennou, S., Khalilov, I., Diabira, D., Ben-Ari, Y., and Gozlan, H. (2002). Early sequential formation of functional GABA(A) and glutamatergic synapses on CA1 interneurons of the rat foetal hippocampus. Eur J Neurosci *16*, 197-208.

Hentschke, M., Wiemann, M., Hentschke, S., Kurth, I., Hermans-Borgmeyer, I., Seidenbecher, T., Jentsch, T. J., Gal, A., and Hubner, C. A. (2006). Mice with a targeted disruption of the Cl-/HCO3- exchanger AE3 display a reduced seizure threshold. Mol Cell Biol *26*, 182-191.

Hertz, L. (1978). An intense potassium uptake into astrocytes, its further enhancement by high concentrations of potassium, and its possible involvement in potassium homeostasis at the cellular level. Brain Res *145*, 202-208.

Hiki, K., D'Andrea, R. J., Furze, J., Crawford, J., Woollatt, E., Sutherland, G. R., Vadas, M. A., and Gamble, J. R. (1999). Cloning, characterization, and chromosomal location of a novel human K^+-Cl^- cotransporter. J Biol Chem *274*, 10661-10667.

Horn, R., and Marty, A. (1988). Muscarinic activation of ionic currents measured by a new whole-cell recording method. J Gen Physiol *92*, 145-159.

Howard, H. C., Mount, D. B., Rochefort, D., Byun, N., Dupré, N., Lu, J., Fan, X., Song, L., Rivière, J.-B., Prévost, C., *et al.* (2002). Mutations in the K-Cl cotransporter KCC3 cause a severe peripheral neuropathy associated with agenesis of the corpus callosum. Nat Genet *32*, 384-392.

Hubner, C. A., Stein, V., Hermans-Borgmeyer, I., Meyer, T., Ballanyi, K., and Jentsch, T. J. (2001). Disruption of KCC2 reveals an essential role of K-Cl cotransport already in early synaptic inhibition. Neuron *30*, 515-524.

Huettner, J. E., and Baughman, R. W. (1986). Primary culture of identified neurons from the visual cortex of postnatal rats. J Neurosci *6*, 3044-3060.

Igarashi, P., Vanden Heuvel, G. B., Payne, J. A., and Forbush, B. I. (1995). Cloning, embryonic expression and alternative splicing of a murine kidney specific Na-K-Cl cotransporter. Am J Physiol (Renal Fluid Electrolyte Physiol) *269*, F405-F418.

Ikeda, M., Toyoda, H., Yamada, J., Okabe, A., Sato, K., Hotta, Y., and Fukuda, A. (2003). Differential development of cation-chloride cotransporters and Cl- homeostasis contributes to differential GABAergic actions between developing rat visual cortex and dorsal lateral geniculate nucleus. Brain Res *984*, 149-159.

Irie, T., Hara, M., Yasukura, T., Minamino, M., Omori, K., Matsuda, H., Inoue, K., and Inagaki, C. (1998). Chloride concentration in cultured hippocampal neurons increases during long-term exposure to ammonia through enhanced expression of an anion exchanger. Brain Res *806*, 246-256.

Isenring, P., Jacoby, S. C., and Forbush, B. I. (1998). The role of transmembrane domain 2 in cation transport by the Na-K-Cl cotransporter. Proc Natl Acad Sci USA *95*, 7179-7184.

Janigro, D., and Schwartzkroin, P. A. (1988). Effects of GABA and baclofen on pyramidal cells in the developing rabbit hippocampus: an in vitro study. Dev Brain Res *41*, 171-184.

Jarolimek, W., Bijak, M., and Misgeld, U. (1994). Differences in the Cs block of baclofen and 4-aminopyridine induced potassium currents of guinea pig CA3 neurons in vitro. Synapse *18*, 169-177.

Jennings, M. L., and Schultz, R. K. (1991). Okadaic acid inhibition of KCl cotransport. Evidence that protein dephosphorylation is necessary for activation of transport by either swelling or N-ethylmaleimide. J Gen Physiol *97*, 799-817.

Kahle, K. T., Rinehart, J., de Los Heros, P., Louvi, A., Meade, P., Vazquez, N., Hebert, S. C., Gamba, G., Gimenez, I., and Lifton, R. P. (2005). WNK3 modulates transport of Cl- in and out of cells: implications for control of cell volume and neuronal excitability. Proc Natl Acad Sci USA *102*, 16783-16788.

Kahle, K. T., Rinehart, J., Ring, A., Gimenez, I., Gamba, G., Hebert, S. C., and Lifton, R. P. (2006). WNK protein kinases modulate cellular Cl- flux by altering the phosphorylation state of the Na-K-Cl and K-Cl cotransporters. Physiology (Bethesda) *21*, 326-335.

Kaila, K., and Voipio, J. (1987). Postsynaptic fall in intracellular pH induced by GABA-activated bicarbonate conductance. Nature *330*, 163-165.

Kaji, D., and Tsukitani, Y. (1991). Role of protein phosphatase in activation of KCl cotransport in human erythrocytes. Am J Physiol *260*, C176-C182.

Kakazu, Y., Akaike, N., Komiyama , S., and Nabekura, J. (1999). Regulation of intracellular chloride by cotransporters in developing lateral superior olive neurons. J Neurosci *19*, 2843-2851.

Kakazu, Y., Uchida, S., Nakagawa, T., Akaike, N., and Nabekura, J. (2000). Reversibility and cation selectivity of the K(+)-Cl(-) cotransport in rat central neurons. J Neurophysiol *84*, 281-288.

Kanaka, C., Ohno, K., Okabe, A., Kuriyama, K., Itoh, T., Fukuda, A., and Sato, K. (2001). The differential expression patterns of messenger RNAs encoding K-Cl cotransporters (KCC1,2) and Na-K-2Cl cotransporter (NKCC1) in the rat nervous system. Neuroscience *104*, 933-946.

Kandel, E. R., Schwartz, J. H., and Jessell, T. M. (2000). Principles of Neural Science, Fourth edn).

Kandler, K., and Friauf, E. (1995). Development of glycinergic and glutamatergic synaptic transmission in the auditory brainstem of perinatal rats. J Neurosci *15*, 6890-6904.

Kandler, K., and Katz, L. C. (1995). Neuronal coupling and uncoupling in the developing nervous system. Curr Opin Neurobiol *5*, 98-105.

Kaplan, M. R., Plotkin, M. D., Lee, W.-S., Xu, Z.-C., Lytton, J., and Hebert, S. C. (1996). Apical localization of the Na-K-2Cl cotransporter, rBSC1, on rat thick ascending limbs. Kidney Int *49*, 40-47.

Karadsheh, M. F., Byun, N., Mount, D. B., and Delpire, E. (2003). Localization of the KCC4 potassium-chloride cotransporter in the nervous system. Neuroscience *123*, 381-391.

Karadsheh, M. F., and Delpire, E. (2001). A neuronal restrictive silencing element is found in the KCC2 gene: Molecular Basis for KCC2 specific expression in neurons. J Neurophysiol *85*, 995-997.

Karadsheh, M. S., Shah, M. S., Tang, X., Macdonald, R. L., and Stitzel, J. A. (2004). Functional characterization of mouse alpha4beta2 nicotinic acetylcholine receptors stably expressed in HEK293T cells. J Neurochem *91*, 1138-1150.

Karolyi, L., Koch, M. C., Grzeschik, K. H., and Seyberth, H. W. (1998). The molecular genetic approach to "Bartter's syndrome". J Mol Med *76*, 317-325.

Kelsch, W., Hormuzdi, S., Straube, E., Lewen, A., Monyer, H., and Misgeld, U. (2001). Insulin-like growth factor 1 and a cytosolic tyrosine kinase activate chloride outward transport during maturation of hippocampal neurons. J Neurosci *21*, 8339-8347.

Khazipov, R., Khalilov, I., Tyzio, R., Morozova, E., Ben-Ari, Y., and Holmes, G. L. (2004). Developmental changes in GABAergic actions and seizure susceptibility in the rat hippocampus. Eur J Neurosci *19*, 590-600.

Kim, G. H., Masilamani, S., Turner, R., Mitchell, C., Wade, J. B., and Knepper, M. A. (1998). The thiazide-sensitive Na-Cl cotransporter is an aldosterone-induced protein. Proc Natl Acad Sci USA *95*, 14552-14557.

Klein, J. D., Lamitina, S. T., and O'Neill, W. C. (1999). JNK is a volume-sensitive kinase that phosphorylates the Na-K-2Cl cotransporter in vitro. Am J Phyiol (Cell Physiol) *46*, C425-C431.

Kleta, R., Basoglu, C., and Kuwertz-Broking, E. (2000). New treatment options for Bartter's syndrome. N Engl J Med *343*, 661-662.

Kleta, R., and Bockenhauer, D. (2006). Bartter syndromes and other salt-losing tubulopathies. Nephron Physiol *104*, p73-80.

Kraner, S. D., Chong , J. A., Tsay, H. J., and Mandel, G. (1992). Silencing the type II sodium channel gene: a model for neural-specific gene regulation. Neuron *9*, 37-44.

Krarup, T., and Dunham, P. B. (1996). Reconstitution of calyculin-inhibited K-Cl cotransport in dog erythrocyte ghosts by exogenous PP-1. Am J Physiol (Cell Physiol) *270*, C898-C902.

Kullmann, D. M., Erdemli, G., and Asztely, F. (1996). LTP of AMPA and NMDA receptor-mediated signals: evidence for presynaptic expression and extrasynaptic glutamate spill-over. Neuron *17*, 461-474.

Kurihara, K., Nakanishi, N., Moore-Hoon, M. L., and Turner, R. J. (2002). Phosphorylation of the salivary Na(+)-K(+)-2Cl(-) cotransporter. Am J Physiol Cell Physiol *282*, C817-C823.

Kyrozis, A., and Reichling, D. B. (1995). Perforated-patch recording with gramicidin avoids artifactual changes in intracellular chloride concentration. J Neurosci Methods *57*, 27-35.

Lauf, P. K. (1985). Passive K^+-Cl^- fluxes in low-K^+ sheep erythrocytes: modulation by A23187 and bivalent cations. Am J Physiol *249*, C271-C278.

Lauf, P. K., and Adragna, N. C. (2000). K-Cl cotransport: properties and molecular mechanism. Cell Physiol Biochem *10*, 341-354.

Lauf, P. K., Bauer, J., Adragna, N. C., Fujise, H., Zade-Oppen, A. M. M., Ryu, K., and Delpire, E. (1992). Erythrocyte K-Cl cotransport: Properties and regulation. Am J Physiol *263*, C917-C932.

Lee, V. C., Moscicki, J. C., and Difazio, C. A. (1998). Propofol sedation produces dose-dependent supression of lidocaine-induced seizures in rats. Aneth Analg *86*, 652-657.

Leinekugel, X., Khalilov, I., Ben-Ari, Y., and Khazipov, R. (1998). Giant depolarizing potentials: the septal pole of the hippocampus paces the activity of the developing intact septohippocampal complex in vitro. J Neurosci *18*, 6349-6357.

Leitch, E., Coaker, J., Young, C., Mehta, V., and Sernagor, E. (2005). GABA type-A activity controls its own developmental polarity switch in the maturing retina. J Neurosci *25*, 4801-4805.

Li, H., Tornberg, J., Kaila, K., Airaksinen, M. S., and Rivera, C. (2002). Patterns of cation-chloride cotransporter expression during embryonic rodent CNS development. Eur J Neurosci *16*, 2358-2370.

Liu, Y. W., Mee, E. W., Bergin, P., Teoh, H. H., Connor, B., Dragunow, M., and Faull, R. L. (2007). Adult neurogenesis in mesial temporal lobe epilepsy: a review of recent animal and human studies. Curr Pharm Biotechnol *8*, 187-194.

Lohof, A. M., Delhaye-Bouchaud, N., and Mariani, J. (1996). Synapse elimination in the central nervous system: functional significance and cellular mechanisms. Rev Neurosci *7*, 85-101.

LoTurco, J. J., Owens, D. F., Heath, M. J. S., Davis, M. B. E., and Kriegstein, A. R. (1995). GABA and glutamate depolarize cortical progenitor cells and inhibit DNA synthesis. Neuron *15*, 1287-1298.

Louvel, J., Avoli, M., Kurcewicz, I., and Pumain, R. (1994). Extracellular free potassium during synchronous activity induced by 4-aminopyridine in the juvenile rat hippocampus. Neurosci Lett *167*, 97-100.

Lu, J., Karadsheh, M., and Delpire, E. (1999). Developmental regulation of the neuronal-specific isoform of K-Cl cotransporter KCC2 in postnatal rat brains. J Neurobiol *39*, 558-568.

Ludwig, A., Li, H., Saarma, M., Kaila, K., and Rivera, C. (2003). Developmental up-regulation of KCC2 in the absence of GABAergic and glutamatergic transmission. Eur J Neurosci *18*, 3199-3206.

Luhmann, H. J., and Prince, D. A. (1991). Postnatal maturation of the GABAergic system in rat neocortex. J Neurophysiol *65*, 247-263.

Lux, H. D., Heinemann, U., and Dietzel, I. (1986). Ionic changes and alterations in the size of the extracellular space during epileptic activity. Adv Neurol *44*, 619-639.

Macdonald, R. L., Gallagher, M. J., Feng, H. J., and Kang, J. (2004). GABA(A) receptor epilepsy mutations. Biochem Pharmacol *68*, 1497-1506.

Majid, A., Speake, T., Best, L., and Brown, P. D. (2001). Expression of the Na+K+-2CI- cotransporter in alpha and beta cells isolated from the rat pancreas. Pflugers Arch *442*, 570-576.

Mantyh, P. W., and Hunt, S. P. (2004). Setting the tone: superficial dorsal horn projection neurons regulate pain sensitivity. Trends Neurosci *27*, 582-584.

Marty, S., Wehrle, R., Alvarez-Leefmans, F. J., Gasnier, B., and Sotelo, C. (2002). Postnatal maturation of Na+, K+, 2Cl- cotransporter expression and inhibitory synaptogenesis in the rat hippocampus: an immunocytochemical analysis. Eur J Neurosci *15*, 233-245.

Mason, M. J., Simpson, A. K., Mahaut-Smith, M. P., and Robinson, H. P. (2005). The interpretation of current-clamp recordings in the cell-attached patch-clamp configuration. Biophys J *88*, 739-750.

Mathern, G. W., Babb, T. L., Leite, J. P., Pretorius, K., Yeoman, K. M., and Kuhlman, P. A. (1996). The pathogenic and progressive features of chronic human hippocampal epilepsy. Epilepsy Res *26*, 151-161.

Mercado, A., Broumand, V., Zandi-Nejad, K., Enck, A. H., and Mount, D. B. (2006). A C-terminal domain in KCC2 confers constitutive K+-Cl- cotransport. J Biol Chem *281*, 1016-1026.

Mercado, A., Mount, D. B., and Gamba, G. (2004). Electroneutral cation-chloride cotransporters in the central nervous system. Neurochem Res *29*, 17-25.

Mercado, A., Mount, D. B., Vazquez, N., Song, L., and Gamba, G. (2000a). Functional characteristics of the renal KCCs. FASEB J *14*, A341.

Mercado, A., Song, L., Vazquez, N., Mount, D. B., and Gamba, G. (2000b). Functional Comparison of the K+-Cl- Cotransporters KCC1 and KCC4. J Biol Chem *275*, 30326-30334.

Meredith, R. M., Floyer-Lea, A. M., and Paulsen, O. (2003). Maturation of long-term potentiation induction rules in rodent hippocampus: role of GABAergic inhibition. J Neurosci *23*, 11142-11146.

Michelson, H. B., and Wong, R. K. (1991). Excitatory synaptic responses mediated by GABAA receptors in the hippocampus. Science *253*, 1420-1423.

Mienville, J. M., and Pesold, C. (1999). Low resting potential and postnatal upregulation of NMDA receptors may cause Cajal-Retzius cell death. J Neurosci *19*, 1636-1646.

Mikawa, S., Wang, C., Shu, F., Wang, T., Fukuda, A., and Sato, K. (2002). Developmental changes in KCC1, KCC2 and NKCC1 mRNAs in the rat cerebellum. Brain Res Dev Brain Res *136*, 93-100.

Misgeld, U., Deisz, R. A., Dodt, H. U., and Lux, H. D. (1986). The role of chloride transport in postsynaptic inhibition of hippocampal neurons. Science *232*, 1413-1415.

Morales-Aza, B. M., Chillingworth, N. L., Payne, J. A., and Donaldson, L. F. (2004). Inflammation alters cation chloride cotransporter expression in sensory neurons. Neurobiol Dis *17*, 62-69.

Moriguchi, T., Urushiyama, S., Hisamoto, N., Iemura, S. I., Uchida, S., Natsume, T., Matsumoto, K., and Shibuya, H. (2006). WNK1 regulates phosphorylation of cation-chloride-coupled cotransporters via the STE20-related kinases, SPAK and OSR1. J Biol Chem *280*, 42685-42693.

Mott, D. D., and Lewis, D. V. (1994). The pharmacology and function of central GABAB receptors. Int Rev Neurobiol *36*, 97-223.

Mount, D. B., Delpire, E., Gamba, G., Hall, A. E., Poch, E., Hoover Jr., R. S., and Hebert, S. C. (1998). The electroneutral cation-chloride cotransporters. J Exp Biol *201*, 2091-2102.

Mount, D. B., Mercado, A., Song, L., Xu, J., George, J. A. L., Delpire, E., and Gamba, G. (1999). Cloning and Characterization of KCC3 and KCC4, new members of the cation-chloride cotransporter gene family. J Biol Chem *274*, 16355-16362.

Mueller, A. L., Chesnut, R. M., and Schwartzkroin, P. A. (1983). Actions of gaba in developing rabbit hippocampus: an in vitro study. Neurosci Lett *39*, 193-198.

Muller, D., Oliver, M., Lynch, G. (1989). Developmental changes in synaptic properties in hippocampus of neonatal rats. Dev Brain Res *49*, 105-114.

Murphey, R. K., and Davis, G. (1994). Retrograde signalling at the synapse. J Neurobiol *25*, 595-598.

Nabekura, J., Ueno, T., Okabe, A., Furuta, A., Iwaki, T., Shimizu-Okabe, C., Fukuda, A., and Akaike, N. (2002). Reduction of KCC2 expression and GABAA receptor-mediated excitation after in vivo axonal injury. J Neurosci *22*, 4412-4417.

Neher, E., and Sakmann, B. (1992). The patch clamp technique. Sci Am *266*, 44-51.

Nicholson, C., and Hounsgaard, J. (1983). Diffusion in the slice microenvironment and implications for physiological studies. Fed Proc *42*, 2865-2868.

Nicolet-Barousse, L., Blanchard, A., Roux, C., Pietri, L., Bloch-Faure, M., Kolta, S., Chappard, C., Geoffroy, V., Morieux, C., Jeunemaitre, X., *et al.* (2005). Inactivation of the Na-Cl co-transporter (NCC) gene is associated with high BMD through both renal and bone mechanisms: analysis of patients with Gitelman syndrome and Ncc null mice. J Bone Miner Res *20*, 799-808.

Nielsen, S., Maunsbach, A. B., Ecelbarger, C. A., and Knepper, M. A. (1998). Ultrastructural localization of Na-K-2Cl cotransporter in thick ascending limb and macula densa of rat kidney. Am J Physiol (Renal Physiol) *275*, F885-F893.

Obrietan, K., and Van den Pol, A. N. (1996). Growth cone calcium elevation by GABA. J Comp Neurol *372*, 167-175.

Oike, M., Droogmans, G., Casteels, R., and Nilius, B. (1993). Electrogenic Na+/K(+)-transport in human endothelial cells. Pflugers Arch *424*, 301-307.

Okabe, A., Yokokura, M., Toyoda, H., Shimizu-Okabe, C., Ohno, K., Sato, K., and Fukuda, A. (2003). Changes in chloride homeostasis-regulating gene expressions in the rat hippocampus following amygdala kindling. Brain Res *990*, 221-226.

Okuda, K., Edwards, G. C., and Winnick, T. (1963). Biosynthesis of gramicidin and tryocidine in the Dubos strain of Bacillus brevis. I. Experiments with growing cultures. J Bacteriol *85*, 329-338.

Owens, D. F., Boyce, L. H., Davis, M. B. E., and Kriegstein, A. R. (1996). Excitatory GABA responses in embryonic and neonatal cortical slices demonstrated by gramicidin perforated-patch recordings and calcium imaging. J Neurosci *16*, 6414-6423.

Painter, M. J., Bergman, I., and Crumrine, P. (1986). Neonatal seizures. Pediatr Clin North Am *33*, 91-109.

Palma, E., Amici, M., Sobrero, F., Spinelli, G., Di Angelantonio, S., Ragozzino, D., Mascia, A., Scoppetta, C., Esposito, V., Miledi, R., and Eusebi, F. (2006). Anomalous

levels of Cl- transporters in the hippocampal subiculum from temporal lobe epilepsy patients make GABA excitatory. Proc Natl Acad Sci USA *103*, 8465-8468.

Payne, J. A. (1997). Functional characterization of the neuronal-specific K-Cl cotransporter: implications for $[K^+]_o$ regulation. Am J Physiol (Cell Physiol) *273*, C1516-C1525.

Payne, J. A., and Forbush, B. I. (1994). Alternatively spliced isoforms of the putative renal Na-K-Cl cotransporter are differentially distributed within the rabbit kidney. Proc Natl Acad Sci USA *91*, 4544-4548.

Payne, J. A., Stevenson, T. J., and Donaldson, L. F. (1996). Molecular characterization of a putative K-Cl cotransporter in rat brain. A neuronal-specific isoform. J Biol Chem *271*, 16245-16252.

Payne, J. A., Xu, J.-C., Haas, M., Lytle, C. Y., Ward, D., and Forbush, B. I. (1995). Primary structure, functional expression, and chromosome localization of the bumetanide sensitive Na-K-Cl cotransporter in human colon. J Biol Chem *270*, 17977-17985.

Pearson, M., Lu, J., Mount, D. B., and Delpire, E. (2001). Localization of the K-Cl cotransporter, KCC3, in the central and peripheral nervous systems: expression in choroid plexus, large neurons, and white matter tracts. Neuroscience *103*, 483-493.

Pearson, M. M., Lu, J., Mount, D. B., and Delpire, E. (2000). Expression of KCl cotransporter (KCC3) in the central nervous system: concurrence with myelination. FASEB J *14*, A351.

Pedersen, S. F., O'Donnell, M., E,, Anderson, S. E., and Cala, P. M. (2006). Physiology and pathophysiology of Na+/H+ exchange and Na+ -K+ -2Cl- cotransport in the heart, brain, and blood. Am J Physiol (Regul Integr Comp Physiol) *291*, R1-R25.

Perkins, K. L. (2006). Cell-attached voltage-clamp and current-clamp recording and stimulation techniques in brain slices. J Neurosci Methods *154*, 1-18.

Perkins, K. L., and Wong, R. K. (1996). Ionic basis of the postsynaptic depolarizing GABA response in hippocampal pyramidal cells. J Neurophysiol *76*, 3886-3894.

Perrot-Sinal, T. S., Sinal, C. J., Reader, J. C., Speert, D. B., and McCarthy, M. M. (2007). Sex differences in the chloride cotransporters, NKCC1 and KCC2, in the developing hypothalamus. J Neuroendocrinol *19*, 302-308.

Piechotta, K., Garbarini, N. J., England, R., and Delpire, E. (2003). Characterization of the interaction of the stress kinase SPAK with the Na+-K+-2Cl- cotransporter in the nervous system: Evidence for a scaffolding role of the kinase. J Biol Chem *278*, 52848-52856.

Plotkin, M. D., Kaplan, M. R., Peterson, L. N., Gullans, S. R., Hebert, S. C., and Delpire, E. (1997a). Expression of the Na^+-K^+-$2Cl^-$ cotransporter BSC2 in the nervous system. Am J Physiol (Cell Physiol) *272*, C173-C183.

Plotkin, M. D., Snyder, E. Y., Hebert, S. C., and Delpire, E. (1997b). Expression of the Na-K-2Cl cotransporter is developmentally regulated in postnatal rat brains: a possible mechanism underlying GABA's excitatory role in immature brain. J Neurobiol *33*, 781-795.

Price, T. J., Cervero, F., and de Koninck, Y. (2005). Role of cation-chloride-cotransporters (CCC) in pain and hyperalgesia. Curr Top Med Chem *5*, 547-555.

Prince, D. A., Deisz, R. A., Thompson, S. M., and Chagnac-Amitai, Y. (1992). Functional alterations in GABAergic inhibition during activity. Epilepsy Res Suppl *8*, 31-38.

Race, J. E., Makhlouf, F. N., Logue, P. J., Wilson, F. H., Dunham, P. B., and Holtzman, E. J. (1999). Molecular cloning and functional characterization of KCC3, a new K-Cl cotransporter. Am J Physiol (Cell Physiol) *277*, C1210-C1219.

Randall, J., Thorne , T., and Delpire, E. (1997). Partial cloning and characterization of *Slc12a2*: the gene encoding the secretory Na^+-K^+-$2Cl^-$ cotransporter. Am J Physiol (Cell Physiol) *273*, C1267-C1277.

Reisert, J., Lai, J., Yau, K. W., and Bradley, J. (2005). Mechanism of the excitatory Cl- response in mouse olfactory receptor neurons. Neuron *45*, 553-561.

Rhee, J. S., Ebihara, S., and Akaike, N. (1994). Gramicidin perforated patch-clamp technique reveals glycine-gated outward chloride current in dissociated nucleus solitarii neurons of the rat. J Neurophysiol *72*, 1103-1108.

Rivera, C., Li, H., Thomas-Crusells, J., Lahtinen, H., Viitanen, T., Nanobashvili, A., Kokaia, Z., Airaksinen, M. S., Voipio, J., Kaila, K., and Saarma, M. (2002). BDNF-induced TrkB activation down-regulates the K+-Cl- cotransporter KCC2 and impairs neuronal Cl- extrusion. J Cell Biol *159*, 747-752.

Rivera, C., Voipio, J., Payne, J. A., Ruusuvuori, E., Lahtinen, H., Lamsa, K., Pirvola, U., Saarma, M., and Kaila, K. (1999). The K^+/Cl^- co-transporter KCC2 renders GABA hyperpolarizing during neuronal maturation. Nature *397*, 251-255.

Rivera, C., Voipio, J., Thomas-Crusells, J., Li, H., Emri, Z., Sipila, S., Payne, J. A., Minichiello, L., Saarma, M., and Kaila, K. (2004). Mechanism of activity-dependent downregulation of the neuron-specific K-Cl cotransporter KCC2. J Neurosci *24*, 4683-4691.

Roberts, E. L., and Feng, Z. C. (1996). Influence of age on the clearance of K+ from the extracellular space of rat hippocampal slices. Brain Res *708*, 16-20.

Rohrbough, J., and Spitzer, N. C. (1996). Regulation of intracellulat Cl^- levels by Na^+-dependent Cl^- cotransport distinguishes depolarizing from hyperpolarizing $GABA_A$ receptor-mediated responses in spinal neurons. J Neurosci *16*, 82-91.

Ronen, G. M., Rosenbaum, P., Law, M., and Streiner, D. L. (1999). Health-related quality of life in childhood epilepsy: the results of children's participation in identifying the components. Dev Med Child Neurol *41*, 554-559.

Rorig, B., and Sutor, B. (1996). Regulation of gap junction coupling in the developing neocortex. Mol Neurobiol *12*, 225-249.

Russell, J. M. (1983). Cation-coupled chloride influx in squid axon. Role of potassium and stoichiometry of the transport process. J Gen Physiol *81*, 909-925.

Russell, J. M. (2000). Sodium-potassium-chloride cotransport. Physiol Rev *80*, 211-276.

Sandblom, J., Eisenman, G., and Neher, E. (1977). Ionic selectivity, saturation and block in gramicidin A channels: I. Theory for the electrical properties of ion selective channels having two pairs of binding sites and multiple conductance states. J Membr Biol *31*, 383-347.

Sattler, R., and Tymianski, M. (2001). Molecular mechanisms of glutamate receptor-mediated excitotoxic neuronal cell death. Mol Neurobiol *24*, 107-129.

Scher, M. S. (2003). Neonatal seizures and brain damage. Pediatr Neurol *29*, 381-390.

Scher, M. S., Aso, K., Beggarly, M. E., Hamid, M. Y., Steppe, D. A., and Painter, M. J. (1993). Electrographic seizures in preterm and full-term neonates: clinical correlates, associated brain lesions, and risk for neurologic sequelae. Pediatrics *91*, 128-134.

Schnermann, J. (2001). Sodium transport deficiency and sodium balance in gene-targeted mice. Acta Physiol Scand *173*, 59-66.

Schoenherr, C. J., and Anderson, D. J. (1995). The neuron-restrictive silencer factor (NRSF): a coordinate repressor of multiple neuron-specific genes. Science *267*, 1360-1363.

Schomberg, S. L., Bauer, J., Kintner, D. B., Su, G., Flemmer, A., Forbush, B., and Sun, D. (2003). Cross talk between the GABA(A) receptor and the Na-K-Cl cotransporter is mediated by intracellular Cl-. J Neurophysiol *89*, 159-167.

Schultheis, P. J., Lorenz, J. N., Meneton, P., Nieman, M. L., Riddle, T. M., Flagella, M., Duffy, J. J., Doetschman, T., Miller, M. L., and Shull, G. E. (1998). Phenotype resembling Gitelman's syndrome in mice lacking the apical Na+- Cl- cotransporter of the distal convoluted tubule. J Biol Chem *273*, 29150-29155.

Selvaraja, N. G., Prasada, R., Goldsteinb, J. L., and Rao, M. C. (2000). Evidence for the presence of cGMP-dependent protein kinase-II in human distal colon and in T84, the colonic cell line. Biochim Biophys Acta *1498*, 32-43.

Sen, A., Martinian, L., Nikolic, M., Walker, M. C., Thom, M., and Sisodiya, S. M. (2007). Increased NKCC1 expression in refractory human epilepsy. Epilepsy Res *74*, 220-227.

Shimizu-Okabe, C., Yokokura, M., Okabe, A., Ikeda, M., Sato, K., Kilb, W., Luhmann, H. J., and Fukuda, A. (2002). Layer-specific expression of Cl- transporters and differential [Cl-]i in newborn rat cortex. Neuroreport *13*, 2433-2437.

Singer, J. H., Talley, E. M., Bayliss, D., and Berger, A. J. (1998). Development of glycinergic synaptic transmission to rat brain stem motoneurons. J Neurophysiol *80*, 2608-2620.

Sipila, S. T., Huttu, K., Soltesz, I., Voipio, J., and Kaila, K. (2005). Depolarizing GABA acts on intrinsically bursting pyramidal neurons to drive giant depolarizing potentials in the immature hippocampus. J Neurosci *25*, 5280-5289.

Sipila, S. T., Schuchmann, S., Voipio, J., Yamada, J., and Kaila, K. (2006). The cation-chloride cotransporter NKCC1 promotes sharp waves in the neonatal rat hippocampus. J Physiol (Lond) *573*, 765-773.

Song, L., Mercado, A., Vazquez, N., Xie, Q., Desai, R., George, A. L., Jr., Gamba, G., and Mount, D. B. (2002). Molecular, functional, and genomic characterization of human KCC2, the neuronal K-Cl cotransporter. Brain Res Mol Brain Res *103*, 91-105.

Staley, K. (1994). The role of an inwardly rectifying chloride conductance in postsynaptic inhibition. J Neurophysiol *72*, 273-284.

Staley, K., Smith, R., Schaack, J., Wilcox, C., and Jentsch, T. J. (1996). Alteration of GABAA receptor function following gene transfer of the CLC-2 chloride channel. Neuron *17*, 543-551.

Staley, K. J., Soldo, B. L., and Proctor, W. R. (1995). Ionic mechanisms of neuronal excitation by inhibitory $GABA_A$ receptors. Science *269*, 977-981.

Starke, L. C., and Jennings, M. L. (1993). K-Cl cotransport in rabbit red cells: further evidence for regulation by protein phosphatase. Am J Physiol (Cell Physiol) *264*, C118-C124.

Stein, V., Hermans-Borgmeyer, I., Jentsch, T. J., and Hubner, C. A. (2004). Expression of the KCl cotransporter KCC2 parallels neuronal maturation and the emergence of low intracellular chloride. J Comp Neurol *468*, 57-64.

Strange, K., Singer, T. D., Morrison, R., and Delpire, E. (2000). Dependence of KCC2 K-Cl cotransporter activity on a conserved carboxy terminus tyrosine residue. Am J Physiol (Cell Physiol) *279*, C860-C867.

Su, G., Kintner, D. B., Flagella, M., Shull, G. E., and Sun, D. (2002a). Astrocytes from Na(+)-K(+)-Cl(-) cotransporter-null mice exhibit absence of swelling and decrease in EAA release. Am J Physiol Cell Physiol *282*, C1147-1160.

Su, G., Kintner, D. B., and Sun, D. (2002b). Contribution of Na(+)-K(+)-Cl(-) cotransporter to high-[K(+)](o)- induced swelling and EAA release in astrocytes. Am J Physiol Cell Physiol *282*, C1136-1146.

Sung, K., Kirby, M., McDonald, M. P., Lovinger, D. M., and Delpire, E. (2000). Abnormal $GABA_A$-receptor mediated currents in dorsal root ganglion neurons isolated from Na-K-2Cl cotransporter null mice. J Neurosci *20*, 7531-7538.

Tajima, Y., Ono, K., and Akaike, N. (1996). Perforated patch-clamp recording in cardiac myocytes using cation-selective ionophore gramicidin. Am J Physiol *271*, C524-532.

Tas, P. W. L., Massa, P. T., Kress, H. G., and Koschel, K. (1987). Characterization of an $Na^+/K^+/Cl^-$ co-transport in primary cultures of rat astrocytes. Biochim Biophys Acta *903*, 411-416.

Thompson, S. M., Deisz, R. A., and Prince, D. A. (1988). Outward chloride/cation co-transport in mammalian cortical neurons. Neurosci Lett *89*, 49-54.

Thompson, S. M., and Gahwiler, B. H. (1989a). Activity-dependent dishinibition. II. Effects of extracellular potassium, furosemide, and membrane potential on E_{Cl} in hippocampal CA3 neurons. J Neurophysiol *61*, 512-523.

Thompson, S. M., and Gahwiler, B. H. (1989b). Activity-dependent disinhibition. I. Repetitive stimulation reduces IPSP driving force and conductance in the hippocampus in vitro. J Neurophysiol *61*, 501-511.

Titz, S., Hans, M., Kelsch, W., Lewen, A., Swandulla, D., and Misgeld, U. (2003). Hyperpolarizing inhibition develops without trophic support by GABA in cultured rat midbrain neurons. J Physiol (Lond) *550*, 719-730.

Toyoda, H., Ohno, K., Yamada, J., Ikeda, M., Okabe, A., Sato, K., Hashimoto, K., and Fukuda, A. (2003). Induction of NMDA and GABAA receptor-mediated Ca2+ oscillations with KCC2 mRNA downregulation in injured facial motoneurons. J Neurophysiol *89*, 1353-1362.

Tyzio, R., Ivanov, A., Bernard, C., Holmes, G. L., Ben-Ari, Y., and Khazipov, R. (2003). Membrane potential of CA3 hippocampal pyramidal cells during postnatal development. J Neurophysiol *90*, 2964-2972.

Ueno, T., Okabe, A., Akaike, N., Fukuda, A., and Nabekura, J. (2002). Diversity of neuron-specific K+-Cl- cotransporter expression and inhibitory postsynaptic potential depression in rat motoneurons. J Biol Chem *277*, 4945-4950.

Urbach, V., Van Kerkhove, E., Maguire, D., and Harvey, B. J. (1996). Cross-talk between ATP-regulated K+ channels and Na+ transport via cellular metabolism in frog skin principal cells. J Physiol *491 (Pt 1)*, 99-109.

Vardi, N., Zhang, L. L., Payne, J. A., and Sterling, P. (2000). Evidence that different cation chloride cotransporters in retinal neurons allow opposite responses to GABA. J Neurosci *20*, 7657-7663.

Veliskova, J., Claudio, O. I., Galanopoulou, A. S., Lado, F. A., Ravizza, T., Velisek, L., and Moshe, S. L. (2004). Seizures in the developing brain. Epilepsia *45 Suppl 8*, 6-12.

Vitari, A. C., Deak, M., Morrice, N. A., and Alessi, D. R. (2005). The WNK1 and WNK4 protein kinases that are mutated in Gordon's hypertension syndrome, phosphorylate and active SPAK and OSR1 protein kinases. Biochem J *391*, 17-24.

Vitoux, D., Olivieri, O., Garay, R. P., Cragoe, E., Jr., Galacteros, F., and Beuzard, Y. (1989). Inhibition of K+ efflux and dehydration of sickle cells by [(dihydroindenyl)oxy]alkanoic acid: An inhibitor of the K+Cl- cotransport system. . Proc Natl Acad Sci USA *86*, 4273-4276.

Vu, T. Q., Payne, J. A., and Copenhagen, D. R. (2000). Localization and developmental expression patterns of the neuronal K–Cl cotransporter (KCC2) in the rat retina. J Neurosci *20*, 1414-1423.

Wake, H., Watanabe, M., Moorhouse, A. J., Kanematsu, T., Horibe, S., Matsukawa, N., Asai, K., Ojika, K., Hirata, M., and Nabekura, J. (2007). Early changes in KCC2 phosphorylation in response to neuronal stress result in functional downregulation. J Neurosci *27*, 1642-1650.

Wall, S. M., and Fischer, M. P. (2002). Contribution of the Na(+)-K(+)-2Cl(-) cotransporter (NKCC1) to transepithelial transport of H(+), NH(4)(+), K(+), and Na(+) in rat outer medullary collecting duct. J Am Soc Nephrol *13*, 827-835.

Wallace, B. A. (1990). Gramicidin channels and pores. Annu Rev Biophys Biophys Chem *19*, 127-157.

Walz, W., and Hertz, L. (1984). Intense furosemide-sensitive potassium accumulation in astrocytes in the presence of pathologically high extracellular potassium levels. J Cereb Blood Flow Metab *4*, 301-304.

Wang, C., Ohno, K., Furukawa, T., Ueki, T., Ikeda, M., Fukuda, A., and Sato, K. (2005). Differential expression of KCC2 accounts for the differential GABA responses between relay and intrinsic neurons in the early postnatal rat olfactory bulb. Eur J Neurosci *21*, 1449-1455.

Wang, C., Shimizu-Okabe, C., Watanabe, K., Okabe, A., Matsuzaki, H., Ogawa, T., Mori, N., Fukuda, A., and Sato, K. (2002). Developmental changes in KCC1, KCC2, and NKCC1 mRNA expressions in the rat brain. Brain Res Dev Brain Res *139*, 59-66.

Watsky, M. A., Cooper, K., and Rae, J. L. (1992). Transient outwardly rectifying potassium channel in the rabbit corneal endothelium. J Membr Biol *128*, 123-132.

Williams, J. R., Sharp, J. W., Kumari, V. G., Wilson, M., and Payne, J. A. (1999). The neuron-specific K-Cl cotransporter, KCC2. Antibody development and initial characterization of the protein. J Biol Chem *274*, 12656-12664.

Wilson, F. H., Disse-Nicodeme, S., Choate, K. A., Ishikawa, K., Nelson-Williams, C., Desitter, I., Gunel, M., Milford, D. V., Lipkin, G. W., Achard, J. M., *et al.* (2001). Human hypertension caused by mutations in WNK kinases. Science *293*, 1107-1112.

Winnick, R. E., Lis, H., and Winnick, T. (1961). Biosynthesis of gramicidin S. I. General characteristics of the process in growing cultures of Bacillus brevis. Biochim Biophys Acta *49*, 451-462.

Wong, J. A., Gosmanov, A. R., Schneider, E. G., and Thomason, D. B. (2001). Insulin-independent, MAPK-dependent stimulation of NKCC activity in skeletal muscle. Am J Physiol Regul Integr Comp Physiol *281*, R561-R571.

Woo, N.-S., Lu, J., England, R., McClellan, R., Dufour, S., Mount, D. B., Deutch, A. Y., Lovinger, D. M., and Delpire, E. (2002). Hyper-excitability and epilepsy associated with disruption of the mouse neuronal-specific K-Cl cotransporter gene. Hippocampus *12*, 258-268.

Wu, W. L., Ziskind-Conhaim, L., and Sweet, M. A. (1992). Early development of glycine- and GABA-mediated synapses in rat spinal cord. J Neurosci *12*, 3935-3945.

Yamada, J., Okabe, A., Toyoda, H., Kilb, W., Luhmann, H. J., and Fukuda, A. (2004). Cl^- uptake promoting depolarizing GABA actions in immature rat neocortical neurones is mediated by NKCC1. J Physiol (Lond) *557*, 829-841.

Yang, T., Huang, Y. G., Singh, I., Schnermann, J., and Briggs, J. P. (1996). Localization of bumetanide- and thiazide-sensitive Na-K-Cl cotransporters along the rat nephron. Am J Physiol (Renal Physiol) *271*, F931-F939.

Yin, H. H., and Lovinger, D. M. (2006). Frequency-specific and D2 receptor-mediated inhibition of glutamate release by retrograde endocannabinoid signaling. Proc Natl Acad Sci U S A *103*, 8251-8256.

Yoshimura, Y., and Tsumoto, T. (1994). Dependence of LTP induction on postsynaptic depolarization: a perforated patch-clamp study in visual cortical slices of young rats. J Neurophysiol *71*, 1638-1645.

Zhang, L. L., Delpire, E., and Vardi, N. (2007). NKCC1 does not accumulate chloride in developing retinal neurons. J Neurophysiol *In press*.

Zhou, F. M., and Hablitz, J. J. (1996). Postnatal development of membrane properties of layer I neurons in rat neocortex. J Neurosci *16*, 1131-1139.